STUDIES OF POLYMERIZATION OF α-OLEFINS CARRIED OUT WITH A TRI-NUCLEAR NICKEL CLUSTER

by
Yee-Yue Grace Luk
Bachelor of Science, Ryerson University, June 2011

A thesis presented to Ryerson University

In partial fulfillment of the requirements for the degree of

Master of Science

In the Program of

Molecular Science

Toronto, Ontario, Canada
©(Yee-Yue Grace Luk) 2014

AUTHOR'S DECLARATION FOR ELECTRONIC SUBMISSION OF A THESIS

I hereby declare that I am the sole author of this thesis. This is a true copy of the thesis, including any required final revisions, as accepted by my examiners.

I authorize Ryerson University to lend this thesis to other institutions or individuals for the purpose of scholarly research.

I further authorize Ryerson University to reproduce this thesis by photocopying or by other means, in total or in part, at the request of other institutions or individuals for the purpose of Scholarly research.

I understand that my thesis may be made electronically available to the public.

STUDIES OF POLYMERIZATION OF α-OLEFINS CARRIED OUT WITH A TRI-NUCLEAR NICKEL CLUSTER

Yee-Yue Grace Luk

Master of Science, Molecular Science, Ryerson University, 2014

Abstract

Green coloured crystals of μ_3-chloro-μ_3-hydroxotris (μ-chloro) tris(*N,N,N',N'* –tetramethyl ethylene-1,2-diamine) trinickel(II) chloride (**1**) were synthesized and used as a pre-catalyst, along with methylaluminoxane (MAO) as an initiator, to polymerize styrene and methyl methacrylate. Polystyrene prepared from these Ni catalyzed reactions are highly syndiotactic with some atactic nature. Blue coloured acetonitriletri(aqua) (*N,N,N'N'* -tetramethylethylenediamine) nickel (II) chloride (**2**) has also been synthesized and structurally characterized by X-ray crystallography. Co-polymerization of methyl methacrylate and styrene was also successfully carried out with the MAO-activated **1**. The polymerization kinetics of styrene was studied by molecular weight analysis. Effects of changing the temperature and monomer concentration on the polymerization would be discussed. Polymerization carried out in homogeneous fashion and a mixed system containing both heterogeneous and homogeneous system will also be discussed.

Acknowledgements

I would like to thank my heavenly Father and my family for supporting me in everything I do. I would like to thank Dr. Gossage and Dr. Foucher for their guidance, patience and kindness (and the parties hosted by Dr. Gossage) during these years. I also thank the people I have worked together with in the lab. Aman, Shane, Justin and Jon who have helped me a lot in teaching me how to use the glovebox and in other Schlenk-related work. I would also like to thank Maja and Tamara who worked in the same fumehood with me during the past years and made my working area a pleasant place to work. Mahroo, Khrystyna and Michelle have been great help and comfort during these three years in the lab. I would also like to thank Drs. Wylie and Hyde for being my committee members and providing me with valuable opinions to guide my research.

Table of Contents

List of Tables

List of Figures

List of Abbreviations

AcCN: Acetonitrile

AN: Acrylonitrile

Bpy: *N,N'*-bipyridine

Cp: Cyclopentadienyl

DCM: Dichloromethane

DSC: Differential scanning calorimetry

HDPE: High density polyethylene

i-PP : *iso*-tactic polypropylene

i-PS: *iso*-tactic polystyrene

MA: Methyl acrylate

MAO: Methylaluminoxane

MeOH: Methanol

MMA: Methyl methacrylate

MMAO: Modified Methylaluminoxane

PE: Polyethylene

PMA: Poly(methyl acrylate)

PMMA: Poly(methyl methacrylate)

PS: Polystyrene

PY: Pyridine

STY: Styrene

s-PS: *Syndio*-tactic Polystyrene

THF: Tetrahydrofuran

TMEDA: *N,N,N',N'*-Tetramethylethylenediamine

VAc: Vinyl acetate

ZN: Ziegler-Natta

1. Introduction

1.1 Ziegler-Natta (ZN) Catalysis

Polymers, the macromolecules comprised of many repeat units, are used routinely in our daily lives. For example, each of the commonly known plastics assigned with a different recycling number are all examples of types of polymers.

Not all the types of the plastics assigned by recycling numbers 1 to 6 were available before 1955. Among these six types of plastics, polyethylene (PE) and polypropylene (PP) are polymers comprised solely of a monomeric α-olefin. Only low density polyethylene (LDPE) and atactic polypropylene (PP) were produced before 1955. The absence of high density polyethylene (HDPE) was mainly due to the harsh conditions and the limited availability of polymerization techniques to make polymers of simple α-olefins. Through free radical polymerization, industrial LDPE can be produced under conditions (operating pressure: 1000-3000 bar; operating temperature: 190-210 ℃)[1] that result in highly branched PE. The high degree of branching results in a lack of crystallinity, a low polymer density and the atactic nature of the PE.[2]

The requirement for harsh reaction conditions to make PE and PP was first addressed in 1955 when high density polyethylene (HDPE) was discovered by the German chemist Karl Ziegler. With a combination of a titanium-based compound and a metal alkyl, (aluminum-alkyls being the most common choice), the production of PE no longer required operation under high pressure and temperatures (Eq.1).[2]

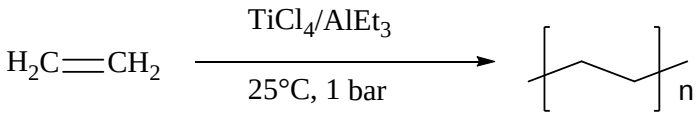

Eq. 1

A year later, another chemist, Italian Giulio Natta, extended Ziegler's findings and

discovered the first synthesis of *iso*-tactic PP (*i*-PP). From then on, catalysts that adapt Ziegler and Natta's findings in polymerization of olefins are generally referred to as Ziegler-Natta (ZN) type catalysts. In the year of 1963, Ziegler and Natta shared the Nobel Prize in Chemistry based on their findings that advanced the production of simple poly α-olefins.

The production of HDPE and *i*-PP demonstrate the ability of ZN-type catalysts to promote stereo-selective polymerization. This finding shed new light in the production of olefin-based polymers. However, ZN catalysts are not a perfect solution for production of polymers of simple olefins. In the original ZN system, solid titanium was used. The active sites of Ti are located both on the surface of the metal and buried within the solid matrix. While the active sites on the surface initiate polymerization, those buried below the surface remain dormant until the monomer can diffuse into the solid matrix.[3] This phenomenon leads to varying initiation times for different polymer sequences. As a result, polymers made by ZN catalysts usually possess broad polydispersities (PDI $\approx$ 9.0).[4] In addition, polymers made from ZN catalysts usually contain residues of the catalyst which requires additional chemical treatment and extraction of the bulk material to prevent the likelihood of unwanted polymer characteristics.[5] As a result, attempts to improve the ZN system have been carried out to prevent these issues. One of these classes of modification is to convert the heterogeneous ZN system into a homogeneous one.

In 1963, Natta reported the production of *syndio*-tactic PP (*s*-PP) with a modified homogenous ZN system.[6] Here the modified ZN system employs a vanadium-based compound with a valence number of 3 or higher instead of the titanium-based compounds. Nevertheless, in order to produce the *s*-PP with this homogeneous ZN system, the polymerization must be operated at a very low temperature (-78˚C). At room temperature (r.t), the system has no activity for the polymerization of propolyene.[7]

Although Natta reported the discovery of *s*-PP with this homogeneous ZN system, this was

not his first report on the attempt to homogenize the system for the polymerization of simple olefins. In 1957, Natta *et al.*[8] and Breslow *et al.*[9] both reported the capability of the first soluble system for the polymerization of ethylene, a system that utilizes titanocene instead of the titanium chloride as used with the original ZN system. However, this metallocene system (Fig. 1) did not receive much attention because of its low activity. In general, modifying the heterogeneous ZN system into a homogeneous system remained a significant challenge for many years until the discovery of "MAO" (methylaluminoxane).

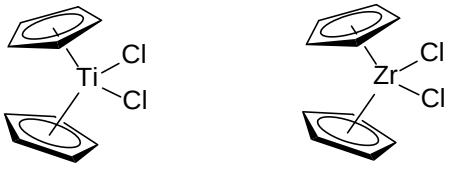

(a) (b)

Figure 1: Metallocene System. (a) Ti-based system reported independently by Natta and Breslow; (b) Zirconocene dichloride.

1.2 Discovery of Methylalumininoxane (MAO)

In 1980, Kaminsky reported on a highly active zirconocene/MAO system for the polymerization of ethylene. This was the first metallocene system (Fig. 1b) to be as active as the original ZN catalyst in ethylene polymerization. The discovery of MAO opened a door that led to a vast array of new plastics-based technologies.[10]

MAO is produced from mixture of water and trimethylaluminum in ratio of about 1:1; the resulting material is soluble in a variety of aromatic solvents.[10] The main elemental composition of MAO is $Al_4O_3(CH_3)_6$ (Fig. 2). It has not been possible to identify the exact molecular structure of MAO due to the lack of any X-ray structure data of a single crystal. In solution, MAO can exist as a linear structure or form cage structures comprised of various oligomers.

Both the linear and cyclic elements of MAO exist at equilibrium with each other in a variety of solvents.[11-14]

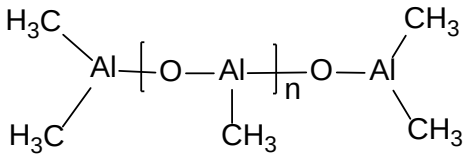

Figure 2: Proposed structure of MAO; n=4-20.

Although other types of co-catalysts exist, MAO is the most frequently used co-catalyst in the industrial polymerization of olefins.[14] One characteristic of MAO is that it behaves as a Lewis acid. It first activates a metallocene catalyst by extracting the halogen ligands and thereafter alkylating the cationic metal center.

1.3 Homogenous system: single site catalysts

The reported zirconocene/MAO system is a homogeneous system that resulted in the production of polyethylene or polypropylene with a PDI values less than 2.[15] The low PDI values result from the presence of a single site activation within the homogeneous system. In this system, the catalysts are soluble in the solvent and therefore the variation in the initiation time of polymerization is limited.

The mechanism of metallocene-based polymerization, whether proposed by Kaminsky *et al*. or by Corradini *et al.*, are based on *Cossee*'s theory.[16, 17] It is now believed that the first step in the polymerization is the activation of the metallocene pre-catalysts by MAO; this involves the extraction of the halogen ligands on the metal center, resulting in the production of a cationic metal center that is a strong Lewis acid (Eq. 2).[17]

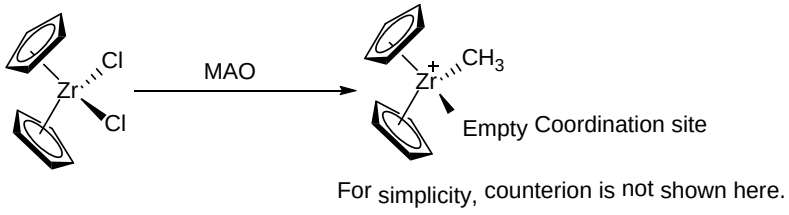

Eq. 2

The olefins then behave as Lewis bases, attacking the cationic metal center. This is known as the " insertion step" (Eq. 3).[17]

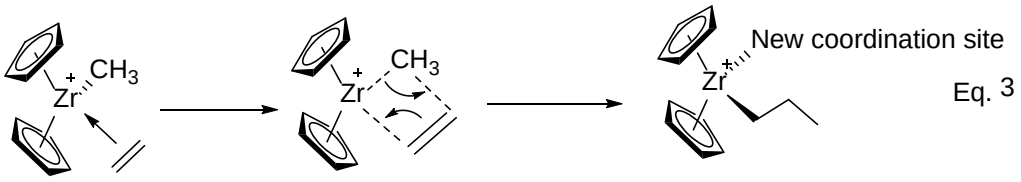

Eq. 3

The polymeric chain grows as the insertion step continues. However, the insertion step does not continue infinitely. At some point, the β-hydride transfer to the metal center can also occur and this causes the termination of the polymerization (Eq. 4).[17]

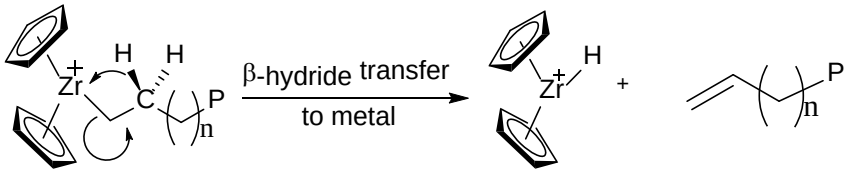

Eq. 4

In such metallocene-based polymerizations, the active site is on the metal center of the catalyst. Due to the fact that the catalyst is soluble in the reaction medium, all catalysts are initiated by MAO at approximately the same time. Hence, the catalysts in metallocene-based polymerization are known as "single-site" catalysts.[17]

1.4 *Ansa*-metallocene system: the development of modifying the metallocene-based catalysts:

Although homogeneous metallocene-based catalyst improved the PDI value of the resulting polymers, the same cannot be said with regard to the tacticity. According to Natta's hypothesis, a *chiral* metal center is crucial in producing *i*-PP. In initial reports, polymerization with a chiral metallocene/MAO system did not produce stereo-selective PP as expected. It was proposed that rotation of the two cyclopentadienyl (Cp) rings around the metal center, during the polymerization can occur readily. As a result, a stable enantiomeric complex is not formed during the polymerization.[10]

The first reported *i*-PP was produced by an *ansa*-zirconocene/MAO system containing a modified metallocene catalyst (Fig. 3).[10, 17(b), 18] This system has high activity (16000 Kg PP/mol Zr·hr) in producing polypropylene with low PDI values (< 2.0 at r.t.) and high isotacticity (95%). The success of obtaining high isotacticity in polypropylene was attributed to the alkyl chain that links the two Cp (or indenyl) rings that restrains the rotation of these two ligands.

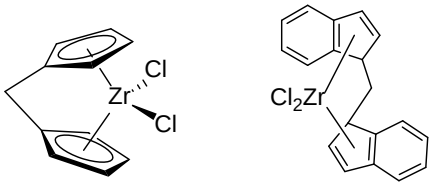

(a) (b)

Figure 3: *Ansa*-zirconocenes. (a) *ansa*-Bis(cyclopentadienyl) zirconocene; (b) *ansa*-Bis(indenyl) zirconocene.

This results in the stable formation of an enantiometric active site during the polymerization. Based on these findings, several inventions on modified *ansa*-metallocene/MAO system to produce stereo-selective polymers have appeared over the last 20 years. Among these studies, the most commonly reported *ansa*-metallocene catalysts usually contain Group 4 elements as the metal center.[14,19,20]

1.5 Catalysts containing late transition metals

While homogeneous, single site metallocene-based/MAO systems can yield polymers with small PDI values, high molecular weight and desired tacticity properties, the high oxophilicity of the early transition metals that are used often imposes an adverse effect on the polymerization of olefins. During polymerization, extreme care is required to avoid contamination by trace amounts of water and/or oxygen that may be present in the solution. In addition, protecting

groups are required if the monomer(s) contains a polar functional group. In order to avoid these disadvantages and to avoid patent controlled Ti/Zr-based catalysts containing metallocenes, the development of non-metallocene catalysts with late transition metals for olefin polymerization has been under increased scrutiny.[21, 22]

For the past two decades, the major focus of catalyst development with late transition metal has been centered on metals such as Co, Fe, Ni, and Pd. Although the lower oxophilicity of late transition metals gives promise for milder experimental condition(s) required for olefin polymerization, a main drawback of such catalysts, particularly in their early development, was the much lower activities in olefin polymerization. This undesirable phenomenon arises from the fact that it is less likely for the olefin double bond to attack the more electron-rich *d* metals because these are less electrophilic than their early transition metal analogs.[23] The improvement in designing catalysts with late transition metals for ethylene polymerization is best demonstrated by the progress of development of catalysts with Group 10 metals such as Ni (Fig. 4).

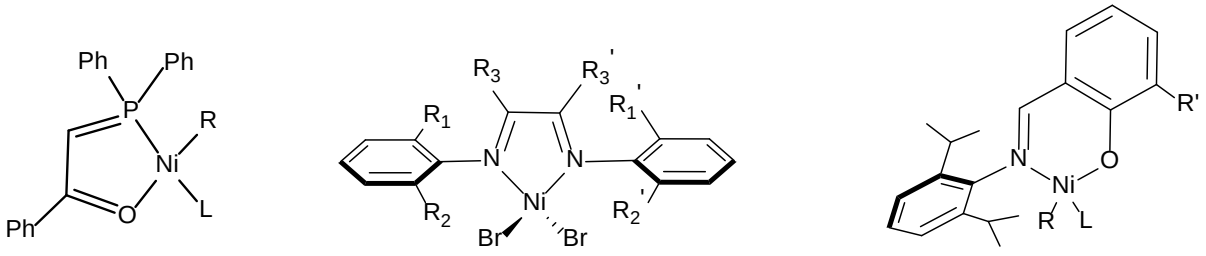

(a) (b) (c)

Figure 4: Evolution of Ni catalysts for ethylene polymerization. (a) SHOP catalyst; (b) Brookhart catalyst; (c) Grubbs catalyst. L= ligand, R= alkyl or aryl groups.

1.6 Ni-Based catalysts for α-olefin polymerization

A: SHOP Catalysts

In the early 1970s, Shell Chemicals developed the "Shell Higher Olefin Process" (SHOP)

which involves ethylene oligomerization processes that manufactures linear ethylene oligomers with chain lengths of between 8 and 20 carbon atoms. The catalyst involved in the SHOP oligomerization is known as the SHOP catalyst (Fig. 4(a)). This is formally a Ni^{2+} metal-centered catalyst which is chelated to a monoanionic *P,O*-donor ligand. It was realized later that removal of the secondary donor ligand "L" (Fig 4(a)) turns the SHOP-type catalyst from a mild oligomerization catalyst to a potent polymerization catalyst, typically yielding polyethylene with molecular weights over 100,000 Da. This can be achieved by different methods depending on the ancillary donor group L. If L = triphenylphosphine (PPh_3), an abstracting reagent such as $Ni(COD)_2$ (COD=1,5-cyclooctadiene) or $B(C_6F_5)_3$ is required to scavenge the ligand from the solution. In cases where pyridine (L = py) is the donor group, an abstracting reagent is not required. The activity of the SHOP–type catalysts in ethylene polymerization was also found to be related to the bulkiness of the substituent groups adjacent to the *O*-atom of the *P*, *O*-ligand. The more bulky the substituent is, the more active the SHOP-type catalyst is in ethylene polymerization (Fig. 5).[23-27]

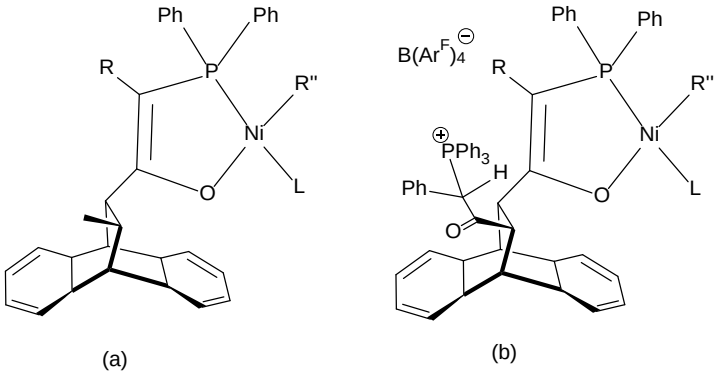

Figure 5: SHOP-type catalysts with substituents adjacent to the O-donor atom. (a): Ni catalyst with less bulky substituent adjacent to the O atom has an activity of 1730 g/mmol·h; (b) Ni catalyst with a more bulky substituent adjacent to the O atom affords an activity of 34880 g/mmol·h.

B: Brookhart Catalysts

In the 1990s, the pioneering work by Brookhart *et al.* re-defined the architectural design of Group 10-based catalyst systems. The square planar Ni^{2+} (or Pd^{2+}) complexes chelating to a neutral bulky diimine ligand through *N*, *N* atoms (Fig. 4 (b); Fig. 6) were the first reported catalysts with late transition metals (with MAO as co-catalysts) that are able to polymerize both ethylene and higher α-olefins into high molecular weight polymers .[23,26,28]

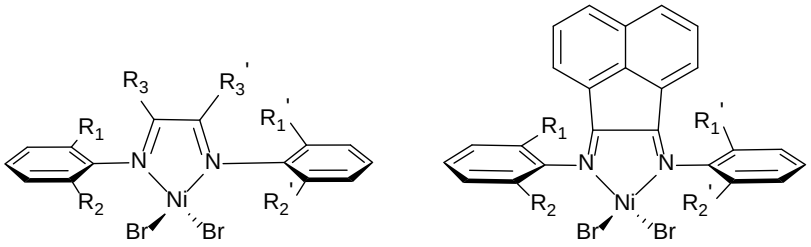

Figure 6: General schematic representations of Brookhart-type catalyst.

The PEs produced by Brookhart-type catalysts have molecular weights ranging from 30,000 to 1 million (g/mol) with very narrow PDI values (1.1-1.3), depending on the catalyst structure and polymerization conditions.[23] It was also noticed that the structures of PEs ranged from highly linear to moderately branched. Moreover, experimental observations suggested that the increase of branching in the produced PEs can be introduced by raising the temperature, lowering the ethylene pressure, or increasing the bulkiness of the *ortho*-substituents on the aryl ring of the diimine ligand (the R_1 and R_2 groups in Fig. 6 (1) and (2)). This phenomenon enables the formation of a copolymer of ethylene-propylene that has its ethylene contents tailored.[29] As a result, ethylene polymerization with this type of catalysts has been extensively studied to gain insight into the polymerization mechanism.

C: The mechanistic insight of insertion coordination through studies of Brookhart-type system

The ability of this class of catalysts to produce PEs in either a desired linear or branched

fashion results from a process known as “chain walking” during polymerization. As with ZN and metallocene-based/MAO system catalysts, the Brookhart-type catalysts carry out polymerization through a coordination-insertion mechanism. The first step is always to activate the catalysts by a co-catalyst to extract the halogens from the catalyst and to alkylate the catalyst, forming a cationic $14e^-$ species (Eq. 5). The most commonly used co-catalyst is either MAO or a modified MAO (i.e., MMAO).[23]

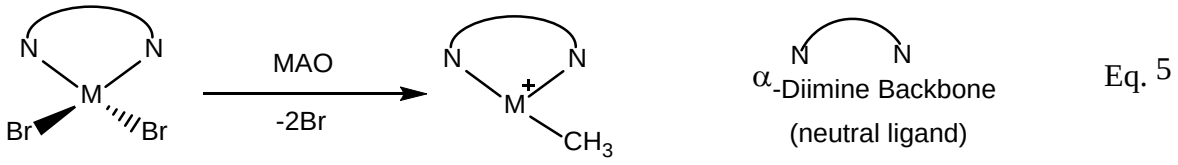

Eq. 5

The introduction of the α-olefins (ethylene in this example) to the activated catalyst is then followed, forming the resting state of the catalyst. Migratory insertion of ethylene is the next step, forming a new active $14e^-$ species that is available for the next ethylene migratory insertion to take place (Eq. 6).

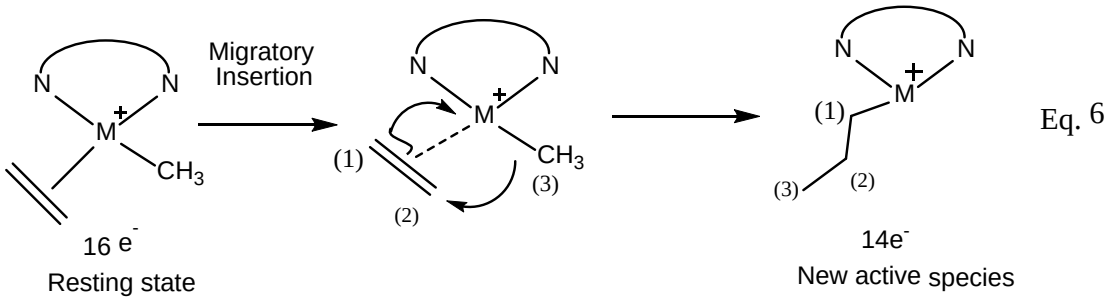

Eq. 6

Through low temperature ^{1}H NMR studies, it was established that after the first insertion of ethylene, the subsequent insertions proceeds with zero-order kinetics in ethylene concentration. Thus, a rationale in mechanism for ethylene has been ascribed. The migratory insertion reaction of the catalyst in a resting state is thought to be the turnover-limiting step.[23,28]

The new active species in Eq. 6 either continues to propagate the ethylene migratory insertion or undergoes β-agostic interaction prior to the next ethylene insertion (Fig. 7).

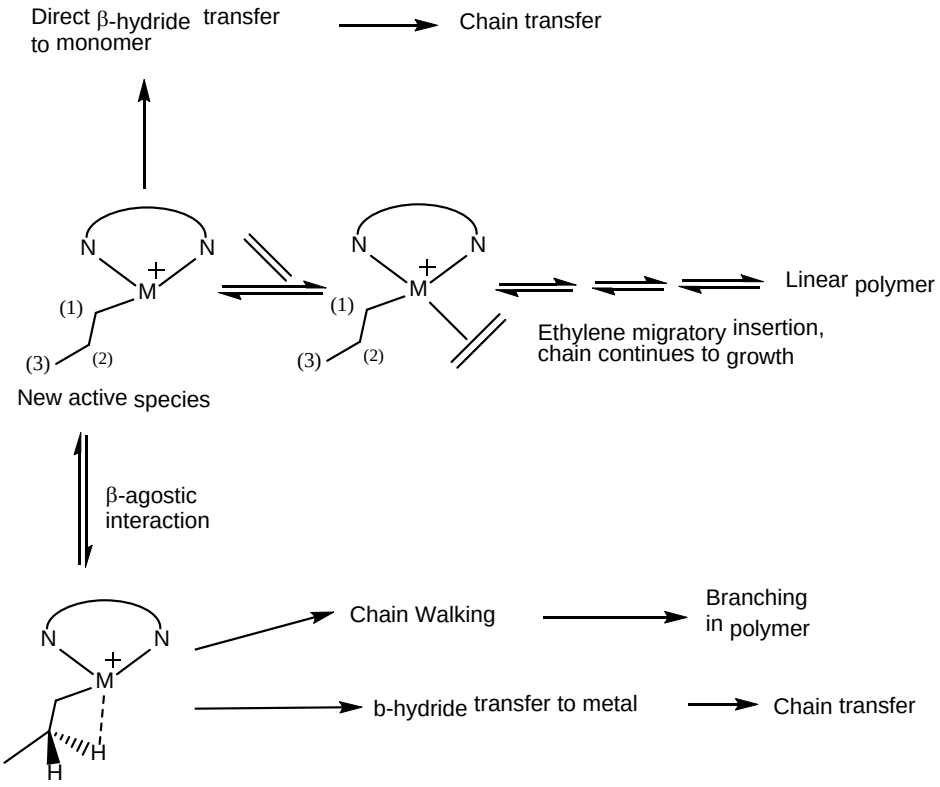

Figure 7: Routes for the new active species that result in linear or branched polymers.

Chain walking is a process such that the new active species undergoes β-hydride elimination from the β-agostic interaction state to form an olefin hydride complex, followed by reinsertion of the hydride. Consequently, the metal "migrates" from one carbon atom along the polymer chain, resulting in branching of the growing polymer chain. The "Chain walking" process could occur several times before the next ethylene insertion takes place (Eq. 7).[30,31]

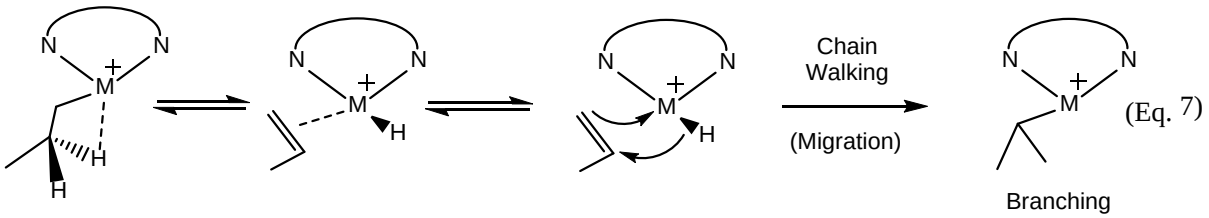

(Eq. 7)

Besides undergoing the chain walking step, it is also possible for the species at β-agostic state to proceed to chain transfer, resulting in the growing polymer chain dissociating from the catalyst, and is sometimes referred to as associative displacement.[23,28]

This chain transfer route, studied and proposed by Brookhart *et al*., involves the same first step as what occurs in chain walking; β-hydride elimination takes place from the species at the β-agostic state, forming an olefin-hydride complex.[23] However, instead of proceeding with further steps that cause branching in the polymer, associative ligand exchange takes place between an incoming monomer and the growing polymer chain. As a result, the growing polymer chain dissociates from the catalyst (Eq. 8). [28, 30, 31]

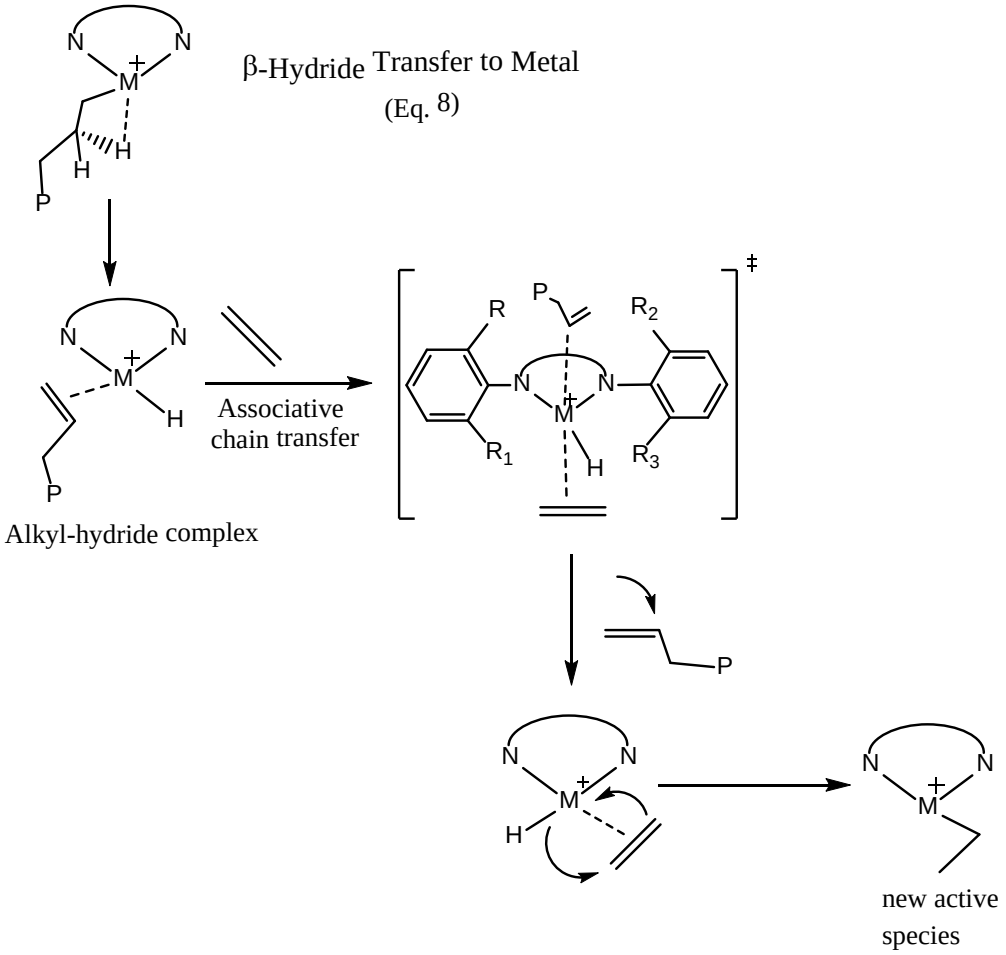

A different pathway for chain transfer to take place was proposed by Ziegler *et al.* through density function calculation.[32] As the new active species proceeds to its new resting state, β-hydride transfer directly from the olefin to monomer, takes place. Consequently, chain transfer follows and the growing polymer chain dissociates from the catalyst site (Eq. 9).[30, 32, 33]

Direct β-Hydride
Transfer to Monomer (Eq. 9)

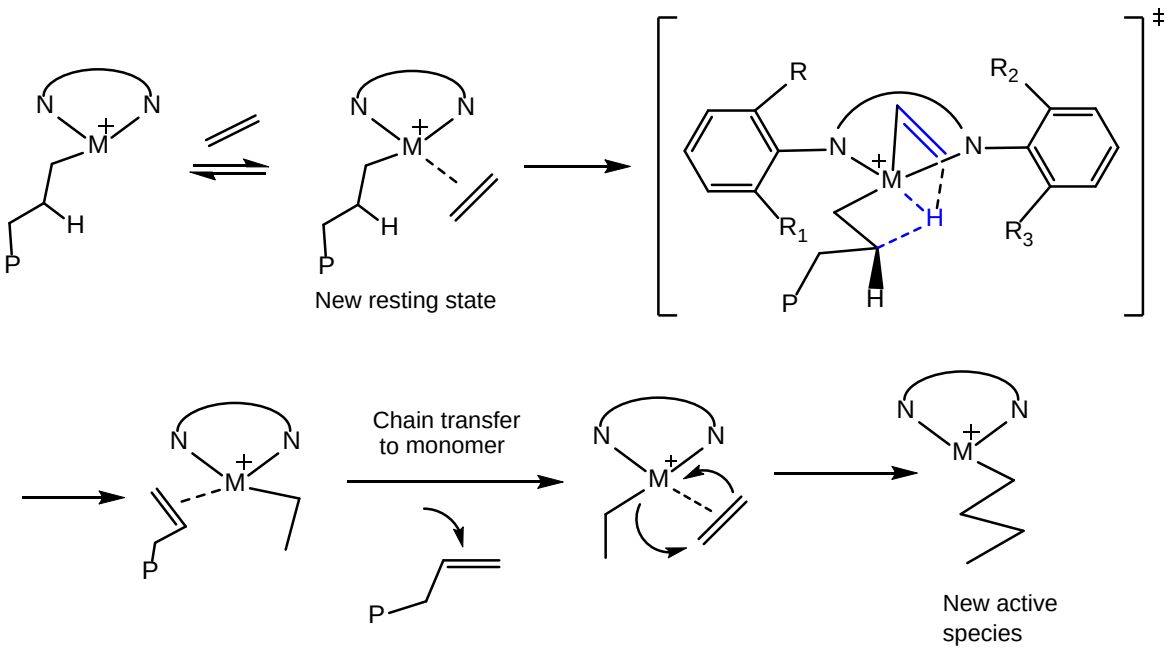

To date, there is no conclusive experimental evidence to favour the mechanism proposed either by Brookhart *et al.*[23] or by Ziegler *et al.*[30] However, both mechanisms agree that increasing the bulkiness of the backbone substituents or the *ortho*-substituents on the aryl ring plays an important role in retarding the chain transfer process that causes premature dissociation of the polymer chain from the catalyst. According to crystallographic studies, the aryl rings lie roughly perpendicular to the square planar α-diimine complex. This phenomenon places the *ortho*-substituents on the axial positions below and above the plane. As the bulkiness of the backbone substituents or the *ortho*-substituents increases, there is less access to the axial position of the coordination plane, and a lower likelihood of the formation of the five-coordinate transition state taking place. As a result, rates of chain propagation are greater than rates of chain transfer and the polymer with high molecular weight is produced.[23, 28, 30-36]

With the mechanistic steps already extensively studied and unveiled, combined with

theoretically calculated or experimentally obtained kinetic data, much of the observed experimental results can be explained. When the monomer is ethylene, the most stable complex in the chain growth is the 16 e^- species at the resting state; therefore chain growth is independent of the monomer concentration. However with other α-olefins, the most stable species is the 14 e^- species at its agostic state. This explains the observed chain growth step to be first-order in the monomer concentration. This also explains the much lower turnover frequency with propylene polymerization.[23,34] Brookhart-type catalysts adopting other metals, such as Pd(II), Fe(II) and Co(II) have also been extensively studied. However, this is a very broad area to explore. For the simplicity of this paper, these will not be covered in the introduction but more information can be obtained from references 34-41.

D: Grubbs' Catalysts

Brookhart-type catalysts replace the [P,O] ligand of the SHOP catalysts with a ligand containing a much harder donor atom: nitrogen. Adopting this rational by choosing the [N,O] salicyladimines as the ligand, a system of neutral, single-component Ni-based catalysts (Fig. 4c) were synthesized by Grubbs *et al*.[42] Depending on the ligand (R in Fig. 4(c)), this class of catalysts can carry out ethylene polymerization without the presence of a co-catalyst. The PEs produced have slightly higher PDI values (1.6-3.0) compared to the Brookhart system. The molecular weight of PEs ranged from 6100 to 347000 (g/mol). One of the advantages of the Ni-based Grubbs catalyst is that even with water as an additive to the polymerization system, the catalyst still remains active. Another advantage is that this class of catalysts can undergo polymerization of a variety of functionalized norbornenes. Branching in the produced PEs is observed. Preliminary mechanistic studies through ^{31}P NMR spectroscopy have suggested the polymerization proceeds through a coordination insertion-type mechanism.

E: Stereo-selectivity in propylene polymerization with Brookhart-type catalysts

Although each of the Brookhart and Grubbs-type catalysts has their own advantages, there is one unique advantage of the Brookhart-type catalysts that is not observed in Grubbs-type catalyst: the ability to produce *i*-PPs or *s*-PPs by stereo-selective polymerization (Fig. 8).

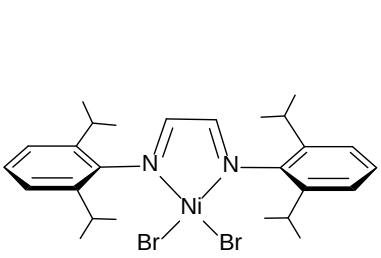

(A): Produced *s*-PP at -78°C[43]

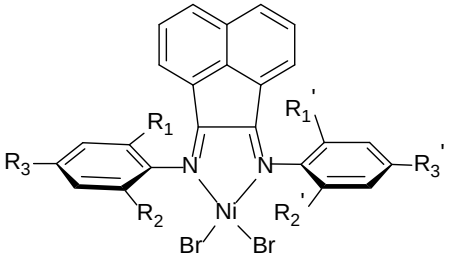

(B) Produced *s*-PP at -45°C[44]

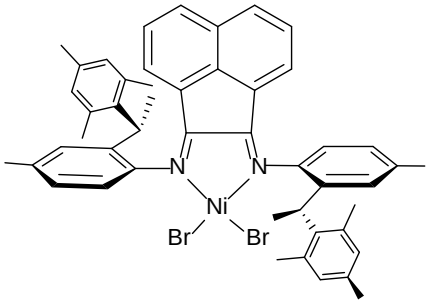

(C): Produced *i*-PP at -78°C[45]

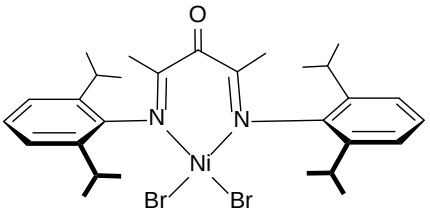

(D): Produced *i*-PP at -60°C[46]

Figure 8: Brookhart catalysts that produced PPs with different tacticity.

Regardless of the differences in the backbone structure of the Brookhart-type catalysts, all four catalysts in Fig. 8 were observed to undergo the stereo-selective polymerization of propylene only at low temperature. As the temperature of experimental condition increases, the resulting PPs lose their tacticity and PPs with a more atactic fraction are produced.[30,44-,46] The reason for the loss of tacticity in PPs at increased temperature was not extensively studied.

However, it may be attributed to the fact that as the temperature increases, the rotation of the N-C bond between the aryl ring to the diimine ligand also increases (Fig. 9).[30,34]

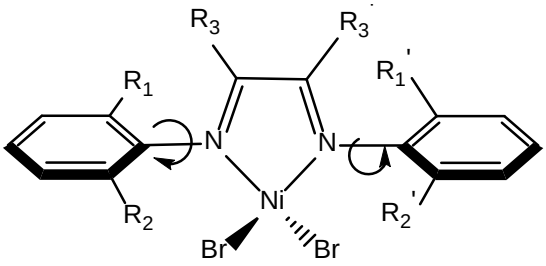

Figure 9: Rotation between the N-C bond becomes more flexible as temperature increases, causing higher access to the axial position below and above the square plane.

Stereo-selective polymerizations of propylene through a coordination insertion mechanism has been extensively investigated and well understood *via* the ansa-metallocene/MAO system. Fundamental principles established during polymerization by ansa-metallocene/MAO system leading to the production of a PP with tacticity have been applied in the preparation of PPs with tacticity produced from Brookhart-type catalysts. It was realized that the requirement to produce a PP with tacticity strongly depends on which enantioface of the prochiral propylene is inserted to the metal center. In other words, the tacticity depends on whether the propylene monomer inserts to the metal center through *re* insertion or *si* insertion (Fig. 10).[20(a)] To produce an *i*-PP, all monomer insertions need to proceed in either all *re* insertion or *si* insertion. Alternative *re* and *si* insertion (or *si* to *re*), on the other hand, produces *s*-PP. A chiral environment around the metal center is necessary for the monomer to be inserted energetically favouring one enantioface over the other. In the case in which the chiral environment is mainly controlled by the ligands of the catalyst, the monomer insertion has undergone the so called “enantiomorphic site control”. On the other hand, when the methyl group at the end of a growing polymer chain has influence over

the ligands of the catalysts in the chiral environment around the metal center, the monomer is known to take the "chain-end" mechanism for insertion.

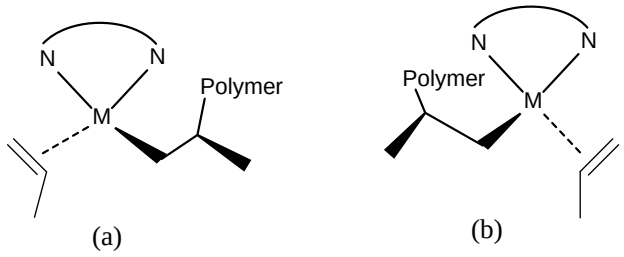

Figure 10: (a) *re* sertion; (b): *si* insertion.

Experimental evidence already suggests that all stereo-selective polymerizations of propylene by Brookhart's catalysts undergo monomer insertion through "chain end" control. As the rotation of N-C bond becomes more flexible at higher temperature (Fig. 9), the *ortho*-substituents on the aryl ring also move away from the axial position and rotate round the plane of the square planar backbone. As a result, the incoming monomer proceeds continuously in an orderly fashion (proceeds *via* all *re*, all *si* insertion, or alternation between *re* or *si*). 1,2- or 2,1-insertion where the metal center coordinates the monomer through a α- or β- carbon has also been extensively investigated in order to understand the defect in tacticity of PPs produced by Brookhart-type catalysts.[47-50]

In contrast to non-polar α-olefins, there have been few cases illustrating the ability of Brookhart-catalyst to undergo stereo-selective polymerization of polar vinyl monomers. Only two specific catalysts have been reported to yield vinyl polymers with tacticity (Fig. 11).

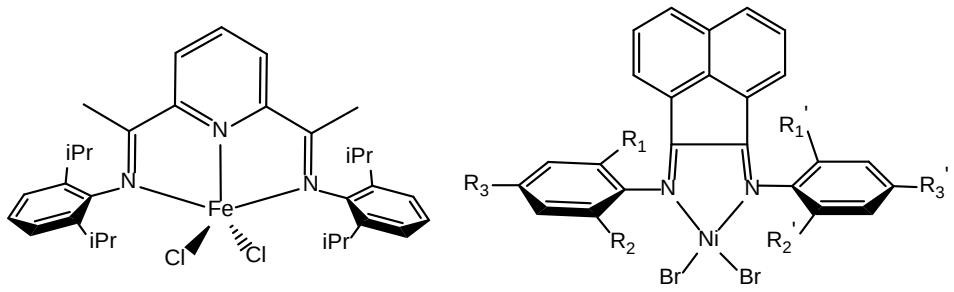

(a) (b)

Figure 11: (a) Reported to produce *syndio*-tactic polystyrene[51]; (b) Reported to produce *syndio*-tactic polymethyl methacrylate.[52]

However, the catalyst shown in Fig. 11(a) possesses very low activity in producing *syndio*-tactic polystyrene (*s*-PS). Interestingly, the most efficient class of catalysts for the production of *s*-PS is the Ti-based metallocene/MAO system.[53]

1.7 Syndiotactic polystyrene

Polystyrene (PS) is a polar vinyl polymer with the recycling number 6. Some of the commercially available PSs are atactic in their nature. This amorphous polymer offers several advantages in its commercial applications which include low cost and ease to foam. However, one of the disadvantages of this atactic polymer is that it possesses a glass transition temperature (T_g) at around 100˚C, which means the polymers cannot be used in applications above this temperature because the atactic polymer softens. The discovery of *iso*-tactic PS (*i*-PS) offers a solution to this limitation. The *i*-PSs possess a T_g at around 100°C and a melting point (T_m) at around 240˚C. These properties offer the possibility for these stereoregular polymers to be used in applications between 100-240˚C as the polymer can still maintain its shape for applications under 250˚C.[54] *i*-PS can be made from early transition metal catalysts such as $TiCl_4$ (ZN system), LiC_4H_9/H_2O,[55] and Ti-based *ansa*-metallocene/MAO system.[56] *i*-PS can also be made with Ni-based catalysts, such as Ni(acetylacetonate)$_2$/MAO system.[57,58] Although ideally *i*-PSs can

be processed below 240°C, one practical drawback of *i*-PSs is that it takes very long time for *i*-PSs to undergo crystallization, which makes *i*-PSs difficult to injection mold.

This issue was solved by the discovery of *s*-PSs in 1980s after the discovery of MAO. Utilizing a Ti-based metallocene/MAO system, the resulting *s*-PSs can reach a high degree of crystallinity in a shorter time.[59]

To date, the Ti-based metallocene/MAO system is favoured for the majority of the industrial production of *s*-PSs. By contrast, *i*-PSs resins are not currently produced for commercial application. More recently, *i*-PSs, copolymers and blends are being more broadly investigated to identify useful materials with new properties.

Styrene (STY) belongs to a class of monomers known as polar vinyl monomers. Some examples of polar vinyl monomers include methyl acrylate (MA), vinyl acetate (VAc) vinyl halide and acrylonitrile (AN). For the past few years, controlled/living radical polymerizations have been employed by industries to produce these vinyl polymers. Synthesis of copolymers of olefin monomers and vinyl monomers have been an interest to both academic and industrial communities because incorporation of vinyl monomers sometimes allows for the physical properties of the olefin polymers to be greatly improved.[53] Discovery of Brookhart-type catalysts has been the breakthrough in synthesizing these types of copolymers. However, it was found that only Pd-based catalysts function best in synthesizing such copolymers.

1.8 Catalysts with more than one metal center

Many catalysts with late transition metals in controlled/living radical polymerization have been reported. The search for new catalyst systems with late transition metals for improved polymerizations remains an active research area. Due to the increasing number of publications and patents regarding this subject, the design of catalysts with new molecular architectures seems

to be the standard pathway in the search for the next generation catalysts. Bi-metallic catalysts are a recently designed class of catalysts that are still novel in the area of catalyst design. Fig. 12 shows a bimetallic catalyst structure that was able to effect the polymerization of ethylene.[62]

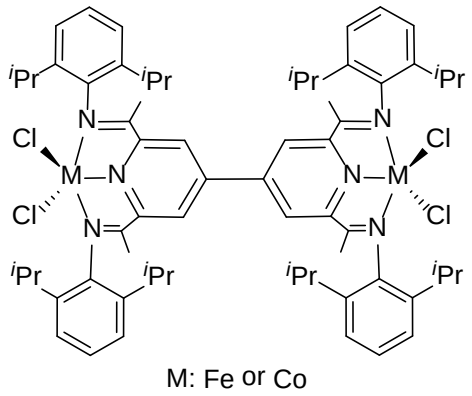

Figure 12: A di-nuclear metal complex. PEs produced by this catalyst have PDIs ranging from 4-10. MAO is required as a co-catalyst.

Very few catalysts with tri-nuclear metal centers have been reported to initiate the polymerization of olefins. One of such catalyst was reported by Hellodorfer *et al.* (Fig. 13(a) : L=κ^2-*N*,*N'*-Ar-N=C(Me)C(Me)=N-Ar; Ar=-C_6H_3-Me-2-Cl-4; X=E=Br). The PEs produced have PDI ranged from 2.7 to 26, highest M_w was 12,240g/mol.[63]

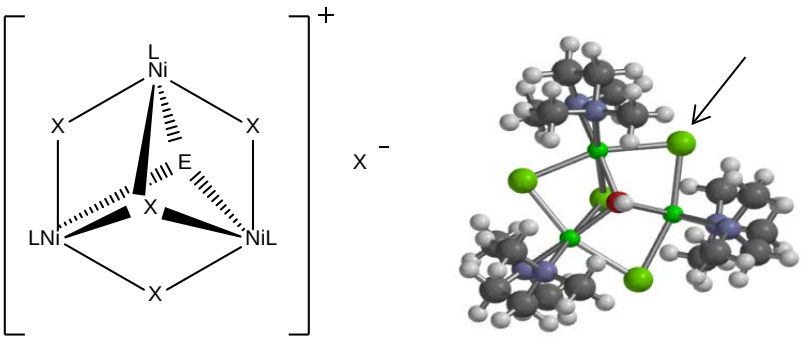

(a) (b)

Figure 13: (a) The general structure of the tri-nuclear Ni catalyst. (b) The pre-catalyst by Gossage *et al.* Small green atom: Ni, larger green atom (arrow): Cl, red atom: O, white atom: H, blue atom: N, black atom: C.

1.9 Project goals

Another tri-nuclear catalyst [complex **1**: μ_3-chloro-tri-μ-chloro-μ_3-hydroxo-tris-*(N,N,N',N'*-tetramethylethylenediamine) trinickel(II) chloride] active in polymerization of STY and methyl methacrylate (MMA) was recently reported by Gossage *et al*.[64] This green coloured Ni-based tri-nuclear catalyst utilizes *N,N,N',N'*-tetramethylethylenediamine (TMEDA) ligands. Each Ni is bridged by a Cl atom, and capped above and below the hexagonal plane with a hydroxyl group and chlorine atom (Fig. 13(a)). Fig. 13(b) is the 3D presentation of the pre-catalyst.

The followings were reported:[64]

1: Polystyrene (PS) and poly(methyl methacrylate) (PMMA) produced by this catalyst exhibit rich *syndio*-tacticity.

2: Polymerization with this Ni catalyst yielded polymers with relatively low PDI values (1.7 or higher) and high molecular weight (up to 2×10^6 g/mol).

3: A stoichiometric amount of MAO is required for polymers to have good PDI value. Increasing

amount of MAO only leads to poorer PDI values. This is different from most late transition metal catalyst in which the required amount of MAO is usually in excess for controlled polymerization.

4: The pre-catalyst itself is air stable and requires no harsh conditions to carry out the polymerization of STY or MMA. The TMEDA ligands incorporated in this tri-nuclear cluster are resistant to both oxidation and nucleophilic attack.

5: The addition of toluene as solvent seems to retard the relative reaction rates (lower yield in polymer weight). This suggests that solvent may compete with the olefins for coordination sites.

6: It was observed that the activated catalysts seem to be unstable in the absence of olefins.

7: According to a DFT optimization, the bridging chlorine atom in the *wide angle* between the TMEDA ligands is energetically favorable to be replaced by the methyl group from MAO.

In general, the reported tri-nuclear Ni-catalyst shows its potential as a promising pre-catalyst for the polymerization of α-olefins.[64] Therefore, the goals of this project are as follows:

1: To examine polymerizations carried out with activated **1** with a variety of different α-olefins.

2: To modify **1** with different ligands in order for better performance in polymerization.

3: To investigate the kinetic aspects of polymerization carried out with activated **1** and to test the hypothesis that this is a coordination-polymerization.

2. Results and Discussion

2.1 Initial observations

The initial stage of this project involved the synthesis of **1** in order to optimize and reproduce **1** in its preferred green coloured crystalline form. Several polymerizations of STY at this stage were also carried out at the same scale and conditions as first reported from our group: room temperature (20-22˚C); ≈ 0.2100g of **1**, 5 mL of toluene, 5 mL of STY, and 0.6 mL of MAO (ratio of complex 1: STY : MAO = 1:150:3). Table A1 in appendix 1 records the all raw data (and the date).[64]

Observations from these synthesis and polymerizations studies are as follows:

1: A single recrystallization solvent (DCM) was used instead of the double layer solvent system (hexane and DCM) reported originally and was sufficient to reproduce the crystalline form of **1** to undergo polymerization of STY. (Table A1, from run PS-2 and onward, all pre-catalyst was obtained from single solvent system).

2: The polymerization system is heterogeneous. Activated catalysts are not soluble in toluene. (Please see pg 79 for further discussion on this)

3: Activated catalysts in toluene (without addition of STY) were placed in a -20˚C fridge under nitrogen atmosphere for seven days. The activated catalyst was then taken from fridge and monomer (STY) was added. As a result, polymers readily formed. This demonstrates that the activity of the activated catalyst can be maintained if stored at low temperature (Appendix 1: Table A1, PS-4 & 4(b)).

4: In the presence of an excess of MAO, the green coloured powdered form of the pre-catalysts transform into large black coloured solids (PS-6 & 7).

5: The most activated catalysts are usually in solid form (heterogeneous).

6: PS recovered from these reactions typically possess PDI values of 1.6-1.7, and $M_w \approx$ 330,000 g/mol.

The relatively low yield of polymers (highest yield was 58% by weight) could be the result of having only a very small amount of the activated catalyst soluble in toluene; and it is these soluble homogeneous fractions that promote polymerization. Therefore, a test was designed to confirm this result.

Prior to addition of STY, pre-catalysts were activated in toluene. A filtration was performed, separating the activated catalysts in their solid forms from the "suspected" activated catalysts present in liquid form (in the filtrate). As a result, two portions were isolated for testing: solids (heterogeneous) and filtrate (homogeneous). Fresh solvent toluene was added to the recovered activated solids and filtrate. STY was then added to both testing portions. It was observed that the activated catalysts in the solid form were able to initiate successful polymerization whereas the filtrate portion produced no polymers. (Table A1, PS 10 & 12) It is the concluded at this point that the **polymerization has to be carried out in a heterogeneous fashion**.

7: It is easy to lose small amounts of polymers during the process of washing.

8: The polymerization carried out by **1** can be performed in the fumehood area instead of in the glovebox.

2.2 Attempts to modify the framework of 1

Because the polymerization carried out by **1** has been confirmed to be a heterogeneous system, several attempts to modify **1** have been carried out to identify a possible more useful homogeneous Ni system. Due to the paramagnetic nature of **1**, all crude products obtained in this section were characterized by infrared (IR) spectrum. Fig. 14 gives the summary for all attempts

that was carried out on **1**.

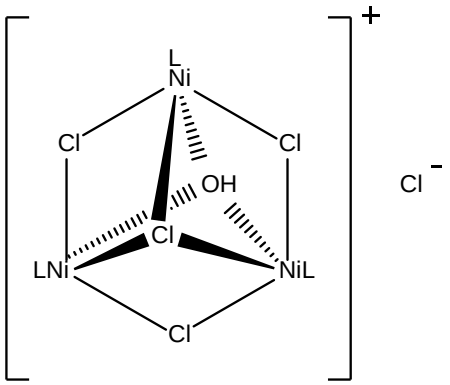

Figure 14: The attempted modifications of **1** included: 1) replace the counter anion Cl^- atom with a nitrate anion; 2) adding a hydrogen to the bridging hydroxyl group; 3) replacing the hydrogen atom of μ_3-hydroxyl group with a protecting group; 4) replace one ligand (L =TMEDA) with *N*,*N*'-bipyridine.

A: Attempts to replace the counter anion Cl with a nitrate group

One method to make **1** more soluble in toluene would be to replace the counter-anion Cl^- atom with a NO_3^-. $AgNO_3$ was used as the nitrate source. The recovered crude light green coloured product displayed different bands from the IR bands of cluster **1**.

Table 1: Synthesis carried out to replace the anion Cl^- with NO_3^- using $AgNO_3$ as nitrate source.

Run	Starting material	Molar ratio of **1**:$AgNO_3$	Solvent	Condition	Result	Solvents for recrystallization
1	Pre-catalyst **1**	1:1.1	DCM	Reflux overnight	Green crystals obtained. No changes*	N/A
2	Pre-catalyst **1**	1:1.1	THF	Reflux overnight	Crude light green powder Changes observed**	Acetone (✗) Methanol (✗) DCM (✓) Acetonitrile (✓)

*: No change: the IR bands displayed no difference between the starting material and the product.

**: Changes observed: there are different IR bands in the spectrum of product and starting material.

Fig. 15 displays the difference of IR bands between the starting material and crude product from Run 2 (Table 1). The different peaks between these two spectrums are listed in Table 2. In general, a compound that includes nitrate(s) as counter anion(s) shows a strong peak at around 1350 to 1380 cm^{-1}.[65] The crude product obtained from run 2 (Table 1) had a IR band at around this area. In addition, there were other IR peaks that were initially found in **1** disappearing from the crude product. It was realized that the crude product obtained might be different from the starting material. The best method to identify the crude product would be to recrystallize the crude product and obtain the crystallography data. The solvents tested for recrystallization were listed in Table 1.

Table 2: IR Peaks of starting material 1 and product from table 1.

Peaks of starting material **1** (cm^{-1})	Peaks of crude product (cm^{-1})
No peak	1505 & 1495(s)*
1468 /1471	1460
No such peak	1384 (s)
1354	No peak
No peak	750

*: S: strong

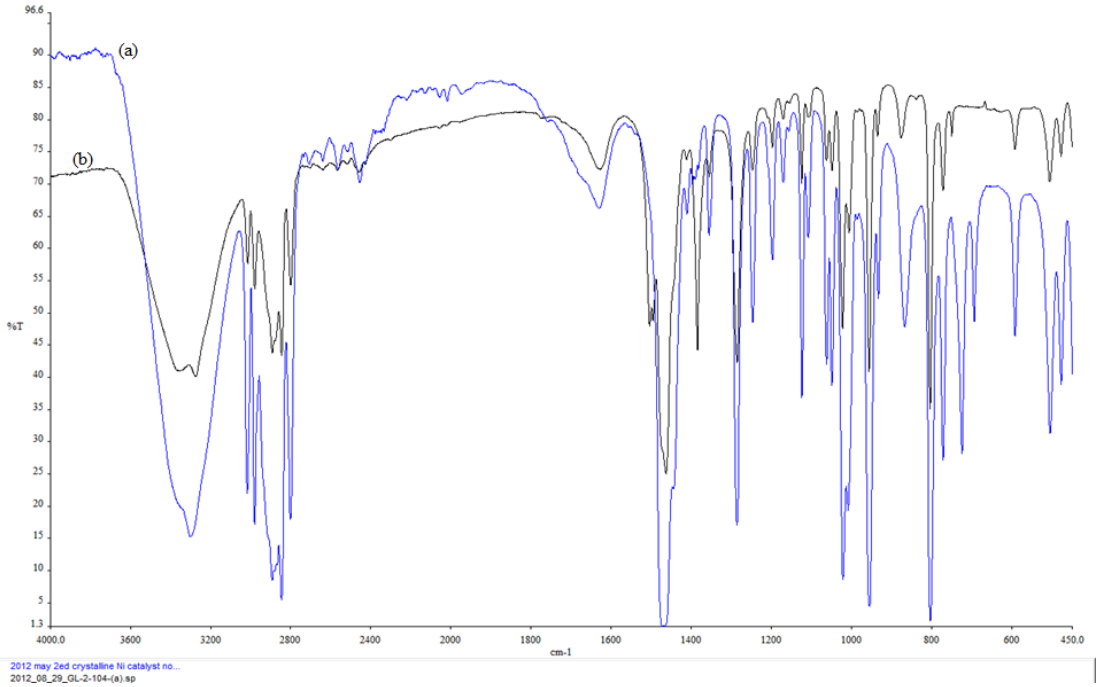

Figure 15: Comparison between the starting material **1** and the crude product from synthesis in run2 (Table 1). (a): Starting material; (b): Crude light green product.

With DCM as the recrystallization solvent (Run 1, Table 1), green coloured crystals were obtained. However, the IR spectrum of these green crystals did not differ from the starting material **1**. With acetonitrile (AcCN) as the recrystallization solvents, blue crystals appeared in in 2-3 days. After a further period of time (6-7 days), green coloured crystals also appeared in the same solution (Fig. 16 (a)). The green coloured crystals from this solvent were confirmed to have the same band positions in IR spectrum as those of complex **1**.

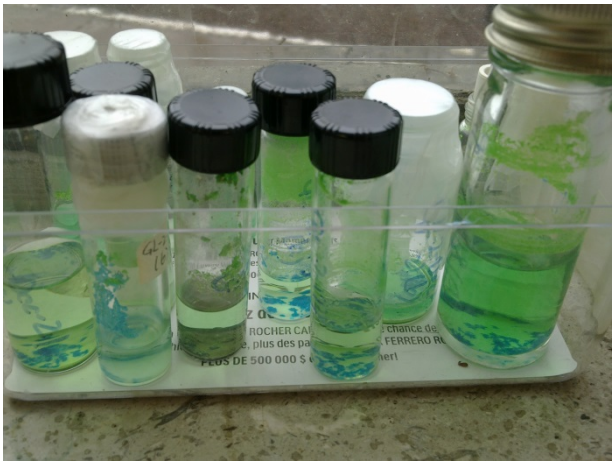

Figure 16: Blue and green crystals appearing in the acetonitrile solvent. Nitrate sources for the three different bottles at the front of picture: (a): $AgNO_3$; (b): $Ni(NO_3)_2 \cdot 6H_2O$; (c): $NaNO_3$.

The blue crystals (**2**) were sent for crystallographic analysis. The blue coloured crystal **2** was identified to be acetonitriletri(aqua)(*N,N,N'N'*-tetramethylethylenediamine) nickel (II) chloride (Fig. 17), an octahedral Ni salt. The cationic part of **2** is formed by the Ni atom coordinated to one TMEDA ligand, one AcCN ligand, and three hydroxyl groups. There is one Cl^- counter-anion. The two bond lengths of Ni to N1 (2.140 Å) and Ni to N2 atoms (2.138 Å) in TMEDA are similar.

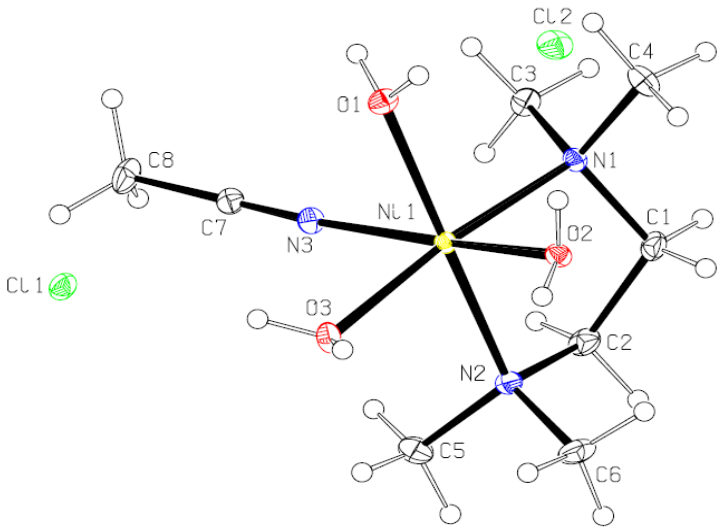

Figure 17: The ORTEP structure of **2**.

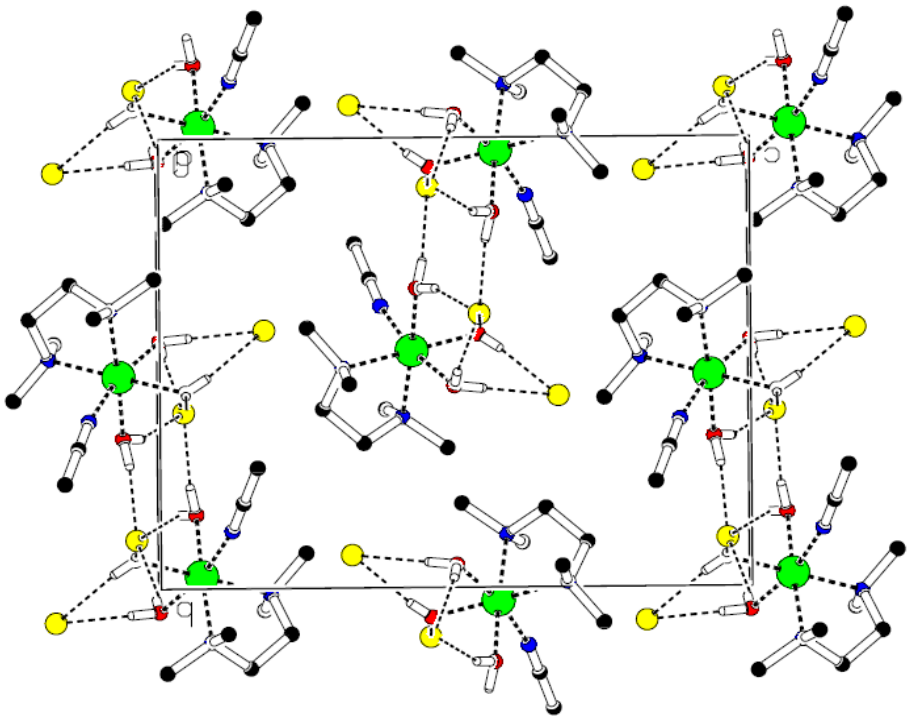

Figure 18: The unit cell diagram of **2.**

The bond angle between N(3)-Ni-O(2) is 168˚, between N(1)-Ni-O(3) is 174˚, and between N(2)-N-O(3) is 177˚. All three angles are less than 180˚, demonstrating slight distortion from a perfectly octahedral structure. The bite angle of the TMEDA ligand in **2** is comparable to the same ligand in complex **1**, which is around 85˚. Fig. 18 shows the unit cell of **2**. All other crystallographic data for **2** are listed in appendix 2.

Using the same method in Table 1 with AcCN as recrystallization solvent, two other nitrate sources, $Ni(NO_3)_2 \cdot 6H_2O$ and $NaNO_3$ were also tested and the IR results shown in Fig. 16 (b) and (c). The IR spectra also showed that the blue complex **2** obtained *via* different nitrate sources have the same IR bands (Fig. 19). One of the significant bands in Fig. 19 is the band at position around 3348 cm^{-1}, which is likely due to the OH stretching. However, compared to most hydrogen-bonded OH stretch bands, this band appeared quite sharp. Typically, -C≡N stretches are centered around 2250 cm^{-1}.[66] With crystal **2**, the typical -C≡N stretches diminishes and is

not observed. Instead, there are two bands at around 2317 and 2287 cm^{-1}.

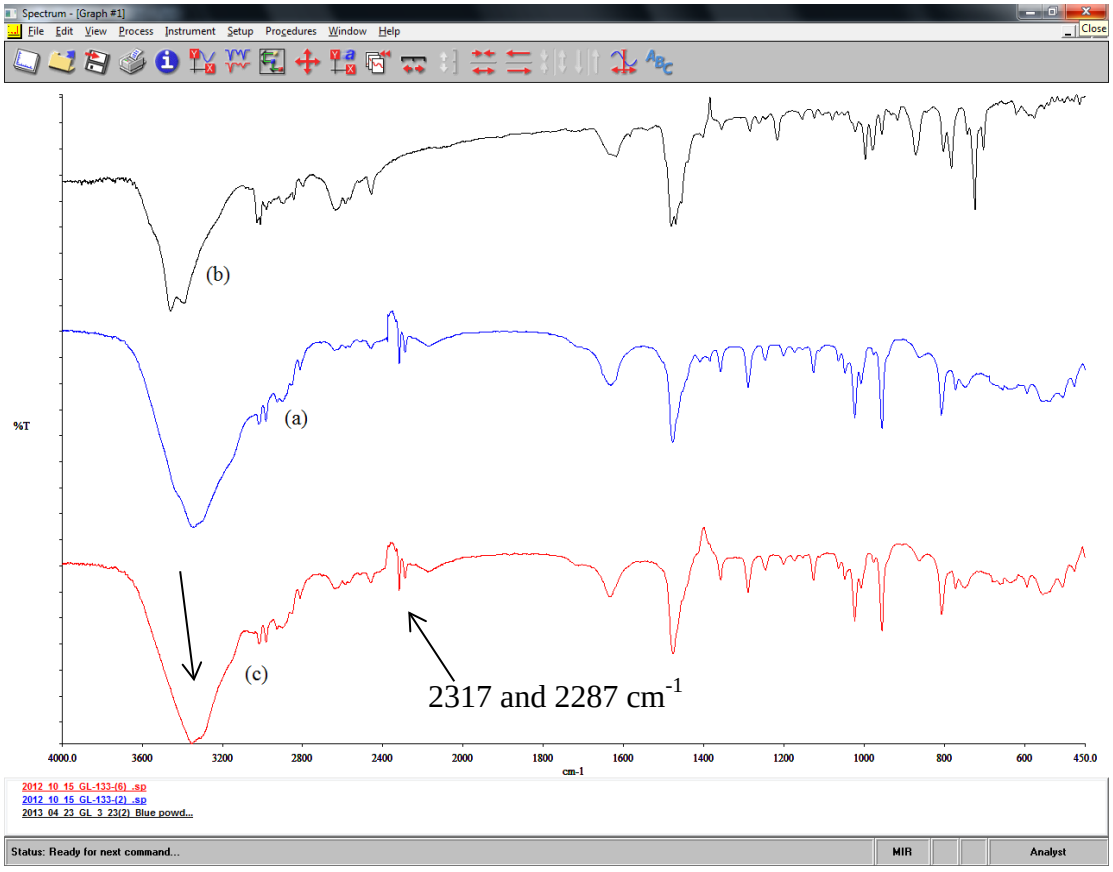

Figure 19: Comparison between blue complex **2** from different nitrate sources. (a): $AgNO_3$; (b): $NaNO_3$; (c): $Ni(NO_3)_2 \cdot 6H_2O$

If Fig. 19 (b) is examined more closely, the bands at 2317 and 2287 cm^{-1} are not apparent in comparison to spectrum (a) and (c). This might due to the fact that the blue crystal used that resulted in 19(b) spectrum was exposed to air for a long period of time prior to analysis. Although the crystal remained blue, the moisture from the air might already affect the crystals.

Based on this finding, it was assumed that in order to produce the Ni **2** complex, it was necessary to treat the Ni **1** complex with a nitrate-containing compound and then recrystallize the product in AcCN. Several attempts were undertaken to see whether there a different route to the Ni **2** complex could be identified.

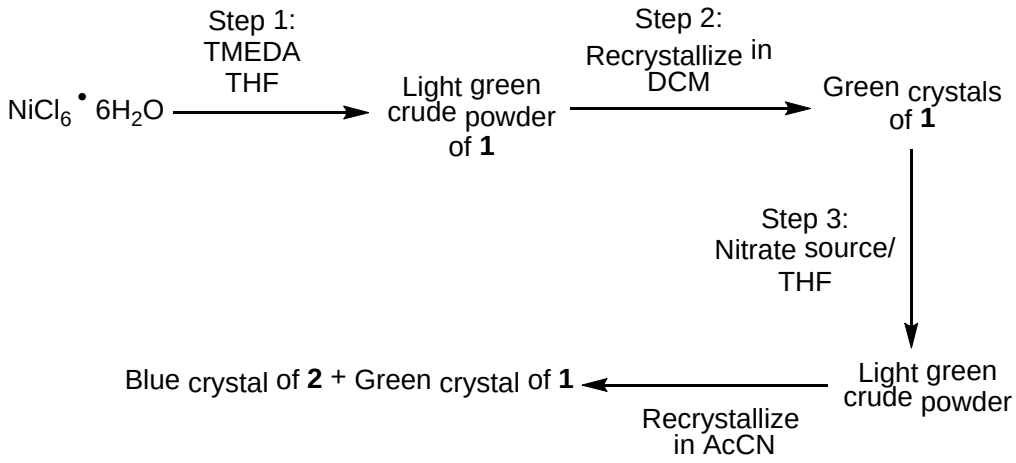

Figure 20: The assumed route to synthesize Ni 2 complex.

The attempts under taken are listed below:

1: Change the reaction solvent to AcCN during the synthesis of Ni **1** complex (step 1, Fig. 20) and do not carry out step 3 and 4.

2: Change the recrystallization solvent to AcCN in step 2 from Fig. 20 and do not carry out step 3 and 4.

3: Change the reaction solvent to AcCN in step 3 from Fig. 20 and recrystallize the crude product in DCM.

All of the attempts taken did not yield the expected blue **2** compound. At this time, the synthetic route from Fig. 20 is the only known method to obtain the blue Ni **2** complex.

The goal of replacing the counter-anion Cl^- with NO_3^- was not achieved. However, considering the size of Cl^- to the NO_3^- anion, the nitrate anion is considerably larger in size. A computational simulation should be done before carrying out the experiment in order to see whether the NO_3^- anion is a suitable anion choice to replace Cl^-. However, based on the IR result, it was certain that the nitrate sources were able to react with the tri-nickel cluster in THF that resulting in a crude products that differ from the starting Ni cluster.

B: Attempt to convert the cationic ion of 1 into a neutral species

An attempt to make the cationic ion of **1** into a neutral species was carried out as follow:

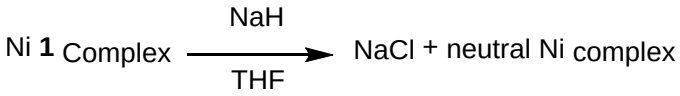

It was anticipated that the sodium ion from the sodium hydride would react with the counter-anion Cl^- in complex **1** to form NaCl as NaH dissolves in THF. This in turn would allow the hydride, acting as a base, to attack the oxygen atom from the hydroxyl group in **1**. This would make the cationic ion of **1** into a neutral species. However, analysis of the crude product after reaction showed that it possessed the same IR bands as the starting material. Hence, the attempt to synthesize a neutral Ni **1** compound in this fashion was unsuccessful.

The reason that THF was chosen as the reaction solvent was because it the choice solvent for the preparation of several Ni based compounds.[67] Ni **1** complex has been reported to be soluble in THF as well.[67] However, the solubility of Ni **1** complex in THF does not seem to be high while testing the solubility of Ni **1** complex in THF. Therefore, this reaction is suggested to be carried out again under the reflux condition to see whether the NAH would react with Ni **1** complex.

Another method to be carry out in order to see if the strong base hydride would attack the hydroxyl group is to change the reaction solvent that only the chloride salt (source of Cl^- is from the counter-anion in the cluster) is insoluble in the reaction solvent.

C: Attempts in modifying the framework of 1

One of the goals of this project was to modify the framework of **1** by changing the ligands. Because the chemistry of the Ni **1** complex was not extensively studied, the choices for reaction solvents were usually DCM (because **1** is soluble in DCM) or THF (**1** is less soluble in THF). Attempts to modify the ligands of **1** included two parts: replacement of the H with a protecting

group with the expectation that complex **1** would be more soluble in toluene; and replacement of a TMEDA ligand with a *N,N'*-bipyridine (Bpy) ligand to enhance the polymerization rate.

Table 3: Attempts to modify the framework of **1**.

Attempts carried out to replace the H atom on the hydroxyl group				
Trials	Protecting group (PG)	Solvent	Molar ratio of 1/ (PG)	Results[(b)] (or noticeable observation)
1	Benzyl bromide	THF	1:5.5	No result*
2	Benzyl bromide	DCM	1:1.9	No result
3	Chlorotrimethyl silane	DCM	1:1	Reaction solution was dark bluish-green, No result
Attempts carried out to replace one ligand with one Bpy ligand				
Trials	Starting material	Solvent	Molar ratio of starting materials	Results (or noticeable observation)
B1	**1**, Bpy	DCM	1/Bpy =1:1	No result
B2[(a)]	$NiCl_2 \cdot 6\ H_2O$; TMEDA & BPY	THF	Ni/TMEDA/BPY Is 1: 7.2: 3.6	Red colour appeared on filtration paper after filtration. Crude green powder turned to grey in two hours. Crude green powder dissolved in ethanol yielded a solid that contains both bluish-green and red colour. Over a period of time, colour was grey outside and red inside Cannot find suitable solvents for recrystallization (does not dissolve in DCM)
B3	**1**, Bpy	THF	1/Bpy = 1:1	Crude powder displayed different band in IR spectrum

(a): IR spectrum was not obtained.

(b): Unless stated otherwise, the colour of reaction solution was green.

*: No result means the IR bands of the crude powder are not different from the starting material **1.**

Although all attempts in modifying **1** were unsuccessful, it was noticed that as **1** was treated with chlorotrimethyl silane in DCM, a dark bluish-green colour appeared. This might suggest that a ligand(s) other than the original ligands (TMEDA, Cl, and hydroxyl group) are now coordinating to the Ni atom. Furthermore, it might indicate the presence of an intermediate in solution. Therefore, even though there appears to be a reaction of components in the DCM solution, analysis of the recovered crude powder indicates that it was still the starting material. This maybe a result of **1** being more energetically favourable in its own recrystallization solvent compared to the unknown end product detected in this reaction.

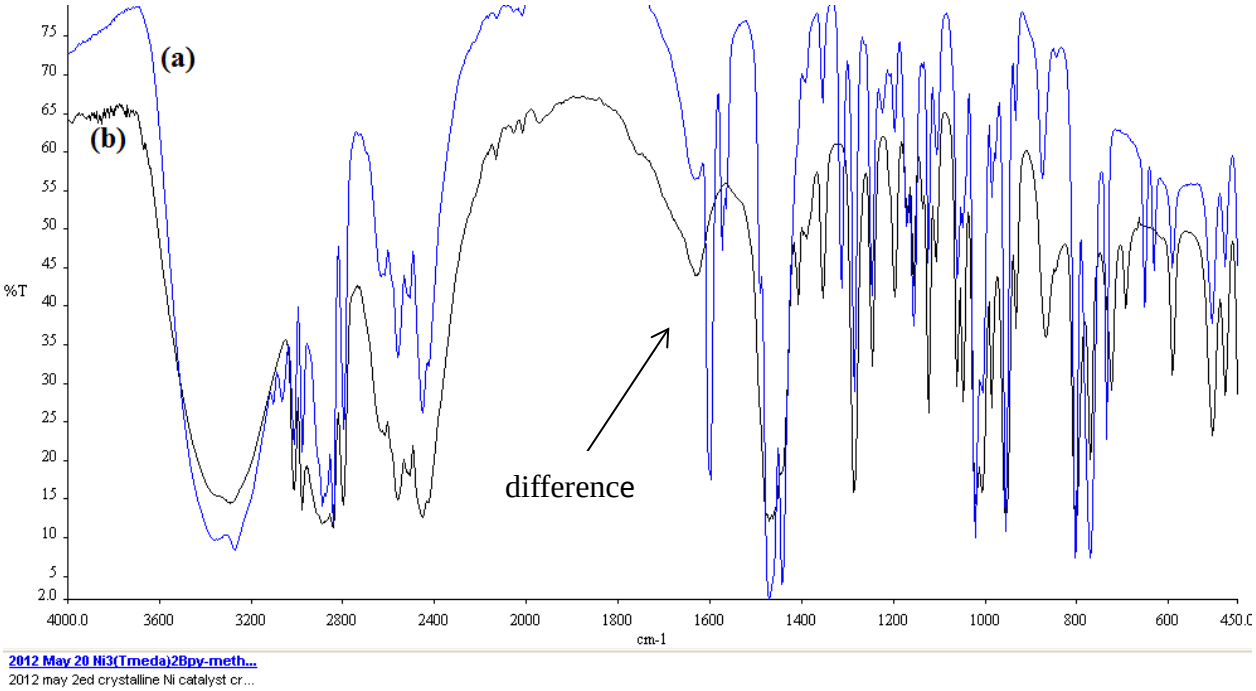

Figure 21: Comparison between crude product from trials B3 (Table 1) and complex **1**. (a): product from Run B3 in Table 1; (b): complex **1**.

Reactions of **1** with Bpy in DCM yielded crude green coloured powders that possess essentially the same IR bands as the starting material of **1**, indicating that no ligand exchange occurred. One method of obtaining crystals of $Ni(Bpy)_2Cl_2$ solvated with methanol (MeOH) was to simply react Bpy with $NiCl_2 \cdot 6H_2O$ in MeOH and have the solvent amount reduced after

reaction over a period of time.[68] Because **1** is soluble in MeOH, a reaction of **1** and Bpy in MeOH should be carried out in future attempts. Reaction of **1** with Bpy in THF (Run B3, Table 1) yielded crude green coloured solids that have different band position relative to the original starting material **1** (Fig. 21). To determine the identity of this compound, it would be best to find a suitable solvent for recrystallization of this crude product.

Replacing one portion of TMEDA with Bpy in the synthesis of **1** (Run B2, Table 3) yielded a product that contained two different colours (see Run B2, Table 3 for observation report). The competition between the formation of **1** and $Ni(Bpy)_2Cl_2$ was expected, but this resulted in neither of these two compounds forming by the end of this reaction. Instead, a blue-green coloured solid was obtained after filtering the reaction solvent. This blue-green coloured solid slowly changed to a grey white coloured solid within 2 hours as it was exposed to the air for further solvent drying. This suggests that the bluish-green coloured compound was unstable and may have undergone decomposition. Additionally, the grey colour appears only on the outside of the solids whereas the interior part of the solids remained red. Tetrahedral or square-planar Ni complexes are often red or orange. The IR spectrum of this dual coloured paramagnetic solid was not performed because the identity of the ligands contained in this compound were unknown (see B2, Table 1).

2.3 Polymerization of monomers

One of the objectives of this investigation was to test the ability of **1** in its activated form to carry out the polymerization of a variety of α-olefins. The α-olefins in Fig. 22 have all been tested for polymerization carried out by **1** activated by MAO, and the results are listed in Table 4.

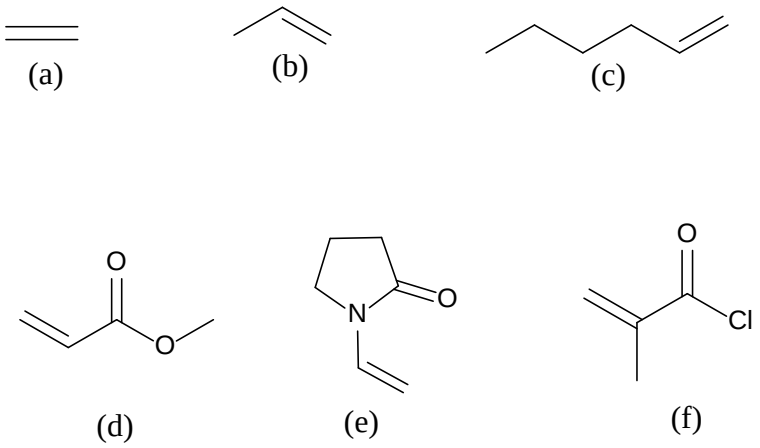

Figure 22: All olefins and α-olefins tested with cluster **1** system for polymerization: (a): Ethylene; (b): Propylene; (c) 1-hexene; (d) Methyl acrylate; (e) 1-vinyl-2-pyrrolidinone; (f) Methacryloyl chloride

Table 4: Polymerization of various olefins carried out by **1**.

Run[(a)]	Monomer/solvent	[Monomer] in solution (mL) % (v/v);	Time*	Result
1	Ethylene/isopar	N.D.	6 hours**	No polymers formed
2	Propylene/isopar	N.D.	6 hours**	No polymer
3	1-Hexene/neat	100% in 5.0 mL	14 days	No polymer
4	1-Hexene/toluene	50% in 10 mL	14 days	No polymer
5	Methyl acrylate/ toluene	45% in 9.0 mL	11 days	Hard, opaque polymers
6	STY/MA/toluene	25% of STY & 25% of MA In 20 mL solution	14 days	White, brittle solids formed
7	Methacryloyl chloride/ toluene	28% in 21 mL	3 days	White soft solids formed
8	1-vinyl-2-pyrrolidinone/ toluene	50 % in 20 mL	14 days	No polymer

(a): General conditions used unless otherwise stated: cluster **1**/MAO = 1:3; cat **1**: 0.2100 g

*: Rxn at R.T.

**: Rxn: at 70°C

A: Polymerization of methyl acrylate

The activated catalyst of **1** was ineffective for the polymerization of simple α-olefins such as ethylene, propylene and 1-hexane in contrast to its activity with STY and MMA (Table 4). Methyl acrylate (MA) is a polar vinyl monomer and is most often polymerized through controlled radical polymerization.[69] Pd-based Brookhart-type catalyst have enabled the production of random copolymer of ethylene and MA with reduced rate compared to that of ethylene polymerization.[53] One of the main reasons for this lower rate was that the oxygen atom in MA monomer favours coordination to the electrophilic Pd(II) center, forming a chelate complex at resting state. This complex in its resting state retards the polymerization rate. Therefore, it is not surprising that homo-polymerization of MA carried out by Pd-based Brookhart system was not reported.[23,53]

Polymerization of MA carried out by **1** activated by MAO was tested. The yield was small (13% by weight), and the recovered product was a hard opaque solid. By contrast, homo-poly(methyl acrylate) prepared by other routes is reported to be a soft material that readily dissolves in THF. The recovered product was very difficult to process with limited or no solubility in common solvents (THF, acetone, MeOH, toluene, chloroform). Therefore, the structure and identity of the product of the MA polymerization was not confirmed. A differential scanning calorimetry (DSC) could have been done to test the T_g of the material. If the material does include a T_g value, it is likely this material is a polymer and the T_g value can be used to identity whether this material is a polymer of MA. However, due to the difficulty in processing the material and in making the material into small pieces so a desirable amount can be measured for DSC testing, the DSC testing was not performed. The only spectroscopic data for this product was its IR spectrum (Fig. 23) by making the material into a neat disc. According to published reports, the band at 1733 cm^{-1} (due to C=O stretching) is the strongest band in the IR spectrum

for poly(methyl acrylate) (PMA).[70] Though the band at this position in Fig. 23 is weak, the crude product from run 6 (Table 4) displayed a C=O stretching at 1733 cm^{-1}, indicating the presence of a C=O functional group. Based on the fact that the material does not dissolve in most of the solvents, it is possible that this material is simply a highly cross-linked polymer. If this opaque, hard solid is indeed a polymer of MA, it would mean that the pre-catalyst **1** could carry out a co-polymerization of STY and MA.

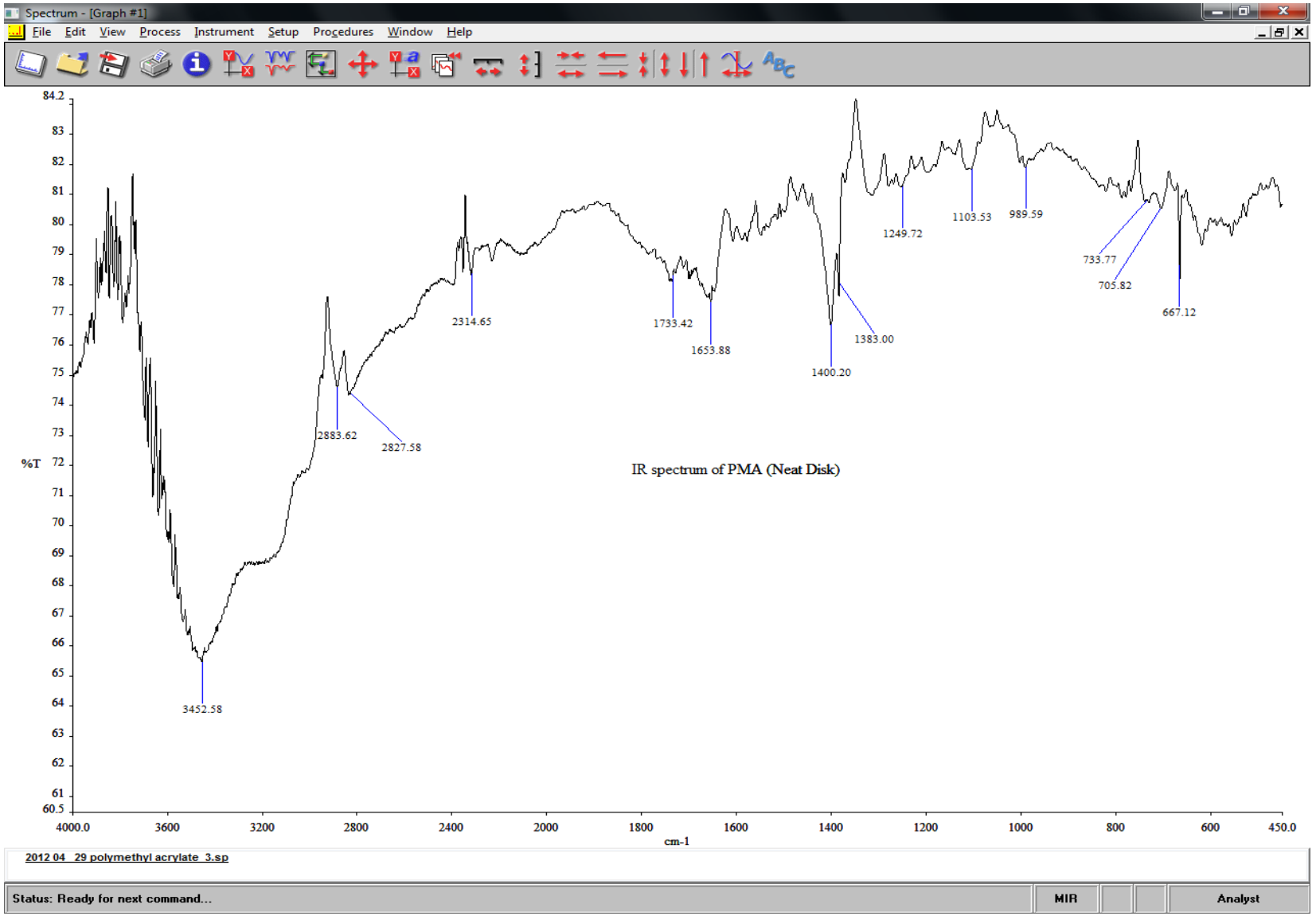

Figure 23: IR spectrum of hard, opaque from polymerization of MA.

B: Co-polymerization of styrene and methyl acrylate

White solids were recovered after carrying out the co-polymerization of STY and MA in the presence of activated **1**. ^{1}H and ^{13}C NMR spectra were obtained for this material (Fig. 24 and 25). ^{13}C NMR spectroscopy was used to determine the identity of the white solids. If the white solid was just a PS that contained no MA units, the carbon peaks belonging to MA would be absent in the spectrum. The ^{13}C NMR spectrum of the synthesized co-polymer was compared with published reports on random co-polymers of STY and MA.[71,72] It was confirmed that the white solid is a random co-polymer of STY and MA. The broad peaks appearing in the ^{1}H NMR spectrum indicates an atactic nature in the co-polymer of STY and MA. GPC results showed that the co-polymer has a PDI value of ≈ 1.63 and M_w≈130,000 g/mol. The single peak observed in the GPC result also ruled out the possibility that the material obtained from this experiment is a blend of STY and MA. For if a blend of STY and MA was obtained instead of a copolymer from this experiment, then two peaks would arise from GPC result because two polymers with different properties are detected from the GPC. And the observation of single peak showing from the GPC result indicates the material is a copolymer, not a blend. DSC test can be carried out in the future if more evidence is required to rule out that this material is a blend. If only one T_g value is observed from DSC analysis, then the material is a copolymer. If two T_g values are observed from DSC result, then this material is a polymer blend.

Compared to the M_w of PS produced by the same system, the rate of polymerization was greatly retarded with MA present in the system. Because activated **1** was able to polymerize STY and MA into a random copolymer, it could be concluded that the hard, opaque solid obtained in section 2.3.A was indeed a polymer of MA. As a result, activated **1** was able to carry out polymerization of MA but with a very limited activity.

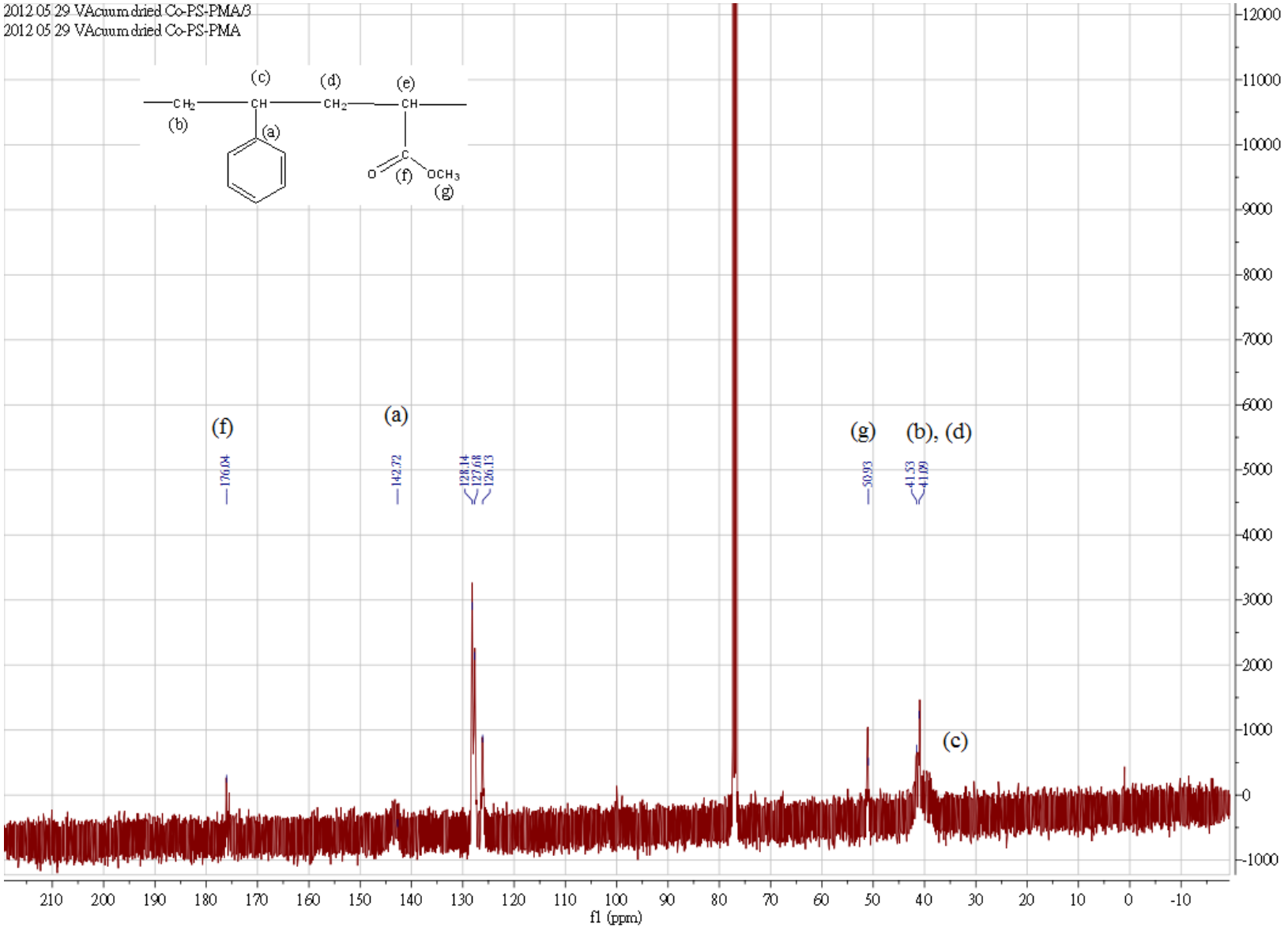

Figure 24: ^{13}C NMR ($CDCl_3$) of white solids from polymerization of STY and MA.

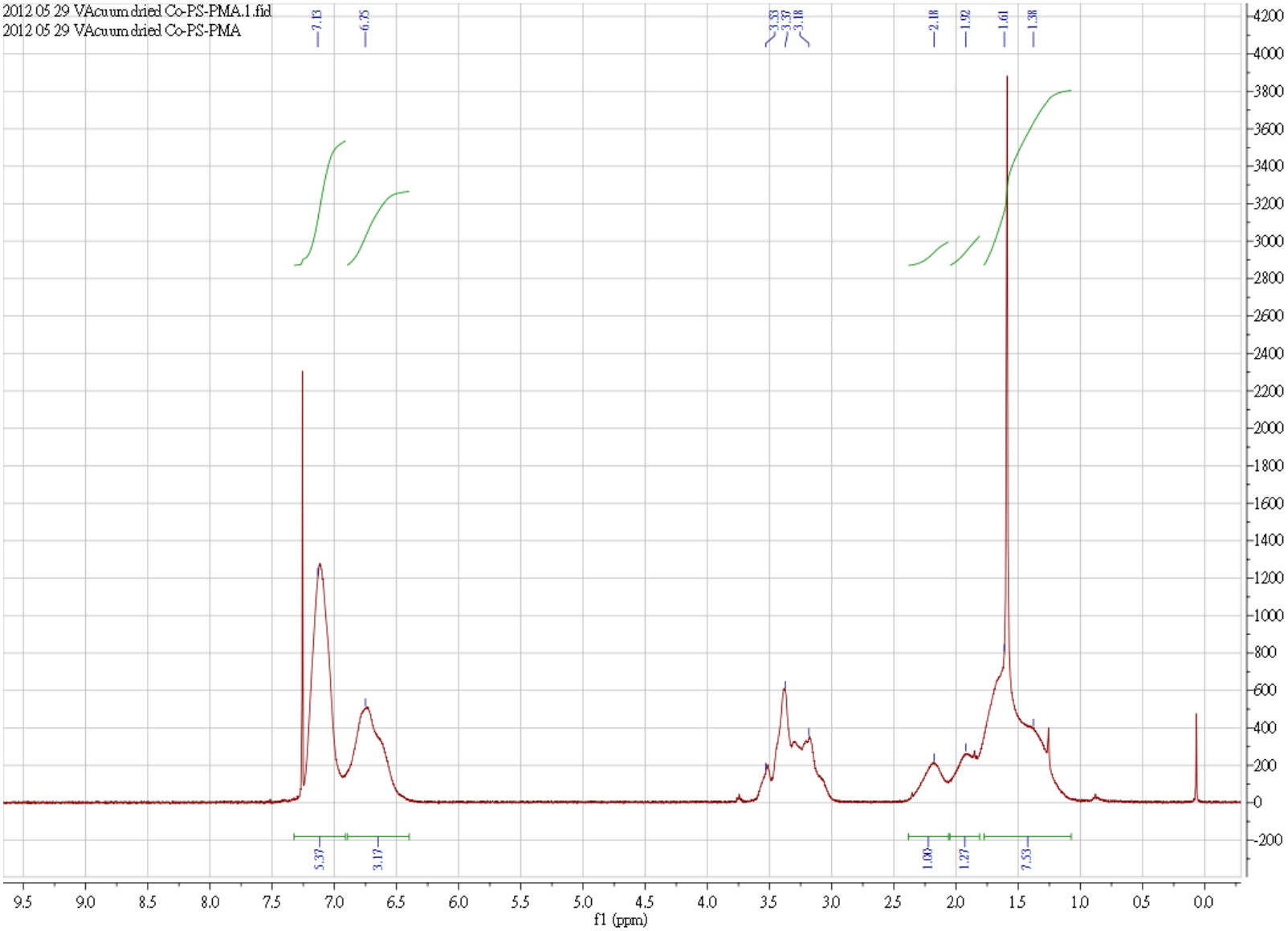

Figure 25: ^{1}H NMR ($CDCl_3$) of white solids from polymerization of STY and MA.

C: Polymerization of methylacryloyl chloride

Polymerization of monomers with other functional groups was also tested with activated **1.** There was no polymer obtained from the polymerization of 1-vinyl-2-pyrrolidinone carried out with activated **1**.

Polymerization of methylacryloyl chloride was also carried out with activated **1**. Upon the addition of MAO, the colour of the solution remained green. However, over a period of three days, the colour of the mixture turned to blue colour and a gel-like product started to appear in the flask. The green to blue colour change might be a result of the Ni atom in activated catalyst **1** experiencing a structural change of the Ni-coordinated ligand framework. Upon the addition of *n*-butylamine, the colour of the mixture changed back to a green colour and the gel-like product dissolved readily in the presence of *n*-butylamine. The recovered product after washing with hexanes was a soft, white coloured solid. Unfortunately, GPC did not detect the presence of any polymer. It was questionable that the material was a polymer of poly(methacryloyl amide). Fig. 26 is the ^{1}H NMR spectra of the obtained product. The expected peak for methylene proton at around 2.0 to 2.2 ppm was not observed. It might be possible this material is a polymer (or oligomer) that is different from the expected poly(methacryloyl amide). MAO is known to extract a halogen and methylated the metal center in a polymerization. Therefore, one concern in considering the identity of this material is that the Cl atom from the acid chloride group of methacryloyl chloride is also a likely to react with MAO, forming a different species that impacts the polymerization. A reaction of methacryloyl chloride with MAO should have been tested to see whether MAO reacts with the monomer, but due to time constraints this was not undertaken.

An IR spectroscopy was performed in order to further determine the identity of this material. The anticipated –C=O stretching band at 1680-1630 cm^{-1} for amide group was not observed. The N-H stretching at around 3400-3180 cm^{-1} is not present in the spectrum as well. Although the

identity of the material remains unanswered, it was realized later that a DSC analysis could be carried out to identify whether this material is an oligomer or a simple organic compound. If a T_g value exist, then the material is possibly an oligomer, Then the test of reacting MAO with the monomer should then be carried out to see if the monomer reacts with MAO to form oligomer.

In conclusion, activated **1** was able to polymerize few polar vinyl monomers into a polymer. All the attempts of carrying out polymerization by activated **1** with simple olefins were not successful. In the case of the unsuccessful polymerization of 1-vinyl-2-pyrrolidinone with activated **1**, it is possible that the oxygen atom on the monomer coordinates to the empty coordination site of Ni atom in the active catalyst, and thus deactivates this monomer towards polymerization.

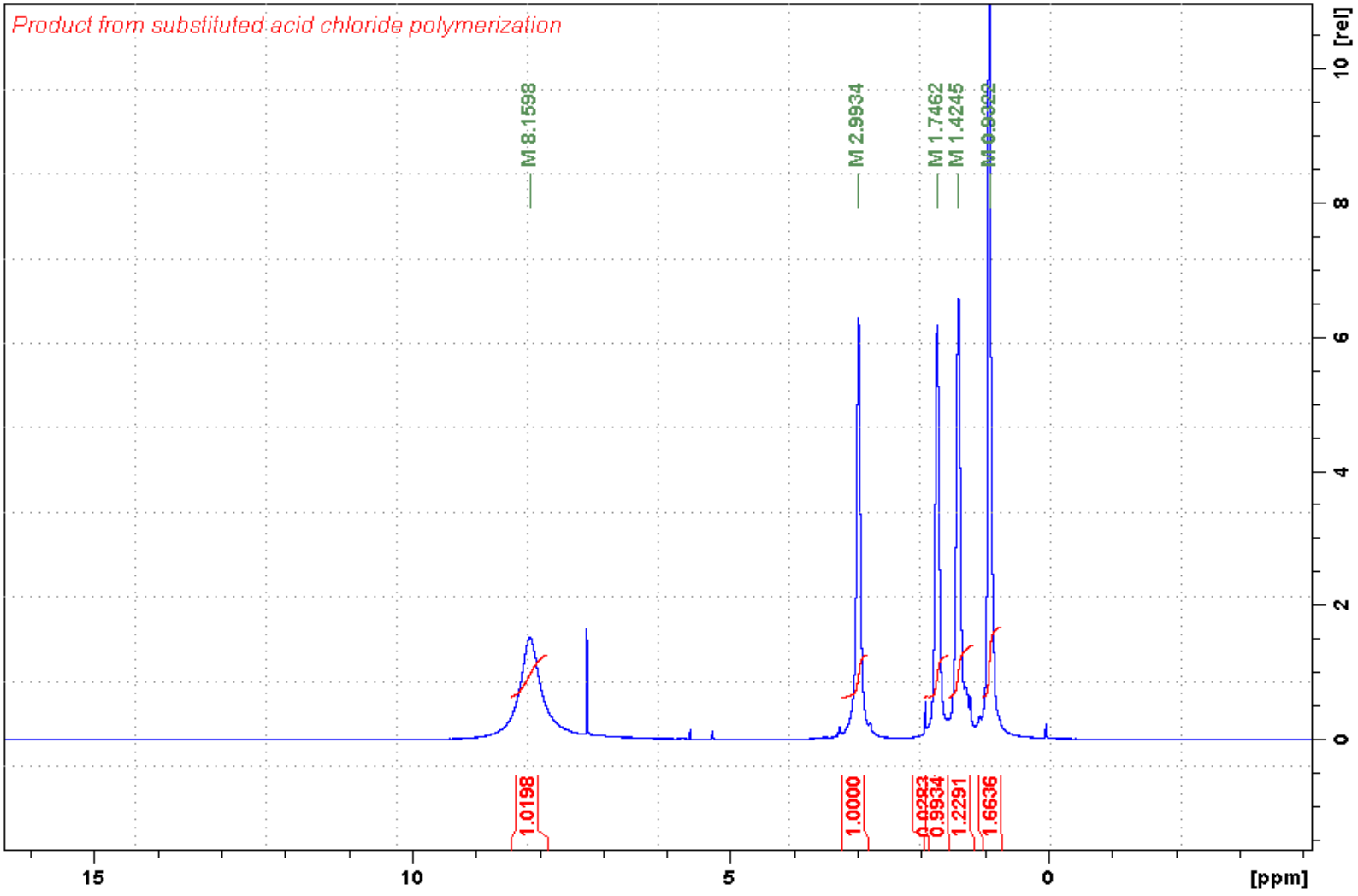

Figure 26: ^{1}H NMR ($CDCl_3$) of the product obtained after polymerization of methacryloyl chloride.

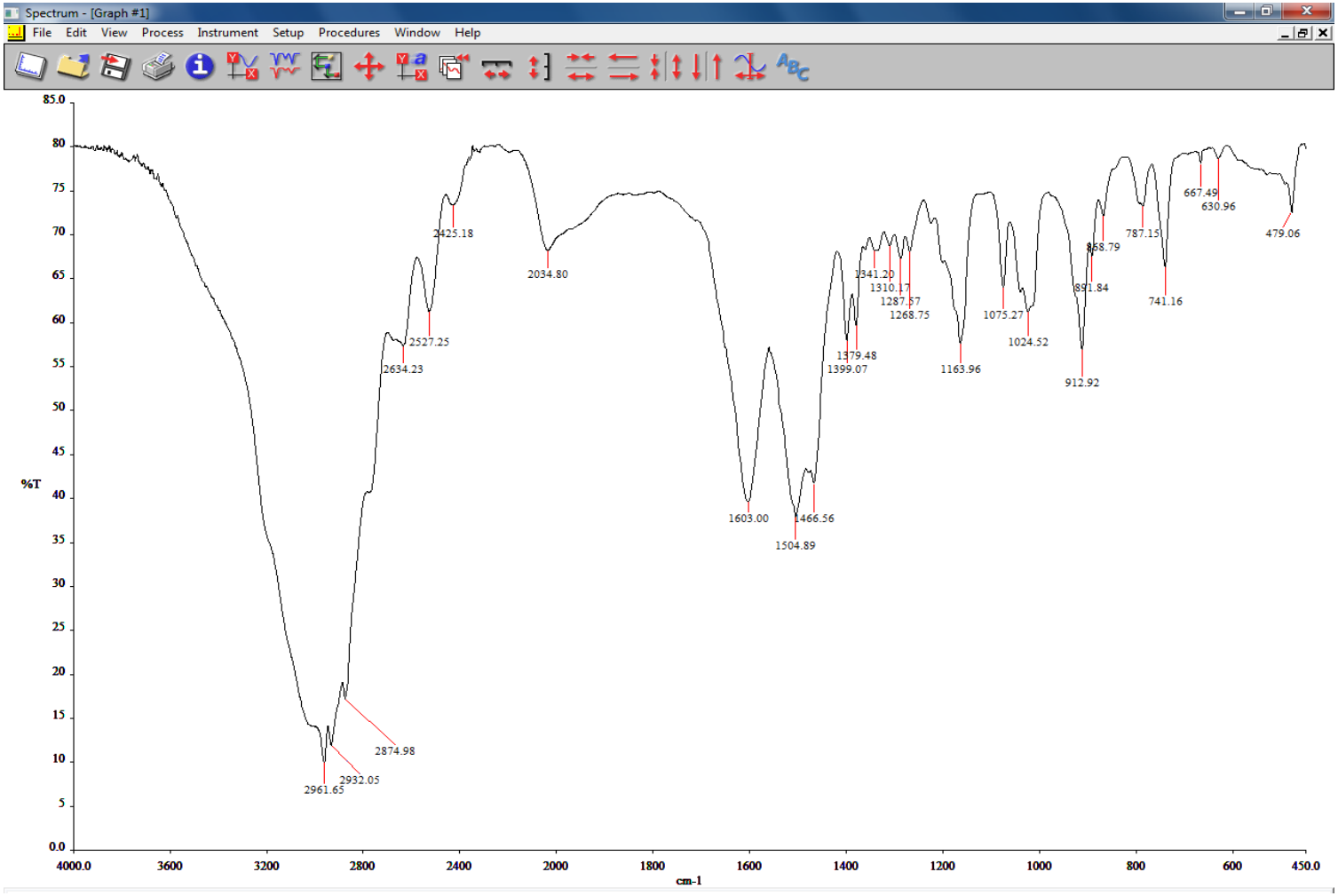

Figure 27: IR spectrum of material obtained from polymerization of methacryloyl chloride.

2.4 Investigation into kinetics of polymerization carried out by pre-catalyst 1

Because the tri-nuclear cluster **1** was reported to be able to carry out polymerization of STY and MMA upon activation by MAO, kinetic studies have been carried out for a better understanding on how the system works. Throughout the project, STY has been tested more often than MMA.

A: Method development

A suitable method is required to investigate the polymerization. Three methods have been considered.

1: **Gas Chromatography (GC) method:** Aliquots are to be taken from the polymerization solution over a period of time. Place the aliquot under high vacuum and collect the liquid portion. By comparing the GC peaks of the aliquot to an internal standard with known concentration, the concentration of unreacted styrene in the collected liquid can be determined.

2: **IR method:** Take aliquots from the polymerization reaction at intervals of time. The aliquot is then to be injected into a sealed liquid cell that has its volume fixed. By measuring the peak area from the C=C stretching band, concentration of styrene been consumed can be determined.

3: **Weight analysis:** Because it is easy to lose small portions of polymer during the washing cycle, the approach of taking an aliquot at each intervals of time and precipitated polymer out in MeOH was not recommended. Instead, the obtained aliquots were placed under high vacuum. Under a high vacuum, unreacted styrene and toluene would be removed from the receiving flask. Hence, only the polymer is left in the flask if the polymerization. The difference of the flask

weight before and after the vacuum is then the weight of yielded polymer.

Each method has its own advantage and disadvantage. While the GC and IR method requires only very small amount of aliquot (less than 1mL), handling the liquid cell or collecting the liquid portion of the aliquot all indicate the requirement of extra steps comparing to the weight analysis method. Therefore, weight determination was applied throughout the kinetic studies.

Table 5 lists the trials carried out for kinetic analysis. For simplicity, the abbreviation as (R5, T5) or (Run 5, T5) was used to indicate 5^{th} trial from Table 5 in the following discussion. In this section, the pre-catalyst would be indicated by **1** (the number assigned to this compound) whereas the activated form of **1** would be indicated by **1/MAO**. MAO was always added last to the temperature-equilibrated solution, and the result of polymer conversion from each aliquot of each trial recorded in Appendix 4.

Table 5: Polymerization trials carried out by **1/MAO** for kinetic studies. Unless otherwise indicated, all monomers used are styrene.

Run	Pre-catalyst (g)	Styrene (v/v %)	Total solution (mL)	Temp. (°C)	Molar Ratio of Pre-cat to MAO	Notable observation or record
1	0.2109	10	20.0	R.T	1 : 4.62	1: reaction duration: 8 days Difficult to sample
2	0.2107	50	20.0	R.T.	1 : 4.12	An 8 day reaction
3	0.2096	10	20.0	R.T.	1 : 4.13	An 8 day reaction; No aliquot sampling
4	0.2095	50	10.0	R.T	1 : 4.12	A 14 days reaction
5	0.2108	50	100.0	R.T.	1 : 5.10	A 14 days reaction Colour of solution turned into brownish red upon activated by MAO, colour gradually turned into yellowish green within 3 days, on the 4th day, colour turned into green M_w ~292,330 ; PDI: 3.53 ^{1}H NMR available
6	0.2103	20	100.0	R.T.	1 : 5.10	Colour changed from light green to yellowish green upon activation by MAO
7	0.2110	50	100.0	R.T.	1 : 5.14	Solution colour: Red brown upon activation by MAO Colour fades to light brown, then yellowish green, then green within 4 days
8	0.2095	50	100.0	70	1 : 4.14	Solution turned into red upon activation by MAO
9	1.0650	50	100.0	70	0	Blank; a 5 days trial

Run	Pre-catalyst (g)	Styrene (v/v %)	Total solution (mL)	Temp. (°C)	Molar Ratio of Pre-cat to MAO	Notable observation or record
10	0.2096	50	50	70	0	Blank; a 3 day trial
11	1.0505	50	100.0	70	1 : 3.3	Solution gradually turned into very viscous solution On 4th day, no more aliquot could sampled as solution was too viscous
12	1.0523	50	100.0	70	1 : 3.0	
13	0.2100	50	100.0	70	1 : 3.1	Colour solution: red upon activation of MAO After polymerization was run for few days, polymerization was no longer monitored and therefore was not placed at high temperature any more. As the solution cooled down, red colour slowly fades and turned into yellowish-green colour.
14	1.0573	50	100.0	70	1 : 2.97	
15	1.0549	50	100.0	70	1 : 2.98	
16	1.0519	50	100.0	R.T.	1 : 2.98	
17	1.0529	50	100.0	R.T.	1 : 2.98	
18	1.0516	50	100.0	70	1 : 2.98	PDI = 1.60
19	1.0516	50	100.0	70	1 : 2.98	PDI = 1.59 Colour slowly turned into brownish as polymerization progress

Run	Pre-catalyst (g)	Styrene (v/v %)	Total solution (mL)	Temp. (°C)	Molar Ratio of Pre-cat to MAO	Notable observation or record
20	1.0520	50	100.0	R.T.	1: 2.98	
21	1.0525	50	100.0	R.T.	1: 2.98	Monomer: MMA
22	1.0536	50	100.0	90	0	Blank
23	1.0506	0	100	90	0	Aborted Rxn; realized added toluene instead of monomer
24	1.0543	50	100.0	90	0	Blank
25	1.0522	50	100.0	90	1 : 2.99	
26	1.0551	50	100.0	90	1 : 3.08	
27	1.0564	50	100.0	90	1 : 3.08	
28	1.0538	25	100.0	90	1 : 3.09	
29	1.0527	50	100.0	90	1 : 2.99	24 hour monitor Solution originally was green Between 3^{rd} to 4^{th} hour, orange colour started to appear in the solution Upon 5^{th} hour, solution already turned into orange At 12^{th} hour, solution became viscous
30	1.0547	75	100.0	90	1 : 3.08	
31	1.0531	25	100.0	25.5	1 : 3.08	Monomer: MMA
32	1.0527	50	100.0	90	0	Blank of MMA

B: General aspects in regards to the calculations

Conversion is calculated as shown below:

Weight of polymer in sampled aliquot =

Weight of flask containing vacuum dried polymer-empty flask weight

$$Polymer\ formed\ weight\ in\ solution = \frac{W.t.of\ polymer\ in\ the\ aliquot}{sampled\ volume} \times total\ volume\ of\ solution\ during\ sampling$$

Polymer formed in the solution = Styrene consumed in the solution

$$\text{Conversion (\%)} = \frac{\text{Consumed monomer at time } t}{\text{Initial monomer concentration}} \times 100\%$$

$$\text{Conversion (\%)} = \frac{\text{Consumed Styrene concentration at time t}}{\text{Initial styrene concentration}}$$

Because it has been confirmed that the polymerization of STY by **1/MAO** is heterogeneous, it was important to make the powder of **1** into very fine particles prior to activation with MAO so that the overall surface area would be maximized. As the polymerization is heterogeneous, then after vacuuming the aliquot, all the remaining material in the flask would be polymer and catalyst **1/MAO** only. Therefore, a little modification was required.

Weight of polymer in sampled aliquot =

W.t of flask containing vacuum dried polymer-empty flask weight-(0.0085g × $V_{aliquot}$)

0.0085g/mL is the average weight of catalyst in 1 mL of the solution. This value can be obtained from (R22,T5) (R24, T5) and (R32, T5).

C: The distribution of catalyst in the polymerization system

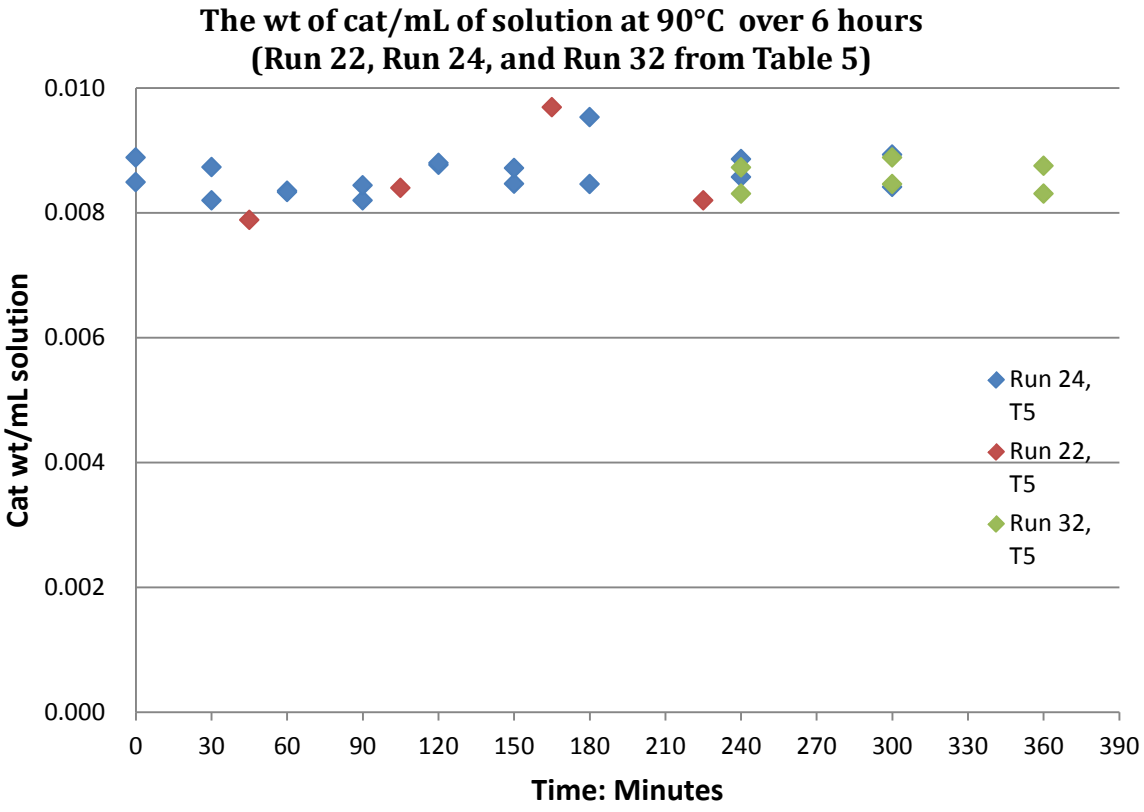

Figure 28: Weight of pre-catalyst **1** distributed in the solution over a period of time at 90˚C. Run 32 displayed how **1** was distributed over time at 90˚ C in the MMA/toluene solution.

In Run 22, Run 24, and Run 32, the toluene solution containing pre-catalyst **1,** monomer STY was placed in a 90˚C oil bath over a period of time for solution to reach 90 ˚C. Aliquots were then taken over a fixed period of time for each trial. If the solid particle of **1** is evenly distributed in the solution, then every time an aliquot is sampled, the amount of the solid/mL should be almost the same. Therefore, in Run 22, Run 24 and Run 32, the obtained pre-catalyst **1** was weighed. The weight distribution of **1** in each mL of solution is between 0.0080 to 0.0100g. (Fig. 28) This showed that **1** was likely to be distributed evenly in the solution. Run 32 used MMA as monomer instead of STY. The similar results of Run 32 in comparison to results obtained from Run 22 and 24 indicated the pre-catalyst is fairly distributed evenly in the

solution regardless of the monomer choice (STY and MMA in this case). One additional piece of information that can be deduced from these results is that the pre-catalysts under these conditions do not react with monomer (STY or MMA) or the toluene because a decrease in weight distribution of pre-catalyst over a period of time at high temperature was not observed.

With these three tests, one additional action was performed to test for the presence of polymer. Each vacuum-dried aliquot was added to THF and MeOH consecutively to see whether there was evidence of polymer formation from self-polymerization. In all instances, there was no white material precipitated out after such action. All vacuum-dried remains in the receiving flask dissolve into a clear liquid upon addition of MeOH. In the case of STY, self-polymerization of the monomer does not occur within 6 hours at 90˚C.

D: Kinetic studies

D.1: Initial findings: Homogeneous vs Heterogeneous system

During the initial kinetic studies, a 10% solution of STY was used for testing. However, it was realized that the 10% solution might not be the ideal solution concentration because it produced only a very small amount of PS after long period of time and it was difficult to obtain reasonable amount of polymer from each aliquot for analysis (R1, T5; R3, T5). As a result, 50% (v/v) STY concentration was used for all kinetic polymerization studies.

The polymerization of STY by **1/MAO** at room temperature was quite slow. In addition, improvement in experimental design was required to get a smoother analysis at this temperature. However, a trend is already observable (Fig. 29) where the polymerization is faster when the concentration of styrene is increased by comparing Run 1 and Run 2.

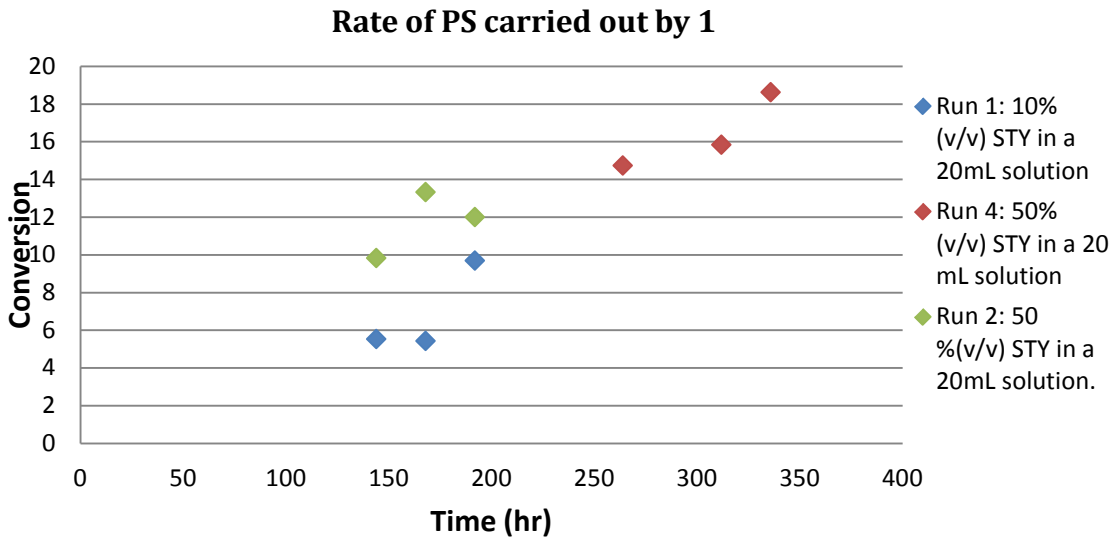

Figure 29: Conversion vs time for polymerization of STY at R.T.

To ensure good sampling practices, a larger polymerization volume would ensure easier sampling and larger aliquot size; therefore a solution with a total volume of 100 mL was used for Run 5 in Table 5. However, the solution colour turned to a brownish red upon addition of MAO. Originally, it was reasoned that there was an error in carrying out this polymerization. Therefore, another trial (Run 6, T5) was carried out with extra caution, and the same phenomenon was still observed. In addition, it was observed that the solution appeared to be homogeneous. As the stirring was slowed during the course of polymerization, there were no solid particles apparent to the naked eye. Prior to these two trials, the red colour was only observed for few trials. When the red colour appeared, it was during the addition of MAO and the appearance only lasted for few seconds. In addition, it was noticed that after the aliquot was vacuum-dried, only a clear gel like polymer was found in the receiving flask and no powdered material was present.

Therefore, a further investigation into the source of the colour change was conducted (Run 7). It was observed that the red colour of the solution would fade away as the polymerization progressed over time (Fig. 30). One of the original reasons to investigate a more homogeneous

catalyst system was that it could yield polymer with lower P.D.I values. However, during the course of investigating the possibility of changing the polymerization from a heterogeneous system into a homogeneous system, it was realized that the polymer obtained from the seemingly homogeneous system had a higher PDI value and a lower molecular weight.

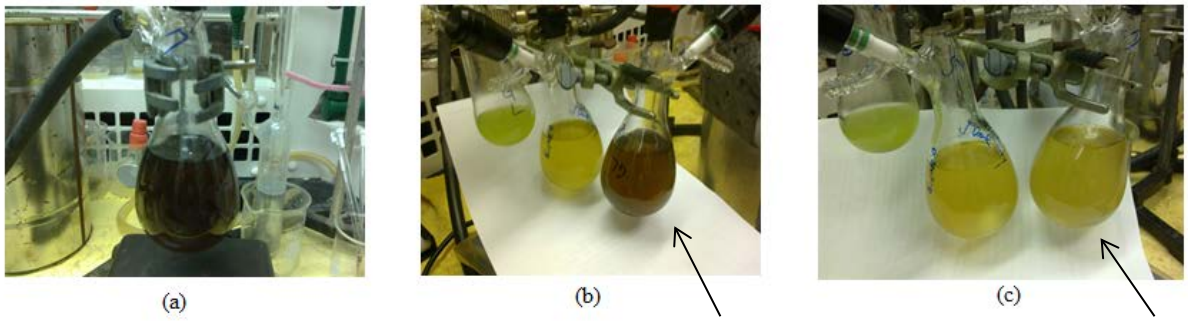

Figure 30: The colour gradually faded away as polymerization progress. (a): Upon activation by MAO; (b): on second day; (c): on 4th day. Run 7 was the observed trial in this figure. Arrow pointed to trial of Run 7. The left most solution in both (b) and (c) is from heterogeneous system Run 4 (Table 5).

At this stage, the reason for the inverse effect of the apparent homogeneous catalyst solution on this polymerization carried with **1/MAO** was not yet realized. The colour-change of the homogeneous polymerization as time progresses could be an indication that the Ni cluster **1/MAO** undergoes coordination changes upon initiation of MAO different from the heterogeneous system.

The polymerization of STY carried out by **1/MAO** in the homogeneous system is also quite slow (Fig. 31). Three trials (Run 5, Run 6, Run 7) only reached 14-15% within 5 days. Run 7 displayed a decrease in the beginning of the polymerization whereas the other three trials displayed an increase of conversion over time. This can only be attributed to a possibility that there was either a flaw in the experimental design or a manual mistake during sampling. It was then realized that a 4 digit analytical balance instead of a 3 digit balance was required because

the total mass of polymer formed was very small as there was only a small aliquot sampled each time. As a result, the weight of polymer obtained from the aliquot after Run 11 was all measured with a 4 digit balance.

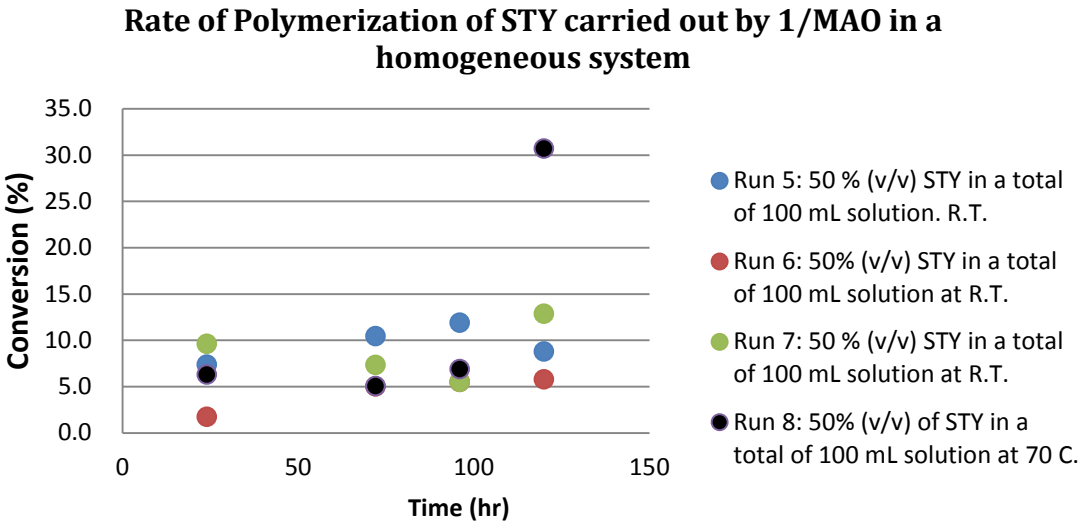

Figure 31: Plot of conversion vs time for polymerization of STY carried out by **1/MAO** in a homogeneous system.

Because polymerization of STY by **1/MAO** was slow in general (Fig. 28 and 29), raising the temperature would be a good option to monitor the polymerization in a shorter time period. A preliminary polymerization (Run 8) run at high temperature (70 ˚C) showed the possibility of obtaining a faster conversion. (Fig. 31) As styrene is known to be able to undergo self-polymerization at high temperatures, and the polymerization of STY carried out by **1/MAO** not as fully explored, blank trials were performed (Run 9 and 10, T5) before carrying out further polymerization at the temperature of 70 ˚C. It was observed that self-polymerization of styrene does not occur at 70 ˚C for over a period of 5 days. As a result, polymerization studies of STY were carried out at 70 ˚C. (Run 11, 12, 13, 14, 15, 18, and 19) (Fig. 32). As described earlier, measurement with an analytical balance with up to 3 decimals is not sufficiently accurate and could only provide a crude observation to how the polymerization progressed. As a result, Run

11 was not taking into consideration when discussing the heterogeneous system of polymerization.

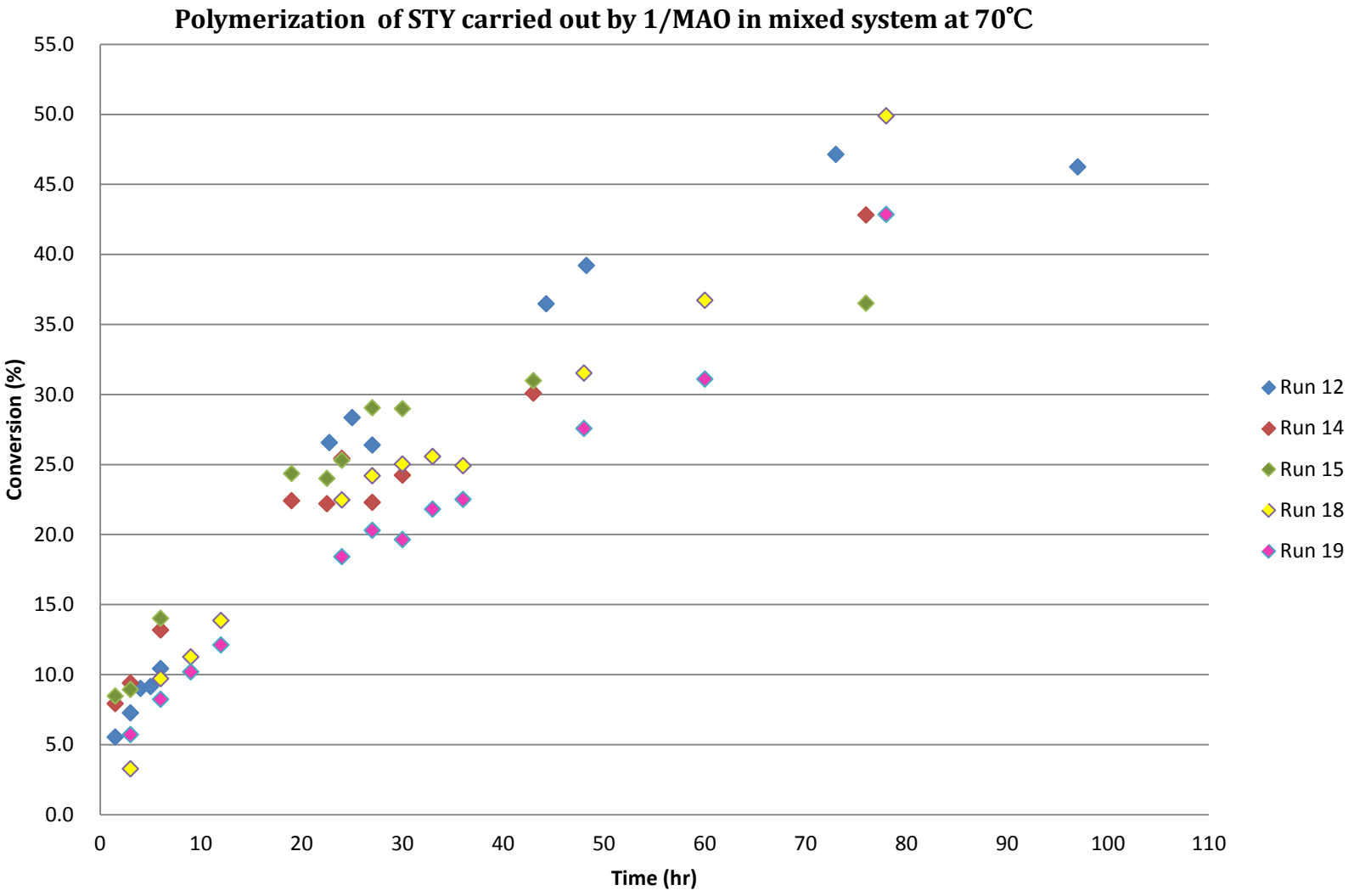

Figure 32: Plot of heterogeneous polymerization of STY carried out by **1/MAO**. All experimental conditions are the same for each run. Repeated trials were to ensure the reproducibility of the results.

It would also be interesting to understand how the homogeneous system (Run 13) behaves at high temperature in comparison to the heterogeneous system (Fig. 33). In general, the conversion with polymerization of STY by **1/MAO** displayed a possibility that the reaction proceeds through a zero-order or a first order reaction in regard to the concentration of STY (Fig. 32, 33).

Homogeneous polymerization carried out by **1/MAO** also displayed a similar curve of conversion over time. An initial assessment of Fig. 33 suggests that the conversion was smaller with a homogeneous system in comparison to the heterogeneous system. However, a more careful examination to Fig. 33 would speak otherwise.

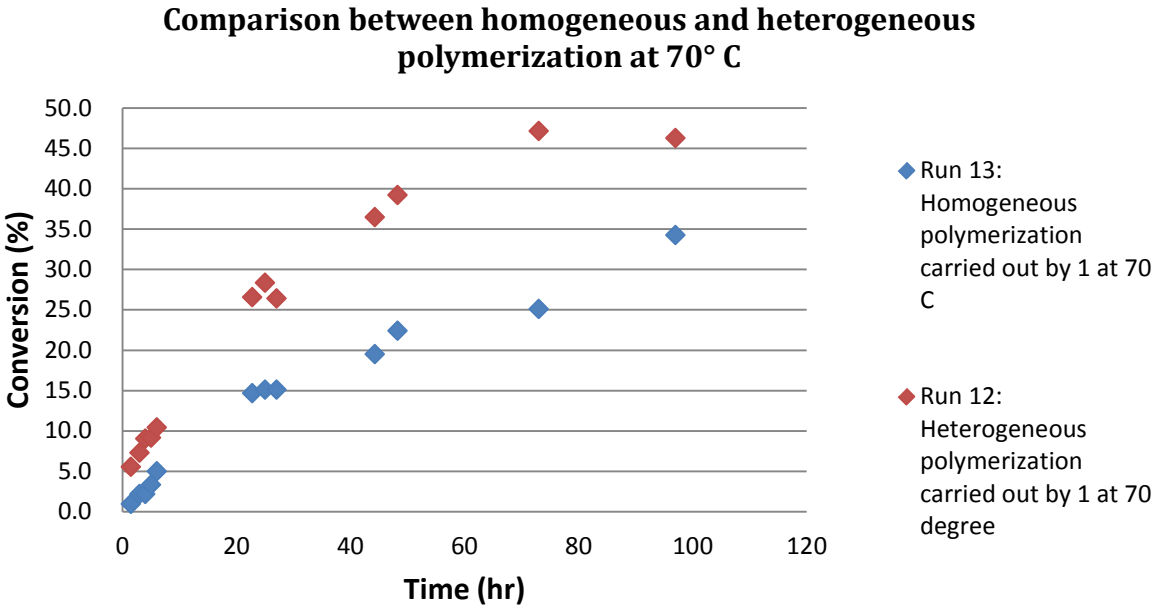

Figure 33: Plot of conversion vs. time for heterogeneous and homogeneous polymerization at 70˚ C.

Evaluation of Fig. 33 suggests that the conversion is smaller with the homogeneous system in comparison to the heterogeneous system. However, a more careful examination to Fig. 33 would speak otherwise. The heterogeneous system likely contains significant dissolved activated

catalyst **1**. From Run 13, it showed that 0.2100g activated catalyst can be totally dissolved in a polymerization solution of 100 mL. Thus, it can be stated that the polymerization Run 12 contained at least 0.2100g of dissolved activated catalyst. And the green undissolved activated catalyst observed in Run 12 was a result from the undissolved activated **1** after the activated catalyst **1** reached its maximum solubility (saturation) in the 100mL polymerization solution. Hence, previous trials that were believed to be carried out in a so called heterogeneous fashion was indeed a polymerization carried out in a mixed system with both homogeneous and heterogeneous phenomenon existing in the polymer solution. Therefore, the heterogeneous system that was mentioned prior to this paragraph should more properly be referred to as a "mixed system" instead of heterogeneous system.

Further examination showed that the activated catalysts in homogeneous system had a better catalytic activity compared to those in the mixed system. Data at 25^{th} hour for both systems indicate that 0.2100g of dissolved activated catalysts generated a 15% conversion of STY into the polymer, and 1.5100g of activated catalyst (where at least 0.2100g of activated **1** was dissolved in the solution) in the mixed system only yielded a 30% conversion. In other words, activated catalyst in homogeneous system underwent polymerization with a faster rate.

Although homogeneous system was found to be more active compared to the mixed system, the PS recovered from homogeneous system has a higher PDI value (PDI=3.5) compared to that recovered from the mixed system. As a result, the trials after Run 13 were all carried out in the mixed system

D.2: Polymerization of styrene carried out at different temperatures

Three trials of polymerization of STY at both R.T. and at 90° C were also carried out. Although it was already established that the polymerization of STY carried out by **1/MAO** is

slow, trials at room temperature are useful for comparison to future trials of polymerization of other monomers. As expected, the conversion of styrene into polymer increased with increasing temperature. There is, however, there was difficulty to determining whether the polymerization proceeds with a faster conversion at 70 ˚C or 90 ˚C after a long period of time. This was due to the reason that while the temperature at 70 ^{o}C can be monitored for a duration of 3 days, the temperature at 90 ˚C was only monitored for a duration of 3 hours. Polymerization carried out at 70˚ C became very viscous on the third day and obtaining the sampling aliquot became extremely difficult at that time. As a result, polymerization carried out at 70 ˚C was only monitored with a period of 3 days.

Before carrying out the polymerization at 90 ˚C, a blank of polymerization (Run 22 and 24) showed that polymerization mixture became very viscous after 1 and half days and sampling the aliquot became extremely difficult. Because it is usually the initial reaction rate that is monitored in studying the kinetics of a system, and polymerization carried out at 90 ˚C started to have orange colour appearing in the polymerization after running for 3 hours, only the polymerization at the beginning of 3 hours was sampled when the polymerization of STY was carried out at 90 ˚C.

However, whether or not the polymerization proceeds with very different conversion rate or similar conversion rate between 70 and 90 ˚C still remained to be answered. In addition, the highest conversion of styrene to PS carried out by **1/MAO** was reported to be ≈ 50% (Fig. 32, Run 18). It was necessary to monitor the reaction to see if conversions exceeded 50%. Therefore, another polymerization trial at 90˚C was carried out over a period of 24 hours (Run 29, T5) (Fig. 34). Plot of conversion vs time at different temperature is presented in Fig. 35. Some notable observations are also included in Table 5. As the polymerization reached the 12th hour, the increase in viscosity of polymerization was easily detected by visual observation. A comparison

of polymerization conversion vs time carried out at temperatures of 70 and 90 ˚C (Fig. 36) clearly show that conversion increased with the increase of temperature. A comparison of polymerization at different STY concentrations indicates that the higher the concentration, the higher the conversion with regard to the polymerization (Fig. 37).

D.3: Temperature effect on tacticity and M_n

It was previously reported that an increase in the temperature of polymerization would greatly reduce the tacticity of a polymer due to the loss of catalyst activity or structure control over the tacticity.[30, 34] Hence, ^{1}H NMR spectra of PSs produced at different conditions were compared (Fig. 38). But before any suggestion can be drawn from Fig. 38, a ^{1}H NMR (Fig. 39) and ^{13}C NMR (Fig. 40) of *s*PS recovered from the mixed system at R.T. with stoichiometric amount of MAO to activated catalyst (ratio = 3:1 of MAO to activated catalyst) should be examined. Table 6 lists the values of peaks obtained from the proton and carbon NMR in Figs. 39 and 40. Proton resonance peaks from Fig. 39 are compared to peaks from the literature value.[59,73] A syndiotactic polystyrene would give a triplet peak at 1.38 ppm for the two methylene protons. If the polystyrene is atactic or isotactic, values higher than 1.38 ppm would be observed for the methylene protons. The proton resonance signal of the methine proton would also be an indication to the tacticity of the polystyrene. A methine proton from syndiotactic polystyrene would give rise to a resonance at 1.89 ppm. The methine proton from atactic or isotactic PS would give rise to a position higher than this value[53,59,73] (compared the trend of syndiotactic proton vs atactic proton signal in ref 59, then one can make this conclusion from the finding in ref 73).

The ipso carbon on the phenyl group is also an indication to the tacticity of the recovered PS. If a PS is 100% isotactic, the ipso carbon signal is usually represented by a sharp resonance

at 146 ppm. The ipso carbon signal obtained from atactic PS would give rise to 5 main peaks ranging from 145.1 to 146.13 ppm, whereas a 98% syndiotactic PS would show a single sharp peak at 145.13 for the ipso carbon.[53, 59]

The ipso carbon signal from Fig. 40 does not show one single sharp resonance between 145.0 to 145.13 ppm; instead a few smaller resonances between 145.09 (largest) and 145.37 (smallest) ppm are observed. Thus from the examination of ^{13}C NMR in Fig. 40, two conclusions can be drawn:

1: The PS recovered from polymerization carried out by activated **1** is an atactic PS that contains some small segments that are syndiotactic.

2: The PS recovered from activated **1** system in this project are largely syndiotactic PS, with some atactic nature.

Based on the fact that the methylene and methine proton signals from the recovered PS produced by activated **1** have signal positions close to those of a syndiotactic PS, it is then more likely the PS made from activated **1** in this project is likely a syndiotactic PS that contains some atactic nature.

Usually splitting of the proton peak is also examined to distinguish the tacticity of the recovered PS. However, this requires the use of high temperature NMR (100 ˚C or higher) so that peaks can be better resolved. This is not the case when carrying out NMR spectroscopy of the polystyrene recovered from the polymerization using activated **1** in this project. Hence, the proton signals arise from the mixture of syndiotactic and atactic environments in the recovered PS in this project are not clearly distinguished or resolved. Therefore, the only conclusion can be drawn from Fig. 39 is that the proton signals of the PS recovered from the polymerization carried out by **activated 1** are in agreement that the PS made from activated **1** system is syndiotactic-rich. A calculation of the % syndiotacticity of the recovered PS by NMR (Fig. 39,

40) is a challenge as the signal ratio between the proton in a syndiotactic environment and the protons from atactic environment cannot be properly resolved at 400 mHz, but maybe separated at higher NMR frequencies.

Table 6: Report on proton and carbon resonance signals from Fig. 39 and 40.

Fig. 39: ^{1}H NMR		
Value from Fig. 39 (ppm)	Lit. Value (ppm)[73]	Assignment from literature [73]
7.07&7.03	δ 7.07	m, 3H, *meta*- and *para*- H
6.57, 6.46 & 6.37	δ 6.59	m, 2H, *ortho*- H
1.86	δ 1.89	m, 1H, CH
1.43	δ 1.38	m, 2H, CH_2
Fig. 40: ^{13}C NMR		
Value from Fig. 40 (ppm)	Lit. Value [73]	Assignment from literature [73]
145.37, 145.09	144.9 [73], 145.13 [53]	C_{ipso}
127.87	127.4	C_{ortho}
127.43	127.3	C_{meta}
125.49	125.0	C_{para}
43.77	43.7	Methine carbon
40.47	40.5	Methylene carbon

As it is reasonably established that the PS made from activated **1** is a mainly syndiotactic PS that contains some atactic nature, Fig. 38 can reexamined and few suggestions can be made:

1: Fig 38 (a) vs Fig. 38(b):

With a different ratio of MAO added to the system, (Cat: MAO=1:3; Cat: MAO=1:5), the major methylene and methine proton peak positions that are related to methylene and methine proton peaks from *s*PS are not shifted. However, a sharp resonances arises at $\delta \sim 1.26$ ppm was observed.

2: Fig. 38 (b) vs Fig. 38 (c):

A comparison between PSs recovered from polymerization carried out at different catalyst concentration can be made from spectra (b) and (c) in Fig. 38. Again, the signals arise from methine and methylene protons are at the same position with the peaks obtained from spectrum (a) in Fig. 38. However, a sharp peak at 1.26 ppm arise from the broad peak methylene are observed in both (b) and (c) spectra.

3: Fig. 38 (a) vs Fig. 38 (d):

A comparison between PSs recovered from polymerization carried out at different temperatures is shown in spectra (a) and (d) in Fig. 38. The signals result from methine and methylene protons remain at the same position. There is no observation of shifting of these two proton signals from highly shielded region to the lower shielded region.

Fig. 41 and Fig. 42 are the spectra of (c) and (d) in Fig. 38 presenting in their original scales. There is a signal that arises at a resonance of $\delta = 0.84$ ppm in Fig. 41 and $\delta = 0.87$ ppm in Fig. 42. It could be said that this peak arises because the atactic nature increases in the recovered PS produced if the MAO to pre-catalyst ratio is increased or the temperature is increased. Nevertheless, a reference to prove this signal is an indication of the presence of atactic PS is required. Moreover, it is also likely that impurities in the sample cause the signal at $\delta = 0.84$

ppm/0.87 ppm to appear in Fig. 41 and Fig. 42.

Although increases in atactic nature would produce a signal with broad peak in proton NMR, the peaks of 4 spectra in Fig. 38 are all broad due to the reason that peaks are not well resolved. Hence, it cannot be determined at this stage whether increases in temperature, increases in the ratio of MAO to pre-catalyst, or decreases in the concentration of the activated catalyst to the overall polymerization system result in the loss of syndiotacticity of the recovered PS. However, one point is worth mentioning is that because the methine and methylene proton signals in all 4 spectra from Fig. 38 are appearing at the position in agreement with those from pure syndiotactic PS, the recovered PS obtained from activated **1** system still remains mainly syndiotactic in regards to its tacticity even though the changes to the polymerization mentioned from the above have been encountered.

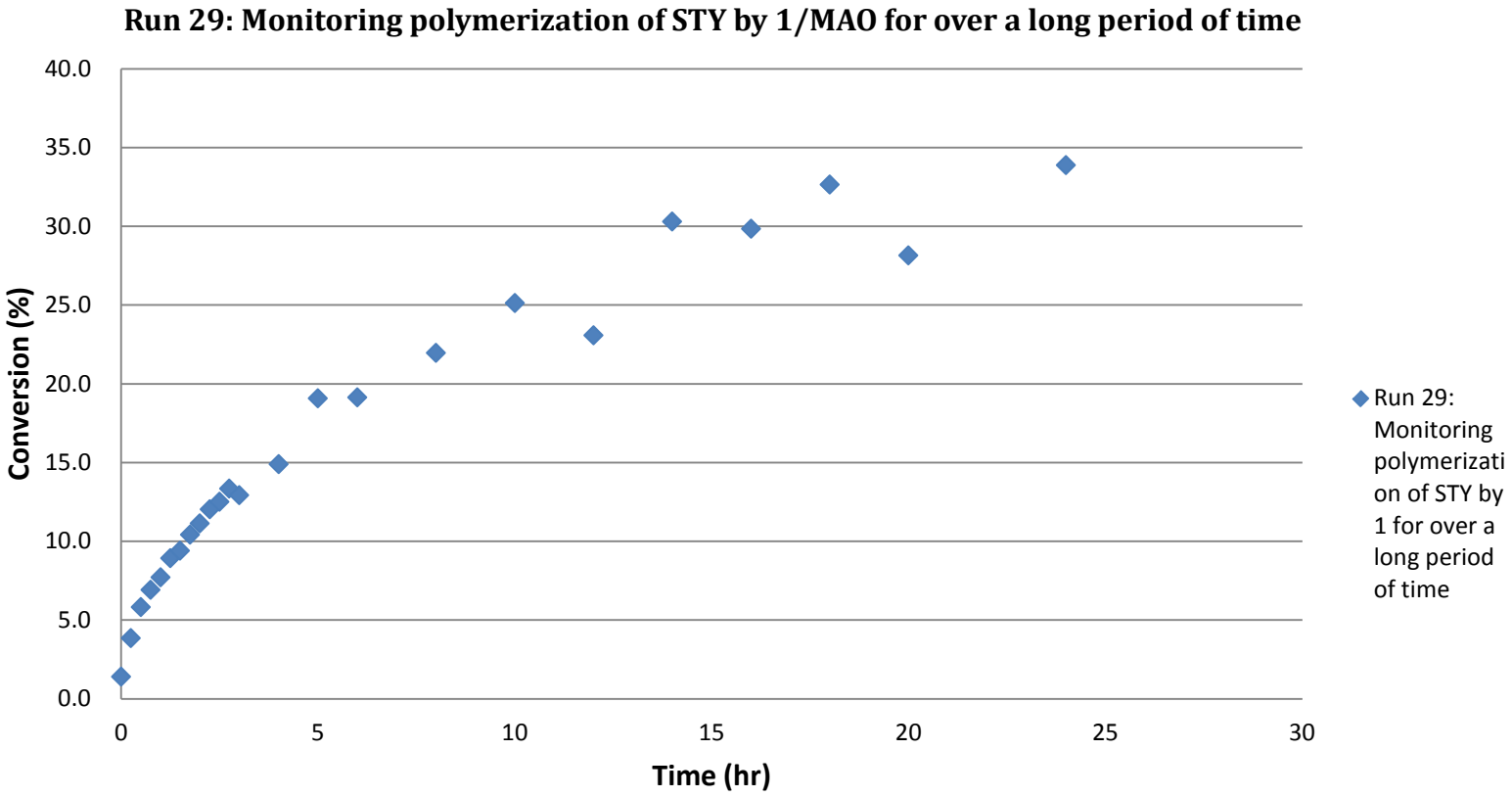

Figure 34: Conversion of STY into PS carried out by 1/MAO at 90° C. Note at time = 0 hr, there is already conversion of STY into PS.

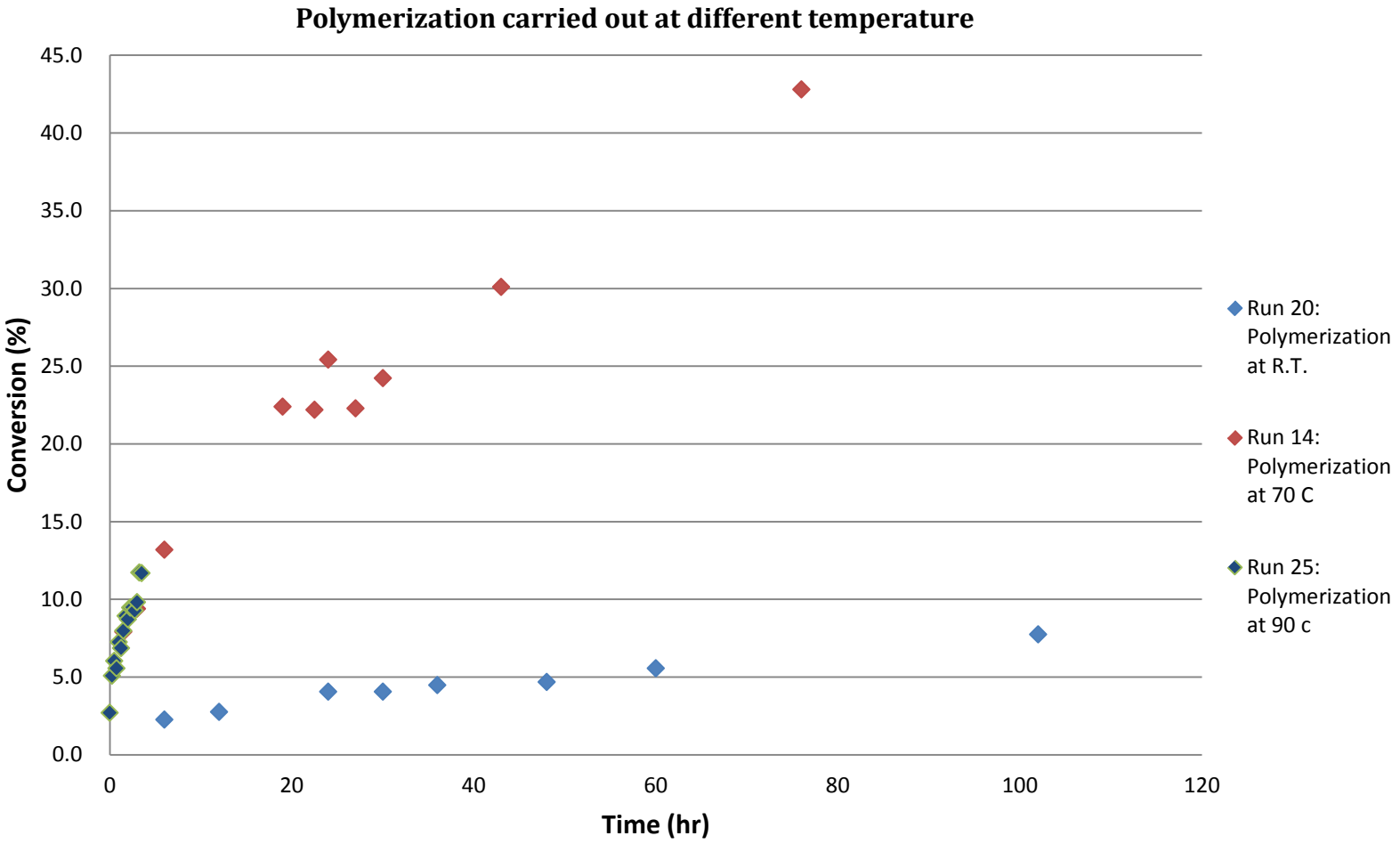

Figure 35: Plot of conversion vs time with polymerization carried out at different temperature.

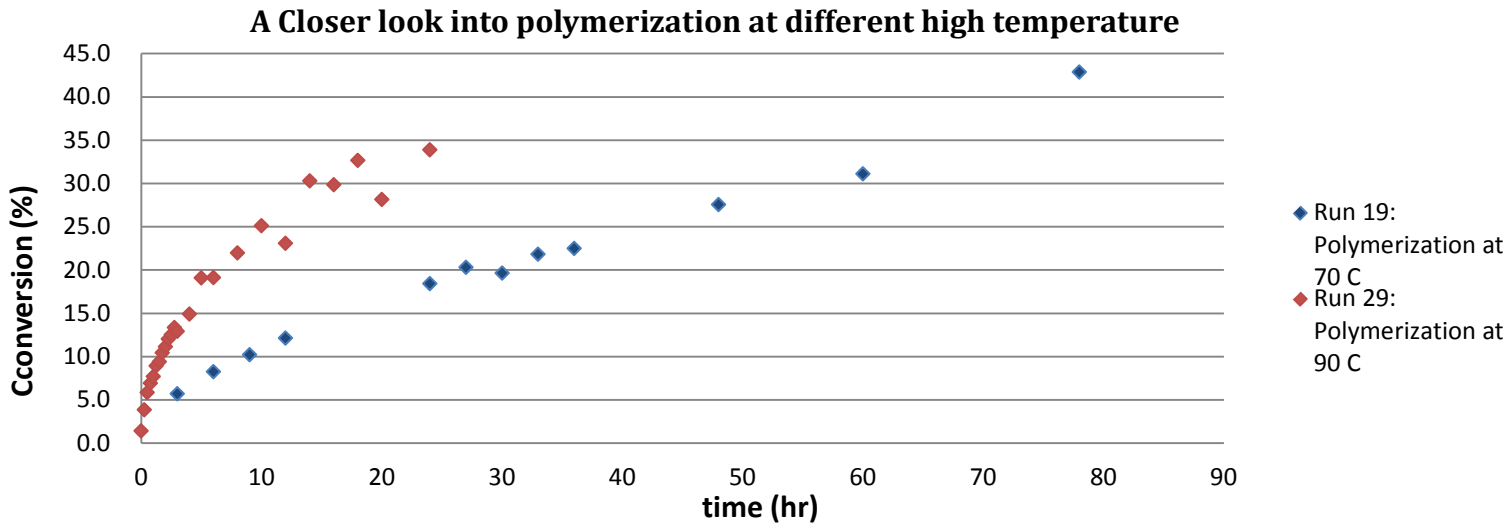

Figure 36: Comparison of polymerization carried out by **1/MAO** at 70 and 90˚ C.

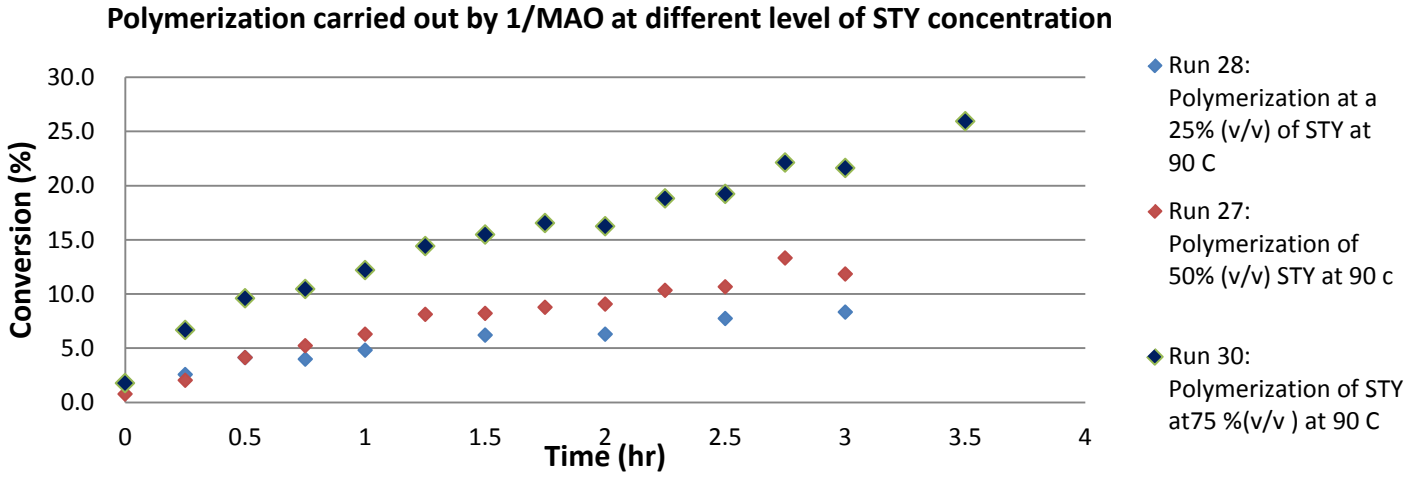

Figure 37: Polymerization of STY at different concentration level carried out at 90° C.

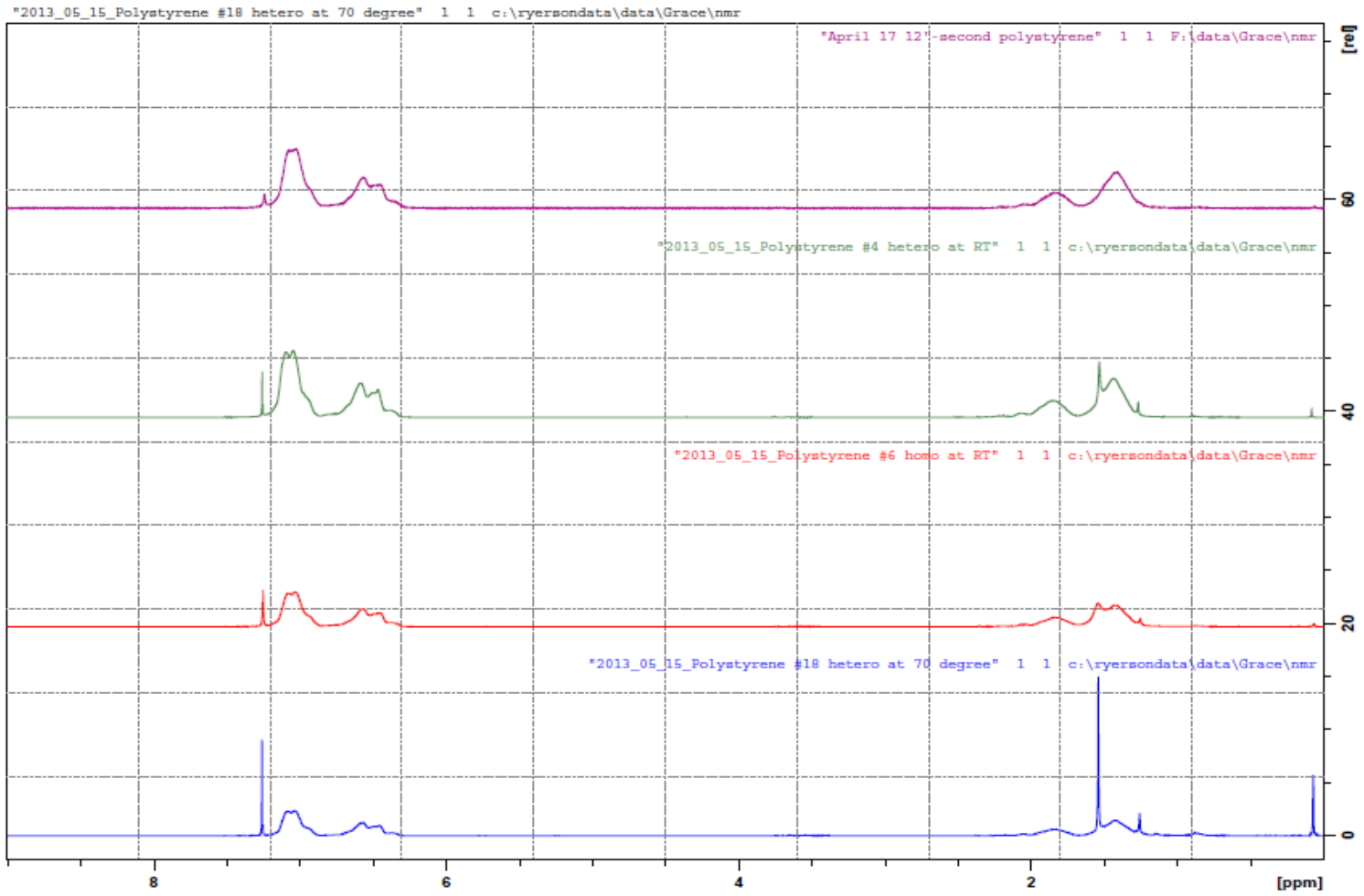

Figure 38: Comparison of ^{1}H NMR ($CDCl_3$) between polymers produced at different experimental conditions. (a): Polymer produced at R.T. ; (b): Mixed system (Run 4, T5); (c) Homogeneous system (Run 6, T5); (d): Mixed system at 70 ◦ C (Run 18, T5).

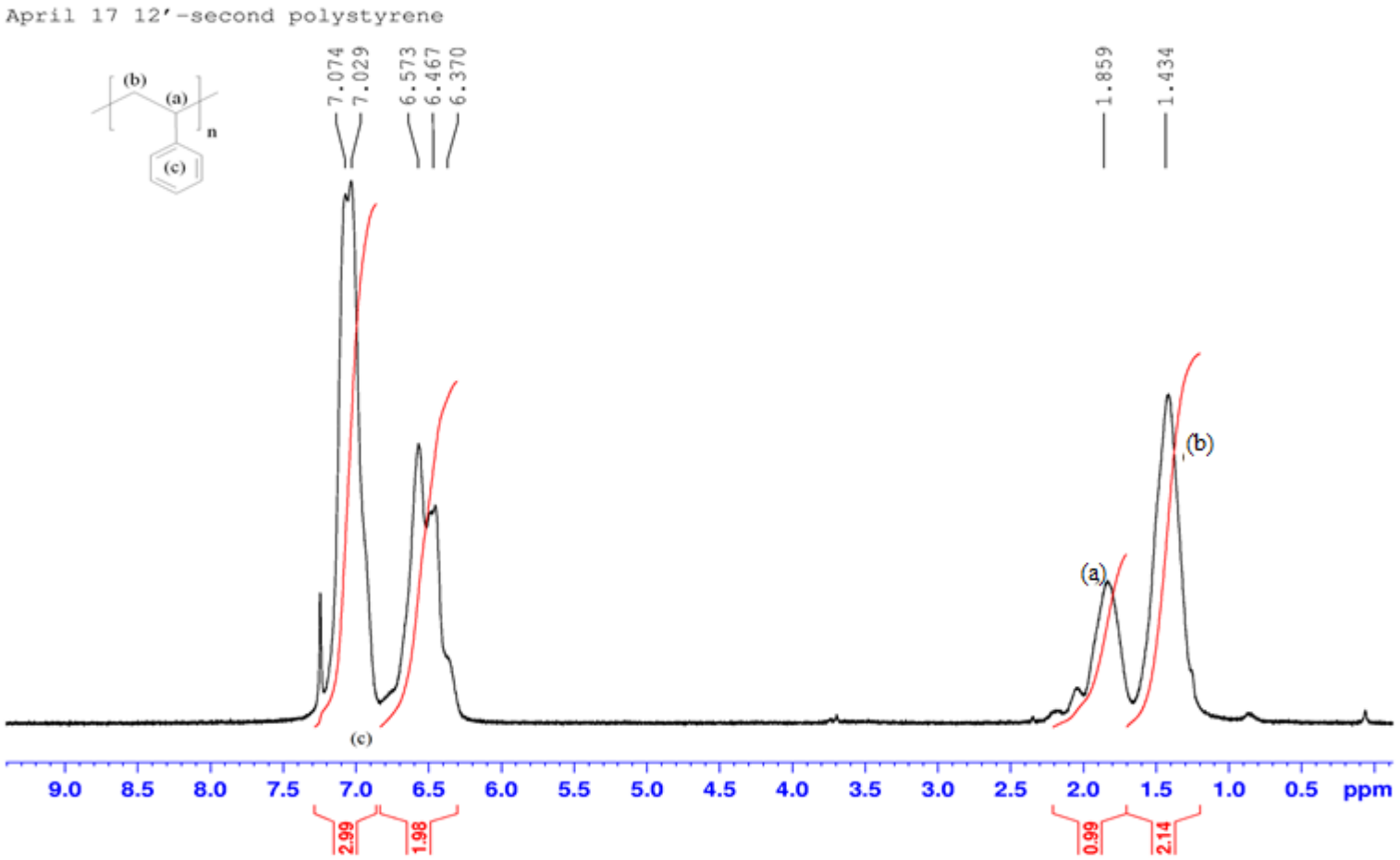

Figure 39: ^{1}H NMR ($CDCl_3$) of recovered PS from R.T. in mixed system, MAO ratio t pre-cat is in 3:1.(Trial was taken from PS-2, Table A1 from appendix 1) .

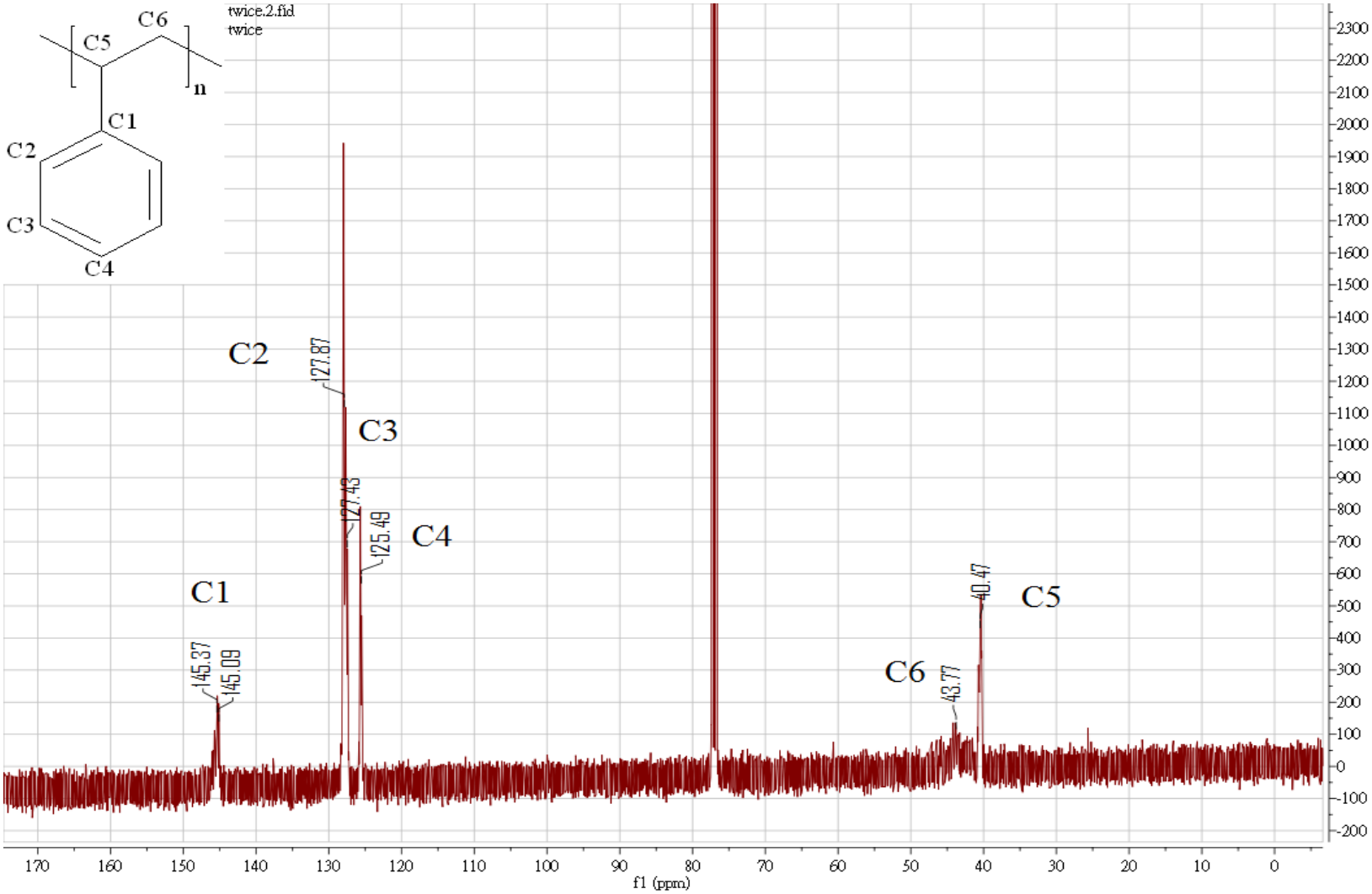

Figure 40: ^{13}C NMR ($CDCl_3$) spectrum of the recovered PS in this project. This is from the same sample used for ^{1}H NMR in Fig. 39.

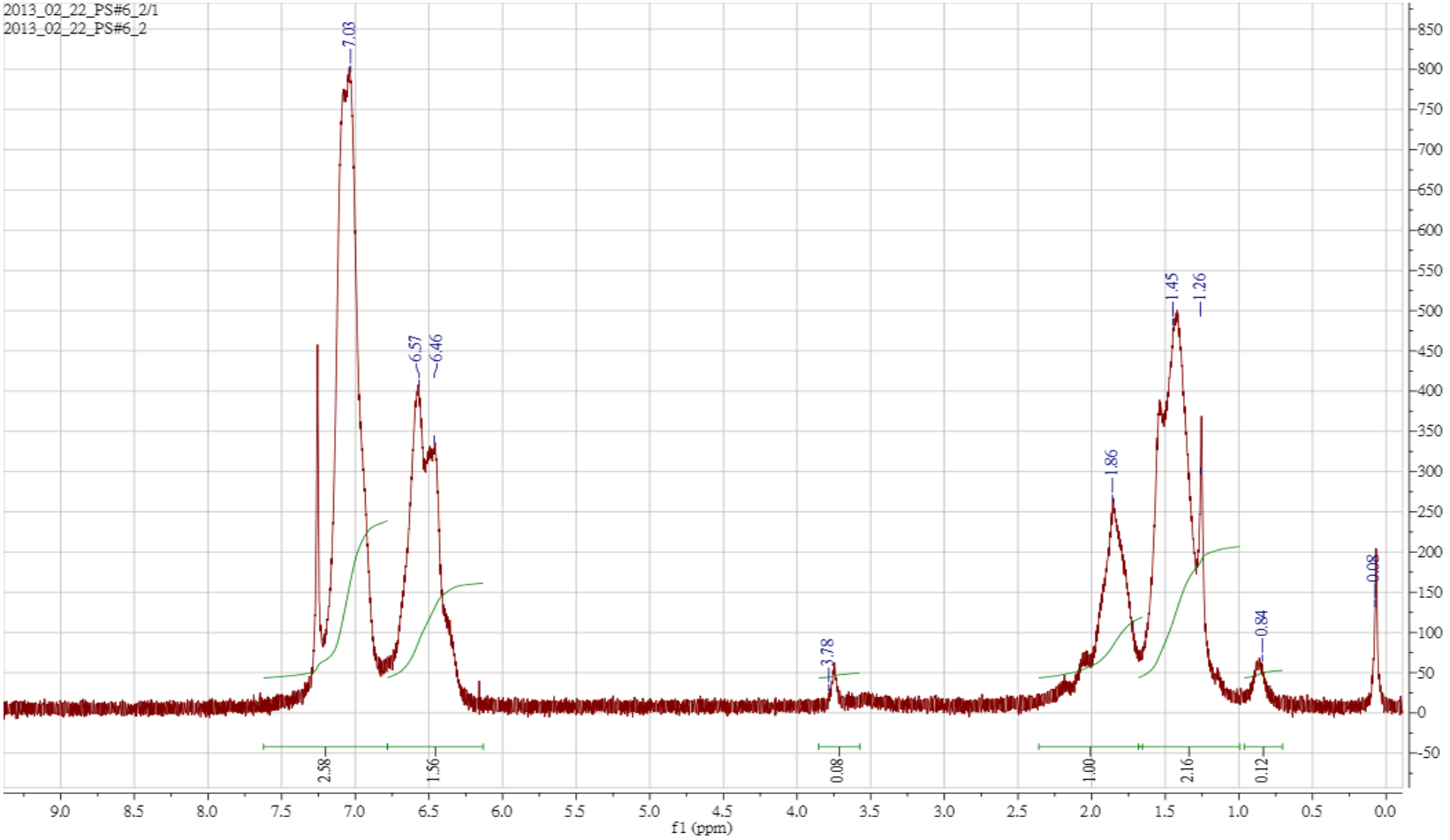

Figure 41: ^{1}H NMR ($CDCl_3$) spectrum for RUN # 6. Atactic nature increases with the PS obtained from homogeneous system.

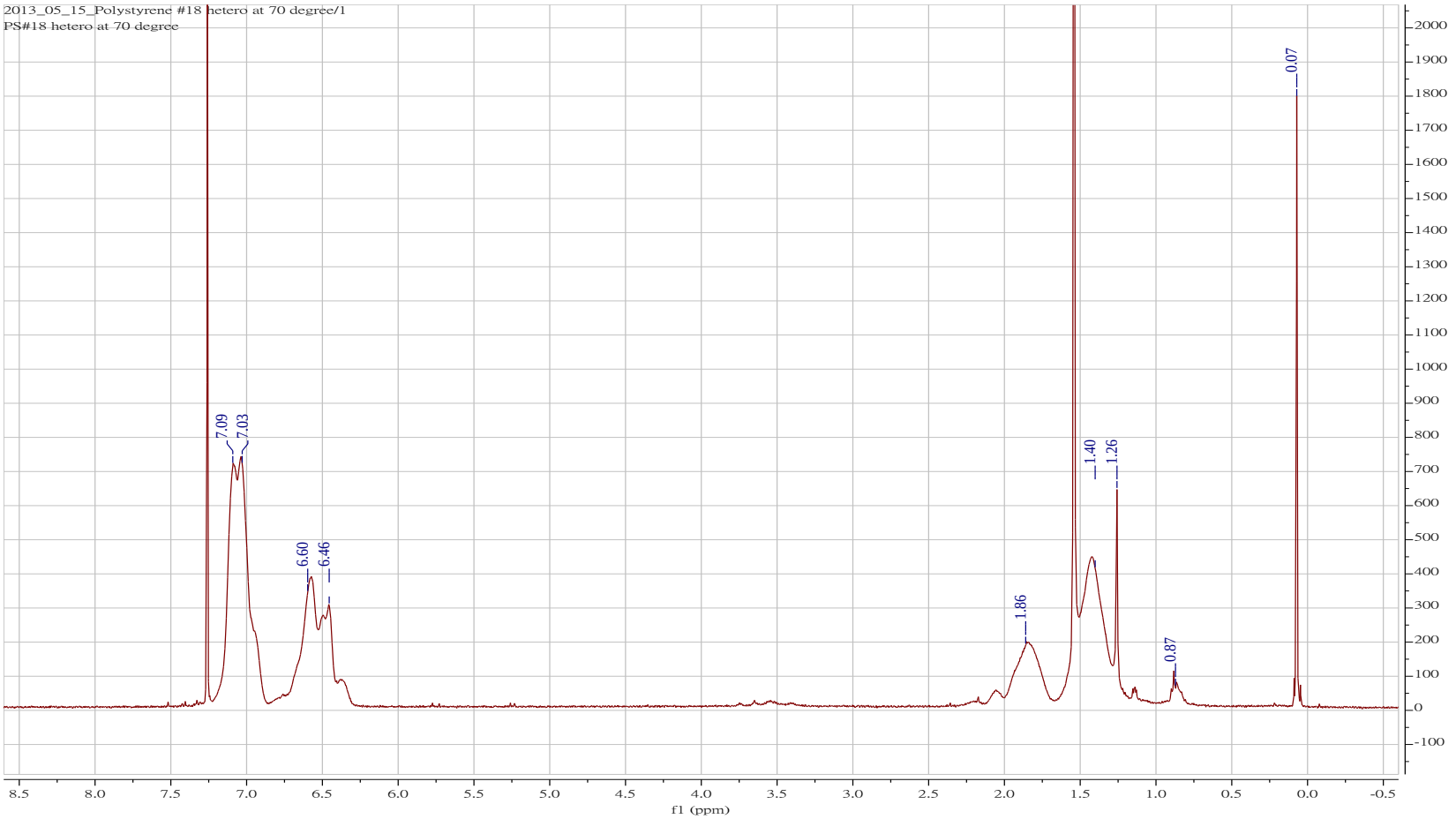

Figure 42: ^{1}H NMR ($CDCl_3$) for the polymerization of STY carried out at 70 ^{o}C (Run 18). The increase of the atactic nature is shown by the appearance of the peak at 0.87 ppm, and an increased intensity at 1.26 ppm.

With polymerization that undergoes insertion coordination pathway, the value of the number average molecular weight (M_n) provides insight to the rate of chain propagation. A large M_n value indicates a polymerization that undergoes chain propagation without encountering frequent β-hydride transfer. [23, 28] In Table 7, the M_n values of the PS produced in different conditions are shown.

Table 7: Result of PS using **1**/MAO as the catalyst.

Trials	Temp.	Conversion (%)	M_n	PDI	TOF
PS 15 (Appendix 1)	25	11.3	205797	1.63	4.2
Run 5, T5 (homogeneous)	25	8.7	76742	3.81	2.4
Run 19, T5: 3rd aliquot (Mixed)	70	[10].0	38876	1.78	7.7
Run 19, T5: 5th aliquot	70	18.1	59775	1.74	5.2
Run 19, T5: 11th aliquot	70	31.1	93344	1.67	3.5

The results in Table 7 indicate that as the temperature increases, the M_n value decreases (PS15 vs Run 19, T5, 3rd aliquot). In an earlier report published by Gossage, *et al.*,[65] a fair assumption is that the polymerization carried out with **1**/MAO proceeds via a coordination insertion mechanism. If this is the case, then the decrease in the M_n values suggests that the rate of chain transfer increases faster than chain propagation as temperature is increased, causing a lower molecular weight in the recovered polymer.

Comparing the polymerization results carried out with different activated catalyst concentration at room temperature (Table 7: PS 15 vs Run 5, T5), it suggests that M_n value of PS

obtained from a polymerization with lower activated catalyst concentration is drastically decreased compared to the PS prepared with higher activated catalyst concentration. However, the suggestion that a higher ratio MAO to catalyst ratio produced a polymer with lower M_n value can also be made because Run 5 was carried out with the ratio of 5: 1 in regards to amount of MAO to the pre-catalyst. AS a result, there is no conclusion whether catalyst concentration in the polymerization or different MAO to catalyst ratio have effect on the M_n value of the obtained PS. GPC data from Run 4 (T5) is then required in the future to determine whether catalyst concentration in the polymerization affect the number average molecular weight to the recovered PS because Run 4 from Table 5 and Run 5 from Table 5 differs only in the catalyst concentration. In regards to PDI value of the polymers, temperature does not seem to have effect on it.

D.4: Turnover frequency of 1/MAO

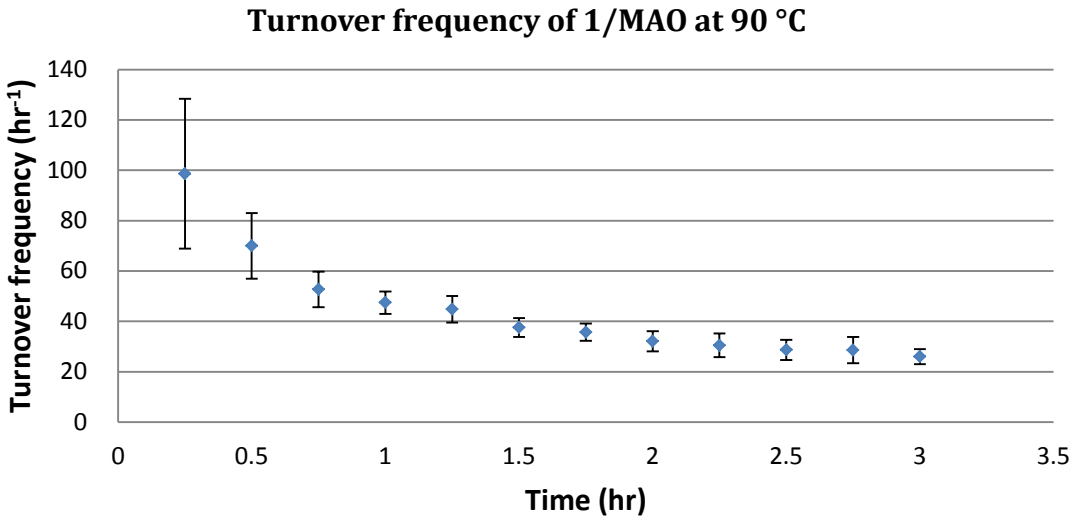

Figure 43: A plot showing the decaying turnover frequency of 1/MAO over time. Data points are average values from 4 trials at 90°C (Run 25, 26, 27, and 29).

Turnover frequency of a catalyst demonstrates the ability, per mole, of a catalyst turning the monomer into a polymer within a given time. Turnover frequency is calculated as turnover

number/time of reaction (hour), in which the turnover number is calculated as "conversion/mole of catalyst".[28] This value is usually reported as a value to indicate the productivity of the catalyst in a short period of time. However, if the turnover frequency of **1**/MAO is calculated over different period of time, it is observed that turnover frequency of **1**/MAO decreased as polymerization progresses (Fig. 43, 44). .

As illustrated in Fig. 43, the turnover ability of activated **1** decays as polymerization of STY progresses. It should be noted that the data in Fig.43 only demonstrates the turnover frequency of **1**/MAO within the first three hours as carrying out the polymerization at 90 ˚C. If the turnover frequency of **1**/MAO is monitored over a longer period of time, then it would be apparent that the catalyst reaches a limit in its ability to turn the STY into a polymer (Fig. 44).

If the turnover frequency of **1**/MAO is compared for polymerization carried out with different concentrations, it appears there is a higher turnover frequency with higher concentration at the beginning of the reaction (Fig. 45). The turnover frequency difference of **1**/MAO shown at different STY concentrations could be explained by a fast/slow diffusion of monomer to the active catalyst site. In polymerizations with a higher concentration of monomer, it is easier for the monomer to diffuse to the active catalyst site. However, the turnover frequency of **1**/MAO does not differ too much between the concentrations of 50% (v/v) STY and of 75% (v/v) STY. When the polymerization reaches its 4^{th} hour, the turnover frequency between each concentration assumes approximately the same value. This could be an indication that diffusion plays a minor role for the active catalyst's turnover ability at the beginning of polymerization. If diffusion plays a role in the beginning of the polymerization, then it is also possible to suggest the causes of the observed declining TOF as the polymerization progresses:

1: The decline of TOF of the catalyst observed as the polymerization continues is due to the slow deactivation of the catalyst;

2: The observed decline of TOF of the catalyst observed as the polymerization progresses is due to increased difficulty of the monomer to be coordinated to the active catalytic site because the elongated growing polymer chain gradually occupies the surroundings of the catalytic metal site as polymerization continues.

At different temperatures, the **1**/MAO appears to possess a higher turnover frequency at higher temperature (Fig. 46). As the polymerization progresses to the 20^{th} hour, the turnover frequency of **1**/MAO at 70° and 90°C begin to reach the same limiting value. The polymerization carried out by **1**/MAO at room temperature, on the other hand, displays a very low activity in converting STY into a polymer. The difference of TOF of **1**/MAO displayed at RT and higher temperatures might arise from the fact that at higher temperature STY has higher energy to overcome the activation energy for insertion step. A low turnover frequency of **1**/MAO at room temperature could be an indication that the activation energy for STY inserting to the active Ni^{2+} center is high. From Fig. 46, it was also demonstrated that the **1**/MAO demonstrates a high turnover frequency in the first five hours of the polymerization.

As mentioned in previous section (Section 2.4: D.2), it was deducted logically that the activated catalysts in the homogeneous system displayed a better catalytic ability in carrying out the polymerization of STY compared to those present in the mixed system. In other words, the dissolved activated catalysts possess a higher catalytic activity in polymerize STY compared to the dissolved & undissolved activated catalysts present in the mixed system. Fig. 47 illustrated such difference in the catalytic ability of the activated catalysts present in these two different systems. As expected, TOF of the activated catalysts present in homogeneous system possess higher value compared to TOF of those present in the mixed system, an indication the activated catalysts present in homogeneous has higher catalytic ability in carrying out polymerization of STY.

One more interesting phenomenon is displayed in Fig. 47. The TOF of the activated **1** seems to increase at the beginning of the first 6^{th} hours of the polymerization, then slowly declines. Polymer recovered from homogeneous has a PDI value of 3.5. Secondly, colour of homoheneous polymerization turned from green to brownish red upon initiation of MAO and no solid particles were observed.From these two observations, one suggestion can be elucidated: upon activation by MAO, all pre-catalysts turned into unknown species that were soluble in toluene (or in the mixture of toluene with STY). Although all pre-catalysts have been turned into a species soluble in the polymerization system, not all new species possess catalytic ability to carry out the polymerization. If all the catalysts were been activated upon the addition of MAO, then the increase in TOF values at the initial stage of polymerization or the PDI values form the recovered PS would not be observed.

Therefore, it is plausible to propose the following might happen upon initiation of MAO:

1: Upon MAO initiation, all pre-catalyst turned into soluble species in polymerization solution.

2: Among the soluble species, there are some that are active in carried out the catalytic activity in polymerizing STY, and others that do not have catalytic activity in polymerization STY.

3: The equilibrium between the catalytic active and non-active species is reached within 6 hours.

The three points listed above are proposed mechanism upon initiation of MAO to explain what might cause the increased value of PDI of the recovered PS. As to what really takes place in regard to the pre-catalysts upon initiation of MAO, more data is required to elucidate the

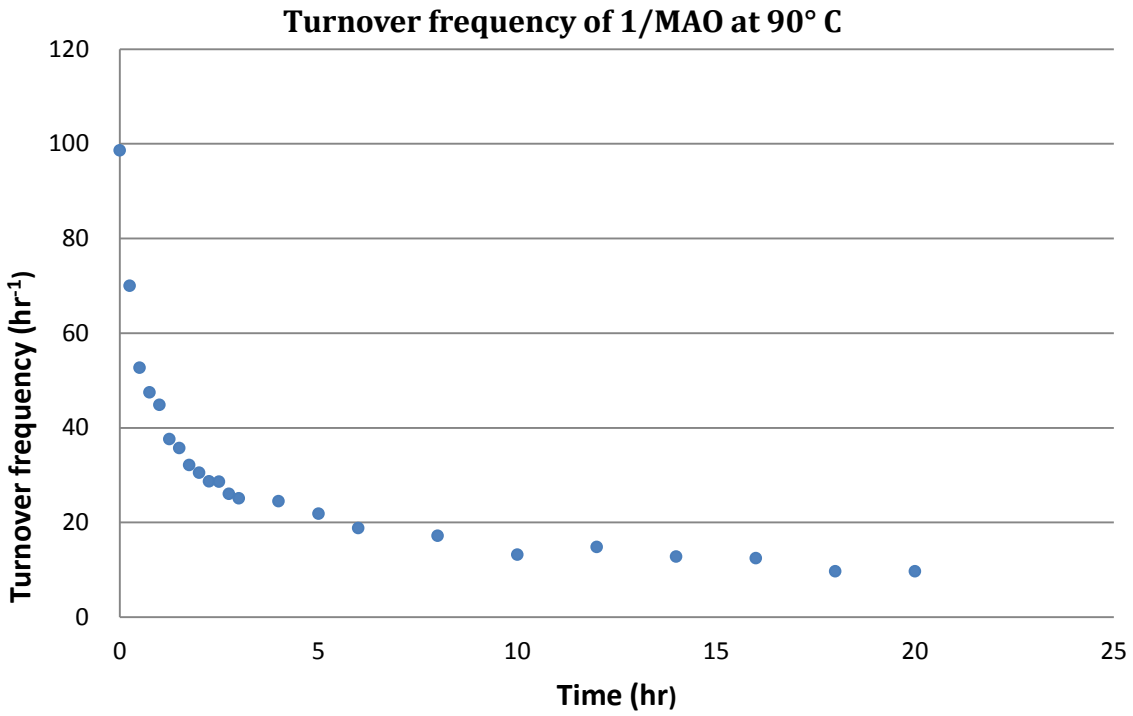

Figure 44: Turnover frequency of **1**/MAO monitored over a period of time. Data obtained from Run 29, polymerization carried out with 50% (V/V) of STY.

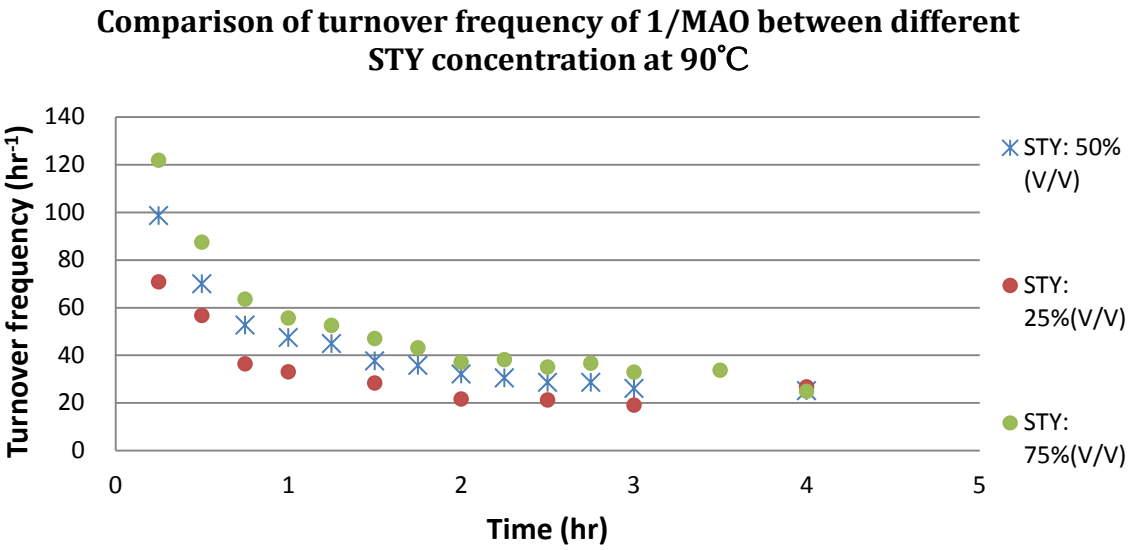

Figure 45: Comparison of turnover frequency between different concentrations at 90° C. Data obtained from Run 28, 29, and 30.

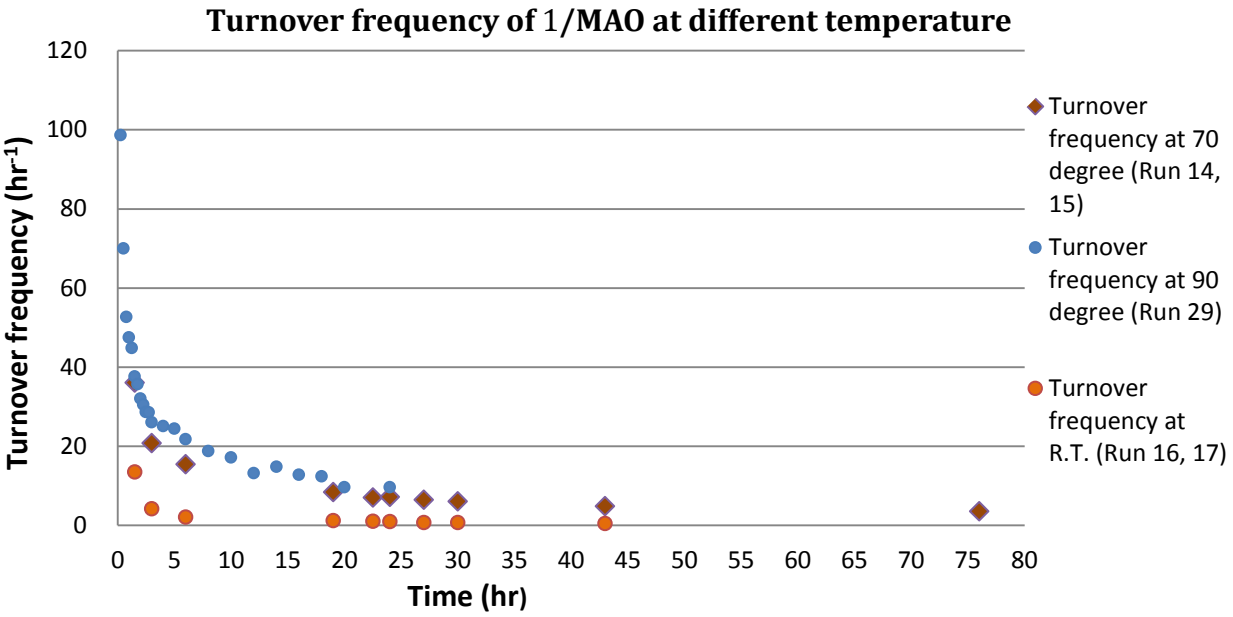

Figure 46: Comparison of turnover frequency of **1**/MAO at different temperature.

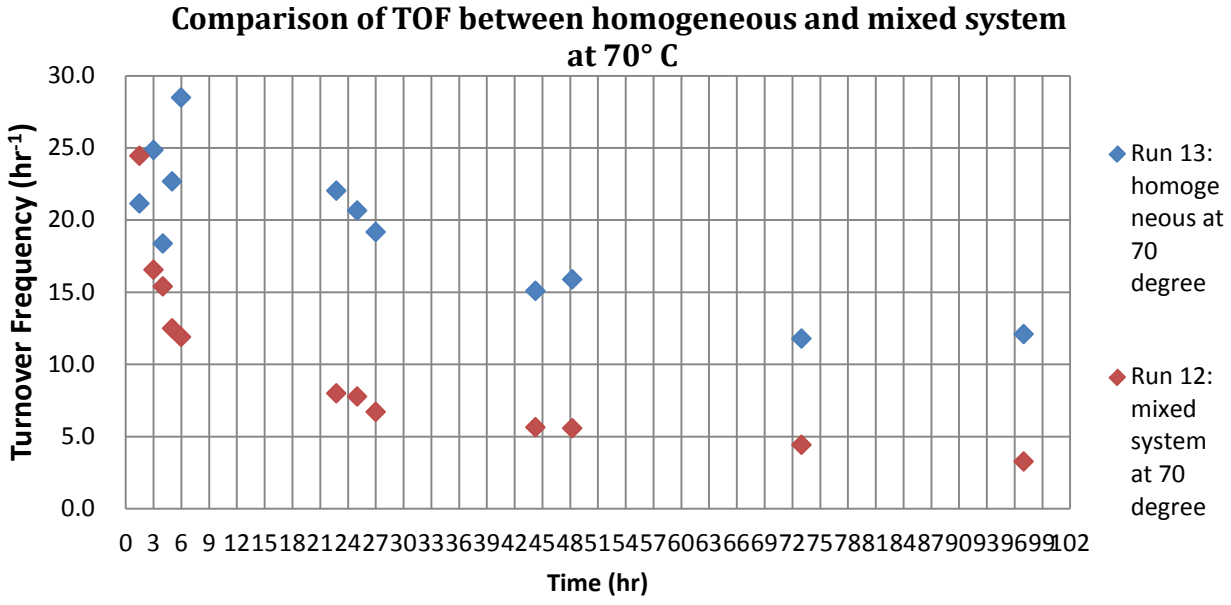

Figure 47: Comparison of TOF between homogeneous system and mixed system. Trials taken from Run 12 and 13 in Table 5

mechanism that occurs at the beginning of polymerization.

At this stage, the following have been confirmed from these studies:

1: As temperature increases, the polymerization conversion increases.

2: As the concentration of STY increases, conversion increases. However, conversion does not increase proportionally according to the increase of STY concentration (Fig. 37).

3: A homogeneous catalyst system has a lower conversion in comparison to the mixed catalyst system at first glance (Fig. 33). However, activated catalysts present in homogeneous systems have a higher catalytic activity compared to those present in a mixed system.

4: When a homogeneous system is initiated, the polymerization colour is reddish brown, indicating possible significant changes in bonding to the Ni center in the activated catalyst. As polymerization progresses over time course, the red colour slowly fades and solution turns to a yellowish green colour. The gradual colour change could be argued that it is due to the deactivation of the catalysts, which also is the cause of the decline of TOF in homogeneous system observed after 6^{th} hour.

5: When a mixed system is initiated, the solution colour gradually turns to an orange-red. (Table 5, Run 29: observation).This is the reverse response in time compared to the homogeneous system.

6: Change in tacticity with respect to the increased temperature is not yet known.

7: If polymer is made in a homogeneous system, the polymer has a high PDI value.

8: At the initial stage of the polymerization, a higher temperature guarantees higher conversion. However, as the polymerization proceeds, the polymerization that is placed at higher temperature does not guarantee higher conversion in long run (Fig. 35).

9: In a mixed system, TOF of the activated catalyst is higher at higher temperature. However, a higher temperature imposes a negative effect on M_n.

10: With the homogeneous system, TOF increases in the beginning of the polymerization and then decreases as the polymerization progresses.

D.5: Fitting the data into models

Ten points have been summarized thus far. As the data is fit into a zero order or a first order model, another point can be drawn for further insight into the mechanistic studies of polymerization carried out by **1**/MAO. However, it seems difficult to determine whether the STY concentration is zero order to the reaction rate or first order (Fig. 48). Another set of data points were also tried to find the best model for this system (Fig. 49, 50, 51).

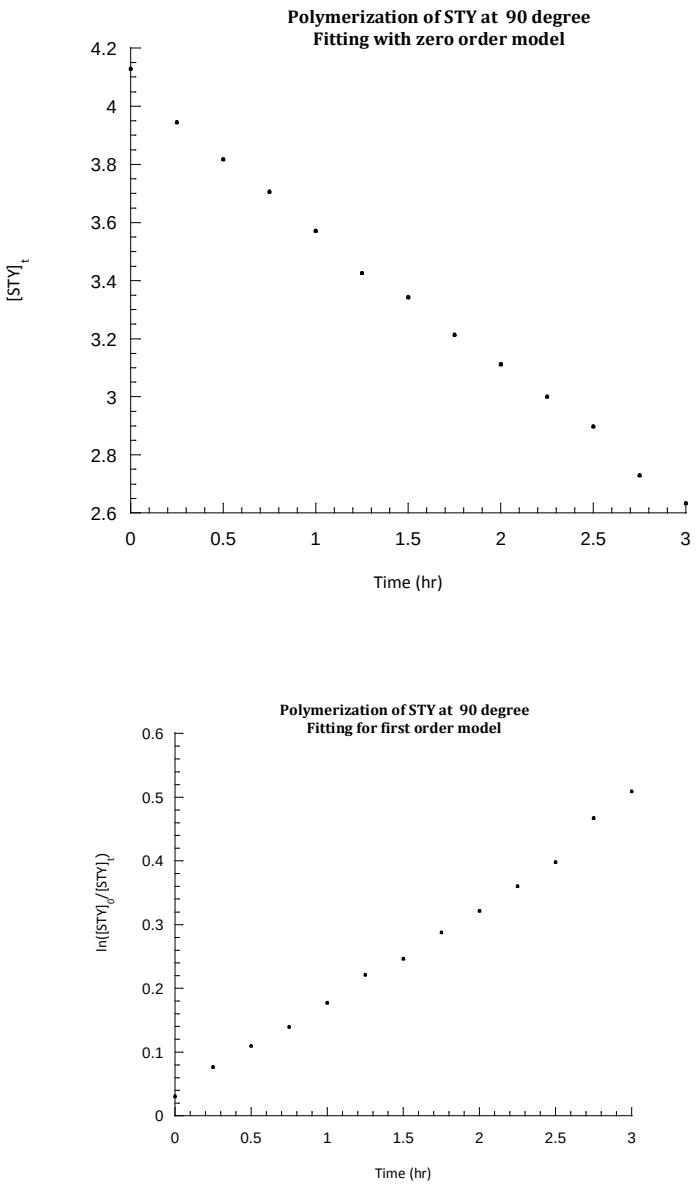

Figure 48: Comparison between two fitting models for polymerization of STY at 90˚ C.

The upper diagram above shows data fit to a zero order reaction model. The lower diagram below represents the model when polymerization is considered to be first order in regards to [STY]. The data points are fairly good fits for both models. Data points in both graphs are average values obtained from Run 25, 26, 27 and 29 in Table 5. The fit for both models with a linear equation, the R^2 values are quite close to each other. R^2= 0.9972 for zero order model and R^2 = 0.9940 for first order model.

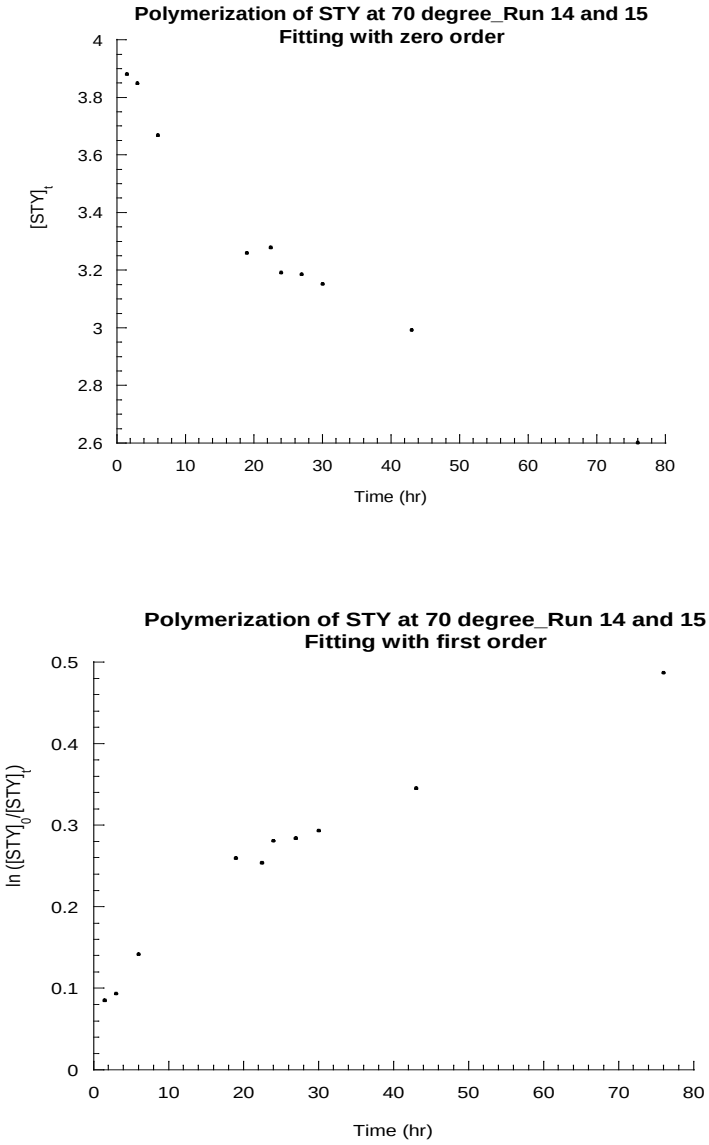

Figure 49: Comparison between zero and first order fitting models for polymerization trials (Run 14, 15) at70℃.

The lower graph represents the model when polymerization is considered to be first order in regards to [STY]. Once again, the data points are fairly good fit for both models. Data points in both graphs are average values obtained from Run 14 and 15 in Table 5. If fit both models with a linear equation, the R^2 values are quite close to each other. R^2= 0.8982 for zero order model and R^2 = 0.9359 for

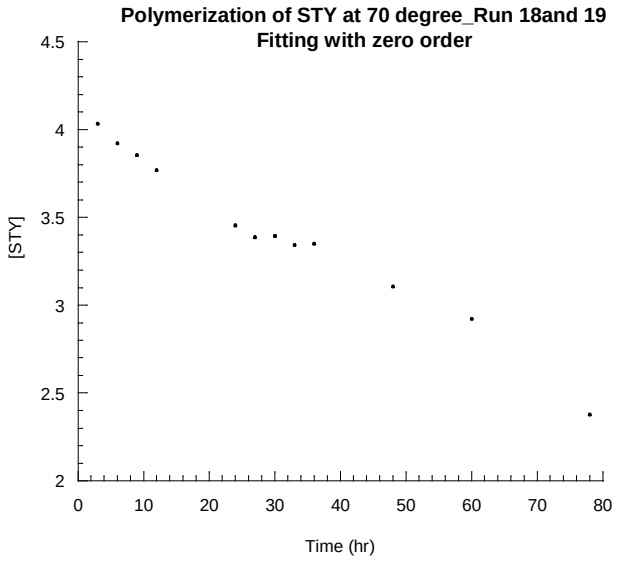

first order model.

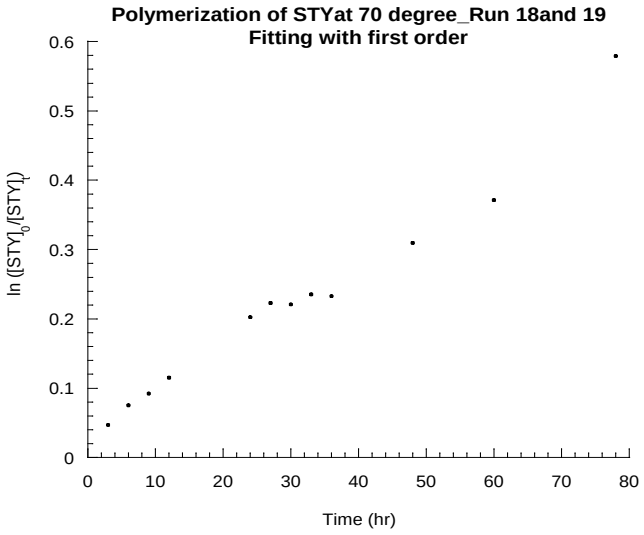

Figure 50: Comparison between two fitting models for two polymerization trials run at 70˚C.

Diagram below represents the model when polymerization is considered to be first order in regards to [STY]. It shows here data points are fairly good fit for both models. Data points in both graphs are average values obtained from Run 18 and 19 in Table 5. If fit both models with a linear equation, the R^2 values are quite close to each other. R^2= 0.9815 for zero order model and R^2 = 0.9717 for the first order model.

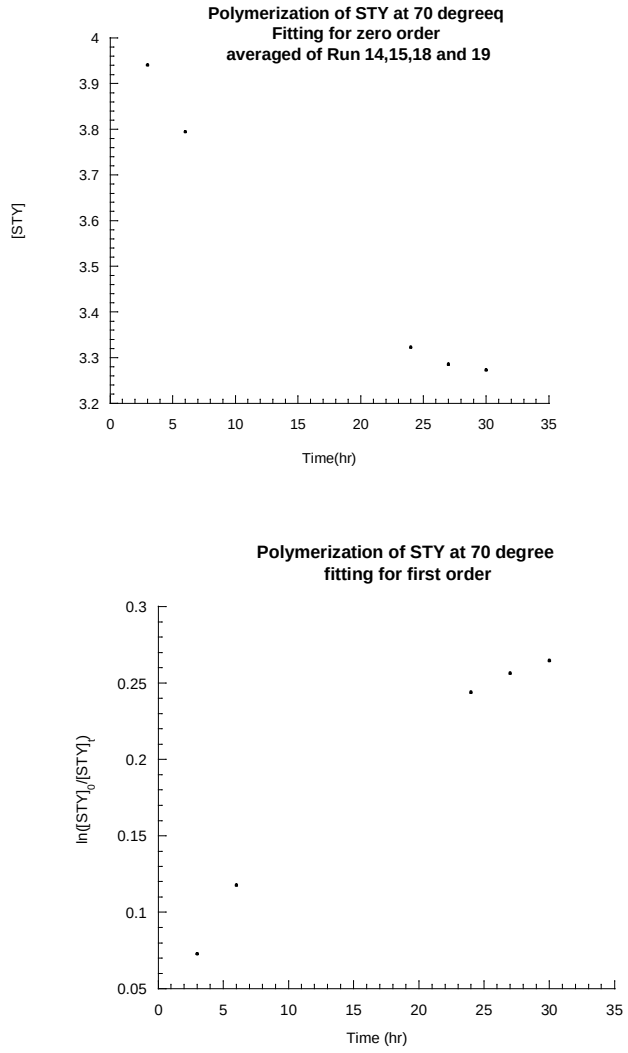

Figure 51: Comparison between two fitting models for two polymerization trials run at 70˚C.

Diagram below represents the model when polymerization is considered to be first order in regards to [STY]. The data points are fairly good fit for both models. Data points in both graphs are average values obtained from average for Run 14, 15, 18, and 19 in Table 5. If both models are fit with a linear equation, the R^2 values are quite close to each other. R^2= 0.9809 for zero order model and R^2 = 0.9822 for first order model. However, there are only five points on the graph. Thus, fitting a linear model would not be very accurate.

The models with fitted equations, including calculations are shown in appendix 5. From Fig. 48 to 51, it seems the polymerization can be regarded either as a zero order reaction or a first order reaction. Reason for the indecisive determination for the reaction order could be that the data obtained to fit the model in Fig. 48 to 51 can only represent the period of polymerization before reaction reaches the plateau. According to Taylor's Theorem expansion, the disappearance of the reactants is linearly proportional to the reaction time at the beginning of a first order reaction. And this is the same phenomenon observed with zero order reaction. In other words, Fig. 48 (the first order model fitting) is well in agreement with zero order because the data obtained represents only the period when conversion is small (~11%). However, Fig. 49 and 50 indicates that even as conversion reaches 30-40%, the polymerization data still fit both zero and first order model well.

In addition, data fit does not go through [0,0] coordinate in Fig. 48 indicating a fast polymerization in the beginning of the reaction, followed by a slower rate of polymerization.

Therefore, the polymerization carried out by **1**/MAO is neither a straightforward first order nor a zero order reaction in regards to the STY concentration. If the polymerization is zero order with respect to STY concentration, then what is shown in Fig. 37 would not be observed. From Fig. 37, it can be concluded the rate of polymerization is in related to monomer concentration. Therefore, STY concentration is not zero order to the rate of polymerization.

In addition to Fig. 48, Fig. 34 and 37 also show that there is a fast polymerization occurring at time 0. The blank trials (Run 22 and Run 24) already rule out the possibility of self-polymerization or side reactions occurring at time 0. Hence, the conversion vs time at the very beginning of polymerization is not strictly linearly, an indication of non-first order of monomer concentration to the overall rate of polymerization. Therefore, STY concentration is not strictly first order to the rate of polymerization.

The rate of polymerization is then more complicated than the anticipated simple form of first order or zero order rate law. In conclusion, the reaction order of the polymerization of STY carried out by **1**/MAO cannot be determined by the data obtained in this project at this stage. The STY concentration order in regards to the overall rate of polymerization might exist in a fractioin form.

Because data used for fitting the model never possess a conversion over 50%, it is then important to investigate experimental conditions in which the activated catalysts yield conversion more than 50%.

In addition, the data used for fitting model are obtained from the mixed system. It is then possible fitting the model with homogeneous data would show the same results obtained from the mixed system or display the fitting results otherwise. Fitting for Run 13 shows the same result as data obtained from mixed system. However, there is not enough data from the homogeneous system. Therefore, the conclusion with respect to the order of STY concentration to the overall rate of polymerization in a homogeneous system should not be hurried to draw.

3. Conclusion and Future work

The activated catalyst **1**/MAO has been found to be stable if it is stored under nitrogen in a -20 ˚C fridge. It is also found that the activated **1** is able to polymerize STY, MMA, and MA into polymers. However, the catalytic activity of activated **1** is very small in polymerizing the MA into a polymer. Nevertheless, activated **1** can be used to polymerize a copolymer of STY and MA.

It is realized that activated **1** is soluble in polymerization solution and possess catalytic activity (TOF = 28.5 (hr^{-1}) at 5^{th} hour) in converting STY into a polymer. However, the polymer recovered has a higher PDI value. In the mixed system in which the polymerization solution is saturated with the soluble activated catalysts, the PS recovered has a better PDI value. It is also noticeable from Table 7 that PDI gradually decreases as polymerization progress (Run 19, three aliquots shown in Table 7). Therefore, few can be done in the future to get a better understanding with regards to the polymerization of STY carried out by **1**:

1: The catalyst turned into soluble species upon initiation of MAO. It is important then to distinguish whether this soluble species present in the polymerization solution is soluble in toluene, or the mixture of toluene and styrene, or soluble in styrene. Investigation of the solvent for the activated catalysts thus becomes important.

If the activated catalysts are soluble in toluene, then same dark brown red colour would be observed in carrying out a homogeneous polymerization of MMA by activated **1**. If the activated catalysts are only soluble in the mixture of toluene and styrene, then homogeneous condition carried out with polymerization of STY might not yield a same result if change the monomer from STY to MAA.

The possibility that activated catalysts are only soluble in styrene is not likely according to

the observation recorded from Run 29. If the activated catalysts are only soluble in STY,then the orange colour would not be observed in Run 29 as STY concentrations gradually decline.

2: It is possible that the higher conversion observed from the mixed system in Fig. 33 resulted from the more soluble activated species (soluble activated catalysts > 0.2100g, but the actual amount of the soluble activated catalysts is not known) present in the Run 12. It is also possible there are activated catalysts present in both the liquid phase (the homogeneous phase) and in the solid phase (activated catalysts are present in the solution as solids). Therefore, it is also crucial to find the critical concentration of the activated catalysts that turn the homogeneous system into the mixed system. Further investigation can then be conducted to see whether the observed higher conversion present in the mixed system comes from activated catalysts that are only soluble in the polymerization solution or from activated catalysts present both in liquid and solid form.

In the beginning of the project, a filtration was performed and it was found homogeneous phase do not yield polymers of PS. Instead, only the activated catalysts in sold form would yield a polymer. This evidence is contradictory to the findings of Run 5-8, and Run 13 from Table 5. If the homogeneous phase does not yield PSs, then there would be no polymer formed in these trials. One possible explanation is that while filtration was carried out, the activated catalysts in homogeneous phase were destroyed. Another possibility is that the acticvated catalysts, though soluble in polymerization solution, have very small solubility to the polymerization solution and therefore not enough amount of activated catalysts present in the liquid phase to yield significant polymer weight to be analyzed.

Hence, it is important to understand the solubility of activated catalysts in the polymerization solution, and to investigate whether the activated catalysts are soluble in toluene, or in the mixture of toluene and STY.

Throughout this project, the tacticity could not be determined due to the broadness of proton peak in the ^{1}H NMR of the recovered PS. It has been reported to dissolve the *s*PS in the methyl ethyl ketone (MEK) and the insoluble part would be isotactic or syndiotactic PS.[53,73] However, a more thorough experimental procedure of the MEK test is required because in some references it was described as "extraction with MEK".[73] As the MEK test procedure is confirmed from literature, the syndiotacticity can then be calculated form the insoluble part of the PS recovered from the MEK test.

Attempts of modifying the trinickel cluster framework of the pre-catalyst all ended in failure. This may be due to a general lack of knowledge in handling or chemically modifying a tri-nuclear crystal. A crystal of the same framework as this Ni cluster but adopts Fe as the metal center was made before together with several other Fe-related dinuclear crystals and was published by Souza, *et al.*[74] Combined with the information of another tri-nuclear crystals published by Gossage *et al.*[64], it might be possible to carry out the modification of this pre-catalyst. Run B2 in Table 3 also conveys certain information in regards to the chemistry of this pre-catalyst.

Because it has been established that a co-polymer of STY and MA could be made with this system, a study could be undertake to make a co-polymer with various compositions of STY and MA. A random tri-co-polymer of MMA, STY and MA is also possible and could be made with ease with this system.

In regards to mechanistic studies, though this pre-catalyst behaves as a catalyst that undergoes a coordination insertion mechanism, a firm piece of evidence required to reject the argument that it undergoes polymerization *via* a radical mechanism rather than coordination insertion would be useful. It was used to believe that a radical trap is sufficient to prove whether the polymerization undergoes a radical or coordination insertion mechanism.

4. Experimental

4.1 General material and procedure.

All reactions in regards to synthesis and attempted modifications of the crystal, {[Ni($C_6H_{12}O_2$)]$_3$$Cl_4$OH}Cl were carried out using standard top bench technique. All experiments in regard to polymerizations were carried out using standard Schlenk techniques under the atmosphere of dinitrogen.

Toluene used in polymerizations was obtained from the M. Braun Solvent Purification System. All other solvents were used as purchased: Acetonitrile (Aldrich, 99.8%), dichloromethane (Aldrich, ACS reagent, ≥99.5%), hexane, mixture of isomers (Aldrich, ACS reagent, ≥98.5%), methanol (Aldrich, ACS reagent, ≥99.5%), Tetrahydrofuran (Aldrich, 99%). Styrene (Aldrich, ReagentPlus®, ≥99%) and methyl methacrylate (Aldrich, 99%) were distilled under vacuum prior to use. The oil bath used for distillation was set at 45˚C. Portions collected at 34-36˚C were discarded. Distillate at 41-43˚C was collected and stored at -65˚C. All other monomers were purchased from Sigma Aldrich and used as received: 1-hexene (99%), methyl acrylate, 1-vinyl-2-pyrrolidinone (98%), methacryloyl chloride (97%). MAO (Aldrich) was used as 10% wt. solution in toluene.

$NiCl_2 \cdot 6H_2O$ (Alfa Aesar, 98%), *N,N,N'N'*-tetramethylethane-1,2-diamine (Aldrich, ReagentPlus, 99%), *N,N'*-bipyridine (Aldrich, 99%), silver nitrate (Aldrich, ACS reagent, >99.0%), nickel nitrate hexahydrate (Fisher Scientific), sodium nitrate(Aldrich, ReagentPlus®, ≥99%), benzyl bromide (Aldrich, Reagent grade, 98%), trimethylsilyl chloride (Aldrich), butylamine (Aldrich, 99.5%) were used as purchased.

Nuclear magnetic resonance (NMR) experiments were recorded on a 400MHz Bruker Avance II spectrometer using deuterated chloroform ($CDCl_3$) as the solvent unless otherwise

indicated. ^{1}H and ^{13}C NMR spectra were referenced to the residual $CHCl_3$ (δ_H = 7.26 ppm) and the central peak of $CDCl_3$ (δ_c = 77.0 ppm) solvent signal respectively. The absolute molecular weight and polydispersity index of the polymers were determined by gel permeation chromatography on a Viscotek GPCmax VE2001 GPC solvent/Sample module. Unless otherwise stated, the polymer was dissolved in THF with a concentration of 1mg/ml. The broad and narrow polystyrene standards were used as reference in determining the molecular weight of the polymer. Crude powder or crystals yielded from the modification of Ni cluster were characterized by the infrared spectroscopy on a Perkin Elmer Spectrum One. Unless otherwise mentioned, all IR spectra of the compounds were obtained through the making of a KBr disk.

4.2 Synthesis of the pre-catalyst, *μ*3-chloro-*μ*3-hydroxotris (μ-chloro) tris (*N,N,N',N'*-tetramethylethylene-1,2-diamine) trinickel(II) chloride, $\{[Ni(C_6H_{12}O_2)]_3Cl_4OH\}Cl$. (Complex 1)

The pre-catalyst was synthesized according to a modified version of the method in Handley *et al.*[66] In 500 mL round bottom flask was added 4.50 g (19 mmol) of $NiCl_2{\cdot}6H_2O$ and 25 mL (165 mmol) of TMEDA in 250 mL of THF and heated under reflux overnight. A light green crude powder was obtained through filtration of reaction mixture. The pale green coloured powder was then dissolved in DCM and layered slowly with hexanes for recrystallization. Comparison of the IR spectrum of recovered dark green crystals to the previously reported IR spectrum[64b] confirmed the crystals to be $\{[Ni(C_6H_{12}O_2)]_3Cl_4OH\}Cl$. It was found that the crystals obtained through one solvent system (dissolving in DCM without layering in hexane) recrystallized in shorter period of time and could also be used in polymerization of styrene.

4.3 Syntheses carried out in attempt to modify the trinickel cluster.

A: Synthesis of the "blue" Ni complex, acetonitriletri(aqua)(*N,N,N'N'*-tetramethylethylenediamine) nickel (II) chloride (2).

There were three methods used to synthesize the blue coloured complex. Procedures of the three methods differed only in the starting compound that contained the nitrate anion and the molar ratio of the nitrate-containing compound to the trinickel cluster. The amounts of the starting compounds been used in each method were recorded in Table 8.

Table 8: Amounts of starting materials used in the synthesis of **2**.

	Starting material Nitrate-containing compound	Amount of starting material (g)	Amount of second starting material: the trinickel cluster (g)	Solvent	Conditions
Method 1	$AgNO_3$	0.7193 (1.00 mmol)	0.7193 (1.00 mmol)	THF (50 mL)	Reflux overnight
Method 2	$Ni(NO_3)_2 \cdot 6H_2O$	0.058 (0.99 mmol)	0.716 (0.20 mmol)	THF (50 mL)	Reflux overnight
Method 3	$NaNO_3$	0.042 (1.38 mmol)	0.3593 (0.91 mmol)	THF (45 mL)	Reflux overnight

In each method, the weighed nitrate starting material and trinickel cluster were both put into a round bottom flask, solvent added, and the reaction was refluxed overnight. Crude was then collected once the reaction cooled down from the reflux. The crude green powder was then recrystallized in hot boiling AcCN. In the same recrystallizing solvent, blue crystals of **2** would first appear after a 2-3 day period, followed by the appearance of green crystals after a period of about one week.

B: Attempted synthesis to modify the cationic ion of Ni 1 cluster into a neutral species.

NaH (0.033 g, 1.4 mmol) and trinickel cluster (0.6588 g, 0.9160 mmol) was placed in a flamed-dried Schlenk flask. The flask was put under vacuum and then back-filled with dinitrogen, followed by injection of 30mL of THF, the reaction solvent. The reaction was then carried out under dinitrogen atmosphere for 3 days. Dark green coloured crude powder was obtained through filtration under inert condition. This crude powder under vacuum turned from a dark green to the same green colour of that of the trinickel cluster.

C: Attempted syntheses to replace the hydrogen atom of the μ_3-hydroxyl group of cluster 1 with a protecting group .

Several different reagents were explored in an attempt to replace the H atom with different protecting groups. Table 9 lists the amounts of the compounds used in the reaction.

The general procedure in attempt to replace the proton with a protecting group was as follows: weigh out cluster **1** and the protecting group and place both components into a round bottom flask. Add the desired reaction solvent to the flask. The solution was then stirred at room temperature for a period of two days. Crude green powders are recovered through vacuum filtration.

Table 9: Attempts to replace the proton on the trinickel cluster with a protecting group.

Trials	Complex **1** (g)	Protecting group (mL)	Reaction Solvent	Conditions
1	0.60 (4.6 mmol)	Benzyl bromide 0.55 (0.83 mmol)	THF (35.0 mL)	Reflux overnight
2	0.63 (1.7 mmol)	Benzyl bromide 0.20 (0.87 mmol)	DCM (50.0 mL)	Stirring overnight at R.T.
3	1.132 (1.6 mmol)	Chlorotrimethyl silane 0.20 (1.58 mmol)	DCM (50.0 mL)	Stirring overnight at R.T.

D: Attempted syntheses to replace one TMEDA ligand in 1 with a Bpy ligand.

The materials and quantities used in attempt to replace one TMEDA ligand with one Bpy ligand are recorded in Table 10.

The general procedure carried out in attempt to replace one TMEDA ligand with one Bpy ligand for trials 1 and 3 in table 10 was as follows: weigh out cluster 1 and Bpy and place in a round bottom flask. Add the desired reaction solvent to the flask and reflux the solution overnight. Crude green coloured powders were then obtained through vacuum filtration.

The procedure carried out for trial 2 was altered. Instead of reacting **1** directly with the ligand Bpy, the ligand was added at the very beginning of synthesis of **1**. In the case, the $NiCl_2 \cdot 6 H_2O$, Bpy and desired amounts of TMEDA were added into a round bottom flask and solvent (THF) added. The reaction was then stirred overnight at reflux. Products were collect through filtration.

Table 10: Amounts of materials used in the attempts of modifying the ligands of **1**.

Trials	Starting material 1 (g)	Starting material 2 (g)	Starting material 3 (mL)	Reaction Solvent	Conditions
1[(a)]	0.089 (0.12 mmol)	0.022 (0.14 mmol)	---------	DCM (10 mL)	Reflux overnight
2[(b)]	0.13 (0.34 mmol)	0.21 (0.87 mmol)	0.40 mL (2.44 mmol)	THF (16 mL)	Reflux overnight
3[(a)]	0.210 (2.92 mmol)	0.0472 (2.92 mmol)	----------	THF (13mL)	Reflux overnight

(a): Starting material 1: complex **1**; starting material 2: Bpy

(b): Starting material 1: $NiCl_2 \cdot 6\ H_2O$; starting material 2: Bpy; starting material 3: TMEDA

4.4 Polymerization

A: Polymerization of styrene/ methyl methacrylate/ 1-hexene/ methyl acrylate

General procedures for polymerization of styrene, methyl methacrylate, 1-hexene and methylacrylate were as follows: pre-catalysts (complex **1)** were measured and crushed *via* a mortar and pestle then poured into a 50 or 100 mL flame-dried Schlenk flask containing a magnetic stir bar. The crushed **1** was then put under vacuum for at least 2 hours and stirred by a magnetic stir bar which further converted the pre-catalyst into a fine powder. Solvent (toluene) was then introduced into the flask *via* syringe. Addition of the monomer then followed *via* a second syringe. Reaction was then initiated by the addition of MAO. The molar ratio of pre-catalyst to MAO to monomer was 1 to 3 to 150. The volume of solvent added was added in 50% (v/v) solvent to monomer ratio. The crude polymers were then precipitated in excess

amount of MeOH. To obtain pure polymer, the crude polymer was re-dissolved in THF and then re-precipitated in excess MeOH. The washing cycle was repeated 2-3 times.

During polymerization of styrene or methyl methacrylate, the reaction mixtures would turn from a light green to a dark green colour upon addition of MAO. Colour change upon addition of MAO was not observed in polymerization of 1-hexene, 1-vinyl-2-pyrrolidinone, or methylacrylate. Comparisons of ^{1}H NMR spectrum of polystyrene and polymethyl methacrylate to those obtained in Gossage *et al.*[64] confirmed that the recovered polymers of this work were the same as the earlier reported ones. Polymerization attempts using 1-hexene did not yield polymers. Polymerization of methylacrylate yielded only a very small amount of a rubbery material (21% yield according to weight). The rubbery material over a period of few hours would turn into a hard, opaque solids. This solid did not dissolve in THF, acetone, methanol, or chloroform. Therefore, GPC results, ^{1}H and ^{13}C-NMR spectrum of this rubbery material could not be obtained.

B: Polymerization of random co-polymer of styrene and methyl acrylate

The pre-catalyst **1** (0.2915 mmol, 0.2096 g) was crushed with mortar and pestle and introduced into a 50mL Schlenk flask. It was then stirred by the magnetic stir bar into fine powder under vacuum. 10mL of toluene was then introduced into the flask *via* syringe. Pre-catalyst was then activated by MAO (0.80 mmol, 0.60 mL). Addition of styrene (5.0 mL, 40 mmol) was then followed. Methylacrylate (5.0 mL, 55 mmol) was added last to the reaction flask. Methylacrylate was put under vacuum first, then back filled with dinitrogen for 5 minutes prior to use in polymerization. The light green colour of the mixture did not change upon addition of monomers into the activated catalysts. However, after 12 hours, the colour turned into a dark pink. After 7 days, the stirring was stopped and air was introduced to the reaction mixture. Crude

white polymers were precipitated out in MeOH. The yield determined by weight was 13%.

C: Polymerization of methylacryloyl chloride

Ni cluster crystals (0.4120 mmol, 0.2960 g) were crushed by mortar and pestle and then further powderdized by the stirring with a magnetic stirring bar under vacuum in the Schlenk flask. Toluene (7.0 mL) was introduced into the flask, followed by addition of methacryloyl chloride (61mmol, 6.0 mL). An additional amount of toluene (8mL) was added to the flask. The reaction was then activated by addition of MAO (1.2 mmol, 0.80 mL). After 3 days of reaction, a blue gel-like material appeared on the wall of the flask. The flask was placed in an ice bath and cooled to 5˚ C with stirring. Butylamine (12.50 mL) was then added into the flask dropwisely *via* a syringe. The blue gel colour disappeared with the addition of butylamine. After one and half hours, the stir bar could barely stir in the flask as most of the mixture had turned into gel-like material. The green mixture was then dissolved in THF and a white polymer purified by re-precipitated in an excess of hexanes.

The isolated polymer formed did not dissolve in THF. Therefore, in order to obtain a GPC analysis, 2mg polymer/mL of THF was first sonicated and the solution was filtered through a 0.55μm filter. However, only IR signal was detected during the GPC analysis and absolute molecular weight and P.D.I. determinations were not made.

4.5 Kinetics of the polymerization of styrene and methyl methacrylate catalyzed by the trinickel cluster.

The determination of the kinetics of polymerization of styrene by the tri-nuclear was carried out as detailed below.

A 100mL Schlenk flask containing a stir bar was flamed dried and wrapped with Al foil. 1.0500 g (1.4603 mmol) A sample of the pre-catalyst **1** (1.0500 g, 1.460mmol) was weighed and

crushed into a fine powder by mortar and pestle. The pre-catalyst was then placed into the foil-wrapped Schlenk flask, put under vacuum (1×10^{-3} mmHg) and further powdered by the magnetic stir bar for over a period of 2 hours. The flask that contained the **1** was then placed into an oil bath at the desired temperature. Toluene (50.0 mL) was added to the flask *via* a syringe, followed by injecting 50.0 mL (435 mmol) of styrene *via* a second syringe. The reaction mixture was then allowed to equilibrate at the desired temperature for 2 hours.

Prior to the introduction of MAO, a needle attached to an empty syringe (**A**) would be introduced to the mixture (sitting above the surface of the mixture). The polymerization was then initiated by injecting 2.90 mL of MAO (10% w.t. solution in toluene) *via* a different syringe. An aliquot of the polymerization solution was taken right after the polymerization was initiated *via* syringe **A**. Consecutive aliquots were taken at time interval of 15 min. for a period of three hours in the case of polymerization carried out at 90˚C.

Each aliquot was collected into a pre-weighed two neck round bottom flask. One of the openings of the two neck flask was sealed with a rubber septa and the other opening was connected to the Schlenk line to expose the aliquot to high vacuum. After a period of one hour, the flask that contained the dried aliquot was weighed by an analytical balance to an accuracy of ± 0.0001 g.

In polymerization of methyl methacrylate, the procedure was the same as above except for the experimental set up for the trial taken was at 25.0˚C. In order to better control the temperature at 25˚C, the silicon oil was put into a water-jacketed beaker. The beaker was then connected to a water circulating bath with the temperature of water bath set at 25.0˚C.

Appendix 1: General polymerization of styrene (Non-kinetic studies)

To be noticed: the polymerization recorded in the following table is a guide should you need to check the lab book. The conditions for the polymerization are mostly the same: all carried out in room temperature, roughly 50% (v/v) of STY, total solution roughly 10mL, pre-cat/MAO =1:3.

Table 11: Summary of polymerization of STY.

Polymerization of styrene			
Run	Date	Procedures carried out	Observations
PS-1	2012: 02/15,21,23 ; 03/01,02,06 ,12,13 03/14	Distillation: 1-139 First polymerization: 1-144,148,149,150 (transfer to glove box); 7days reaction,1-157, NMR analysis 1-158; GPC 1-160; totally take out the flask and analyze the overall product (13 days); GPC 1-162; NMR 1-170,WT analysis 1-171 Second one: 03/14 pg1-172	No pink colour observed after adding MAO in the first polymerization
PS-1	2012 02/23; 03/12 04/04,05,18	Re-prepare ^{1}H NMR because the first spectrum was not satisfactory Take out from glovebox on 03/27 Put PS under vacuum with Schlenk line, don't put in heating oven, not working	1-148,149,150,151,170.171,185, 186,187 1-171:58.09% wt 1-195: ^{13}C NMR
Run	Date	Procedures	Observations
PS-2	2012 03/14	Cat: 0.2124g	1-172, 174,183

	.04/09,17,25	Cat from single solvent system Cat stirred in styrene and toluene for 3 hours Tried to have cat soluble in toluene and monomer, then add MAO 2 days after overnight Colour of pink orange appearing Stop reaction on 03/27	1-188: (GPC)0.0021g in 2.1THF 1-194: ^{1}H NMR and ^{13}CNMR 2-28: collect the PS 2-31: wt 0.2g
PS-3	2012/03/23	Cat 0.1061g 5mL toluene 5mL styrene MAO: 0mL	1-180,183 No viscosity observed after 7 days (04/02), stop reaction
PS-4	2012/04/03	Cat 0.2090g 5mL toluene 0mL styrene MAO: 0.6mL-0.8mL	Colour turned from light green to dark green Pre-catalyst was activated, no monomer added The activated catalyst was then placed in the -20°C fridge
PS-4(b)	2012/04/10, 19,24,25 05/18	*USE the activated catalyast from PS-4* 5mL styrene 14 days rxn	1-188,190: put in -20°c fridge again because I want to freeze the polymerization for awhile 2-25: transfer into glovebox 2-31 2-52: collect crude (from MeOH ppte) (0.8g)
Run	Date	Procedures	Observations
PS-5	2012/04/10,	Cat: 0.1048	1-189, 190

	11,19,25,27 05/02	4.6-4.8mL toluene 0.6mL MAO Then 5 mL styrene Transfer to glovebox on 04/11 Out from Glove on 04/19	Solution colour : pink colour appeared on top layer of solution for awhile. Catalysts turned into black (when continue adding MAO over 0.6mL) 2-25,31 2-32: ^{13}C NMR and ^{1}H NMR 2-35: black catalyst ring on the flask
PS-6	2012/04/11	Cat 0.1049g 4.6mL toluene 0.6mL MAO	1-191 Green catalyst became big chunk of black solids, therefore considered the reaction to be failure, originally thought there might be oxygen present
PS-7	2012/04/12, 19 05/15	0.1051g cat 4.6mL toluene 0.6Ml MAO	1-192: Catalyst became black and looks like solidify on the glass wall (large sticky solids) Flask remains in fumehood 2-25: transfer to glovebox 2-47: still no viscosity, finally realize I did not add styrene into the flask
PS-8	2012/05/26 06/04,05,08	0.2101g cat 5mL toluene] 5mL styrene 0.6mL MAO 40°C (sand bath) RXn start: 05/26 Rxn stop: 06/02 (7 days)	2-62 2-68: Rxn stopped Wt: 0.25g 2-70: PPTE in MeOH 2-73: 1.82g polymer from oven
Run	Date	Procedures	Observations
PS-9	2012/05/26; 06/04,05,08	0.2096g Cat 5mL toluene	2-62,68 2-68: rxn stopped

		5mL styrene 0.6mL MAO 38-43°C (sand bath) Start: 05/26 Stop :06/04 (9 days)	Wt: 0.64g crude polymer 2-70:ppte in MeOH 2-74: Wt:2.38g
PS-10	2012/05/28, 30 06/05,08.15	0.2101g cat 5mL toluene 0.6-0.8 mL MAO 2-65: liquid part transferred to ps12, then add monomer and new solvent Start : 05/28 06/05: stopped reaction; viscous brown (8 days)	2-63 2-65: transfer suspension into another Schlenk flask, add new 5mL toluene and 5mL styrene into original flask to see if remaining solids still carry out polymerization 2-70:stopped rxn 2-73: ppte in MeOH 2-78: 0.41g
PS-11	2012/05/28; 06/05,06,08	0.2096g cat 5mL toluene 0.6mL MAO 5mL styrene Start: 05/28 Stop: 06/05 (8 days)	2-63 2-69: reaction stopped; 034g 2-74: 2.93g
PS-12	2012/05/30; 06/05	Suspension from PS-10 and add 5mL styrene 06/05: rxn stopped stirring; viscous brown mixture 06/06: precipitation in MeOH does not yield PS	2-66,70,71
Run	Date	Procedures	Observations
PS-13	2012/06-01, 04	0.2096g cat 40°C	2-67.68 2-68: stopped reaction

		Toluene+MAO+5mL styrene (amount of toluene and MAO not recorded) Start 06/01 Stop 06/04	Considered failed because suspect air goes into the flask
PS-14	2012/06/06, 07,08	0.2101g cat 5mL toluene 0.6mL MAO Then +5mL styrene 40°C Rxn start: 06/07 Rxn stop: 06/08 (1 day)	2-71,72 2-72: add monomer 2-73: ppte in MeOH, no polymer
PS-15	2012/06/06, 07,08	0.2096g cat 5mL toluene 0.6mL MAO 5mL styrene 30°C Rxn start 06/07 Rxn stop 06/011 (4 days)	2-71,72 2-72: add monomer 2-73 2-78: 0.48g 2-87: GPC
PS-16	2012/06/08, 13	0.2101 g cat	2-73,77,78 Problematic later because timer set so don't really know the temperature
PS-17	2012/06/13		2-78 Problematic later because timer does not work according to plan, so don't know what is the temperature of the reaction running
PS-18	2012/07/31	0.21 g cat+5mL styrene+5mL toluene+0.6mL MAO	2-84,87
Run	Date	Procedures	Observations
PS-19	2012/08/08	0.2098g cat+5mL toluene+5mL styrene+0.6mL MAO	

		40°C Start : 08/08	
PS-20	2012/10/22 to 2012/11/05	At 50°C	
PMMA-1	2012/05/17, 18,19,30	0.1051g cat 5mL toluene 0.6-0.8mL MAO 5mL MMA	2-50: cat became black 2-52: once starting to stir, colour gradually turned to green-brown colour 2-54: test, no polymer formed; colour of solution is dark brown red colour 2-60,65,69 (nmr)

Appendix 2: Crystallography data for crystal 2

Table 1. Crystal data and structure refinement for d12312.

Identification code	d12312	
Empirical formula	C8 H25 Cl2 N3 Ni O3	
Formula weight	340.92	
Temperature	147(2) K	
Wavelength	0.71073 Å	
Crystal system	Orthorhombic	
Space group	P 21 21 21	
Unit cell dimensions	a = 7.8722(11) Å	α= 90°.
	b = 12.4209(18) Å	β= 90°.
	c = 16.044(2) Å	γ = 90°.
Volume	1568.8(4) $Å^3$	
Z	4	
Density (calculated)	1.443 Mg/m^3	
Absorption coefficient	1.578 mm^{-1}	
F(000)	720	
Crystal size	0.30 x 0.20 x 0.13 mm^3	
Theta range for data collection	2.07 to 27.52°.	
Index ranges	-10<=h<=6, -16<=k<=14, -20<=l<=20	
Reflections collected	13249	
Independent reflections	3595 [R(int) = 0.0247]	
Completeness to theta = 27.52°	99.6 %	
Absorption correction	Semi-empirical from equivalents	
Max. and min. transmission	0.7456 and 0.6655	
Refinement method	Full-matrix least-squares on F^2	
Data / restraints / parameters	3595 / 0 / 183	
Goodness-of-fit on F^2	1.006	
Final R indices [I>2sigma(I)]	R1 = 0.0141, wR2 = 0.0317	
R indices (all data)	R1 = 0.0150, wR2 = 0.0318	
Absolute structure parameter	0.001(6)	
Largest diff. peak and hole	0.182 and -0.158 $e.Å^{-3}$	

Table 2. Atomic coordinates (x 10^4) and equivalent isotropic displacement parameters ($Å^2$x 10^3) for d12312. U(eq) is defined as one third of the trace of the orthogonalized U^{ij} tensor.

	x	y	z	U(eq)
Ni(1)	4072(1)	4716(1)	4294(1)	12(1)
Cl(1)	3903(1)	1081(1)	4583(1)	21(1)
Cl(2)	4604(1)	5731(1)	6765(1)	25(1)
O(1)	2864(1)	4348(1)	5421(1)	18(1)
O(2)	5922(1)	5505(1)	5003(1)	15(1)
O(3)	5621(1)	3339(1)	4373(1)	19(1)
N(1)	2694(1)	6188(1)	4137(1)	14(1)
N(2)	5190(1)	5111(1)	3119(1)	17(1)
N(3)	2277(1)	3718(1)	3781(1)	17(1)
C(1)	3640(2)	6769(1)	3477(1)	21(1)
C(2)	4138(2)	6006(1)	2784(1)	22(1)
C(3)	915(2)	6009(1)	3865(1)	19(1)
C(4)	2633(2)	6874(1)	4894(1)	23(1)
C(5)	5185(2)	4207(1)	2518(1)	26(1)
C(6)	6981(1)	5464(1)	3219(1)	26(1)
C(7)	1269(2)	3109(1)	3594(1)	17(1)
C(8)	-20(2)	2326(1)	3356(1)	26(1)

Table 3. Bond lengths [Å] and angles [°] for d12312.

Ni(1)-N(3)	2.0522(10)
Ni(1)-O(2)	2.0912(9)
Ni(1)-O(1)	2.0925(9)
Ni(1)-O(3)	2.1039(9)
Ni(1)-N(2)	2.1380(10)
Ni(1)-N(1)	2.1406(10)
O(1)-H(1OA)	0.709(16)
O(1)-H(1OB)	0.827(16)
O(2)-H(2OA)	0.754(17)
O(2)-H(2OB)	0.809(16)
O(3)-H(3OA)	0.850(17)
O(3)-H(3OB)	0.791(16)
N(1)-C(1)	1.4828(15)
N(1)-C(3)	1.4833(14)
N(1)-C(4)	1.4838(16)
N(2)-C(5)	1.4802(17)
N(2)-C(6)	1.4847(14)
N(2)-C(2)	1.4867(16)
N(3)-C(7)	1.1364(15)
C(1)-C(2)	1.5135(18)
C(1)-H(1A)	0.9900
C(1)-H(1B)	0.9900
C(2)-H(2A)	0.9900
C(2)-H(2B)	0.9900
C(3)-H(3A)	0.9800
C(3)-H(3B)	0.9800
C(3)-H(3C)	0.9800
C(4)-H(4A)	0.9800
C(4)-H(4B)	0.9800
C(4)-H(4C)	0.9800
C(5)-H(5A)	0.9800
C(5)-H(5B)	0.9800
C(5)-H(5C)	0.9800

C(6)-H(6A)	0.9800
C(6)-H(6B)	0.9800
C(6)-H(6C)	0.9800
C(7)-C(8)	1.4568(17)
C(8)-H(8A)	0.9800
C(8)-H(8B)	0.9800
C(8)-H(8C)	0.9800

N(3)-Ni(1)-O(2)	168.75(4)
N(3)-Ni(1)-O(1)	84.37(4)
O(2)-Ni(1)-O(1)	87.12(4)
N(3)-Ni(1)-O(3)	86.12(4)
O(2)-Ni(1)-O(3)	86.83(4)
O(1)-Ni(1)-O(3)	91.93(4)
N(3)-Ni(1)-N(2)	93.91(4)
O(2)-Ni(1)-N(2)	94.85(4)
O(1)-Ni(1)-N(2)	177.27(4)
O(3)-Ni(1)-N(2)	90.06(4)
N(3)-Ni(1)-N(1)	96.88(4)
O(2)-Ni(1)-N(1)	90.94(4)
O(1)-Ni(1)-N(1)	93.34(4)
O(3)-Ni(1)-N(1)	174.17(4)
N(2)-Ni(1)-N(1)	84.76(4)
Ni(1)-O(1)-H(1OA)	118.5(14)
Ni(1)-O(1)-H(1OB)	118.6(10)
H(1OA)-O(1)-H(1OB)	106.5(17)
Ni(1)-O(2)-H(2OA)	115.8(13)
Ni(1)-O(2)-H(2OB)	109.9(11)
H(2OA)-O(2)-H(2OB)	102.3(16)
Ni(1)-O(3)-H(3OA)	117.9(11)
Ni(1)-O(3)-H(3OB)	119.0(11)
H(3OA)-O(3)-H(3OB)	103.6(15)
C(1)-N(1)-C(3)	109.68(9)
C(1)-N(1)-C(4)	108.73(10)
C(3)-N(1)-C(4)	107.23(9)

C(1)-N(1)-Ni(1)	104.22(7)
C(3)-N(1)-Ni(1)	112.65(7)
C(4)-N(1)-Ni(1)	114.22(7)
C(5)-N(2)-C(6)	107.27(10)
C(5)-N(2)-C(2)	109.24(10)
C(6)-N(2)-C(2)	110.32(11)
C(5)-N(2)-Ni(1)	113.49(8)
C(6)-N(2)-Ni(1)	111.34(7)
C(2)-N(2)-Ni(1)	105.17(7)
C(7)-N(3)-Ni(1)	171.34(10)
N(1)-C(1)-C(2)	110.50(10)
N(1)-C(1)-H(1A)	109.5
C(2)-C(1)-H(1A)	109.5
N(1)-C(1)-H(1B)	109.5
C(2)-C(1)-H(1B)	109.5
H(1A)-C(1)-H(1B)	108.1
N(2)-C(2)-C(1)	110.27(10)
N(2)-C(2)-H(2A)	109.6
C(1)-C(2)-H(2A)	109.6
N(2)-C(2)-H(2B)	109.6
C(1)-C(2)-H(2B)	109.6
H(2A)-C(2)-H(2B)	108.1
N(1)-C(3)-H(3A)	109.5
N(1)-C(3)-H(3B)	109.5
H(3A)-C(3)-H(3B)	109.5
N(1)-C(3)-H(3C)	109.5
H(3A)-C(3)-H(3C)	109.5
H(3B)-C(3)-H(3C)	109.5
N(1)-C(4)-H(4A)	109.5
N(1)-C(4)-H(4B)	109.5
H(4A)-C(4)-H(4B)	109.5
N(1)-C(4)-H(4C)	109.5
H(4A)-C(4)-H(4C)	109.5
H(4B)-C(4)-H(4C)	109.5
N(2)-C(5)-H(5A)	109.5

N(2)-C(5)-H(5B)	109.5
H(5A)-C(5)-H(5B)	109.5
N(2)-C(5)-H(5C)	109.5
H(5A)-C(5)-H(5C)	109.5
H(5B)-C(5)-H(5C)	109.5
N(2)-C(6)-H(6A)	109.5
N(2)-C(6)-H(6B)	109.5
H(6A)-C(6)-H(6B)	109.5
N(2)-C(6)-H(6C)	109.5
H(6A)-C(6)-H(6C)	109.5
H(6B)-C(6)-H(6C)	109.5
N(3)-C(7)-C(8)	179.83(16)
C(7)-C(8)-H(8A)	109.5
C(7)-C(8)-H(8B)	109.5
H(8A)-C(8)-H(8B)	109.5
C(7)-C(8)-H(8C)	109.5
H(8A)-C(8)-H(8C)	109.5
H(8B)-C(8)-H(8C)	109.5

Symmetry transformations used to generate equivalent atoms:

Table 4. Anisotropic displacement parameters ($Å^2 x\ 10^3$) for d12312. The anisotropic displacement factor exponent takes the form: $-2\pi^2[\ h^2\ a^{*2}U^{11} + ...\ + 2\ h\ k\ a^*\ b^*\ U^{12}\ ]$

	U^{11}	U^{22}	U^{33}	U^{23}	U^{13}	U^{12}
Ni(1)	10(1)	11(1)	13(1)	-1(1)	-1(1)	0(1)
Cl(1)	13(1)	18(1)	30(1)	2(1)	2(1)	-1(1)
Cl(2)	28(1)	31(1)	17(1)	-6(1)	0(1)	-2(1)
O(1)	15(1)	23(1)	16(1)	-1(1)	-2(1)	-3(1)
O(2)	13(1)	16(1)	17(1)	-3(1)	-1(1)	1(1)
O(3)	17(1)	13(1)	27(1)	-1(1)	-5(1)	0(1)
N(1)	14(1)	13(1)	15(1)	0(1)	0(1)	1(1)
N(2)	16(1)	18(1)	17(1)	-1(1)	2(1)	-1(1)
N(3)	17(1)	17(1)	17(1)	0(1)	-2(1)	0(1)
C(1)	20(1)	15(1)	27(1)	6(1)	2(1)	0(1)
C(2)	24(1)	24(1)	18(1)	7(1)	4(1)	0(1)
C(3)	13(1)	20(1)	25(1)	4(1)	-3(1)	2(1)
C(4)	28(1)	19(1)	24(1)	-4(1)	-4(1)	8(1)
C(5)	32(1)	28(1)	18(1)	-8(1)	5(1)	0(1)
C(6)	16(1)	37(1)	27(1)	-1(1)	6(1)	-5(1)
C(7)	21(1)	17(1)	13(1)	2(1)	0(1)	0(1)
C(8)	29(1)	26(1)	24(1)	0(1)	-3(1)	-14(1)

Table 5. Hydrogen coordinates (x 10^4) and isotropic displacement parameters ($Å^2$x 10^3) for d12312.

	x	y	z	U(eq)
H(1A)	4673	7100	3719	25
H(1B)	2921	7353	3248	25
H(2A)	3104	5709	2519	27
H(2B)	4789	6402	2353	27
H(3A)	355	6705	3781	29
H(3B)	306	5600	4294	29
H(3C)	910	5603	3341	29
H(4A)	2082	7559	4760	35
H(4B)	3792	7010	5091	35
H(4C)	1986	6505	5331	35
H(5A)	5744	4432	2001	39
H(5B)	4010	3997	2398	39
H(5C)	5796	3593	2758	39
H(6A)	7466	5624	2670	40
H(6B)	7638	4889	3485	40
H(6C)	7020	6112	3567	40
H(8A)	-963	2354	3754	39
H(8B)	477	1602	3357	39
H(8C)	-441	2495	2796	39
H(1OA)	3070(20)	4658(14)	5778(10)	33(5)
H(1OB)	1820(20)	4272(12)	5422(9)	33(4)
H(2OA)	6750(20)	5211(14)	5052(10)	35(5)
H(2OB)	5600(20)	5564(13)	5480(10)	37(5)
H(3OA)	5140(20)	2739(13)	4476(10)	40(5)
H(3OB)	6410(20)	3345(12)	4679(9)	27(4)

Table 6. Hydrogen bonds for d12312 [Å and °].

D-H...A	d(D-H)	d(H...A)	d(D...A)	<(DHA)
O(1)-H(1OA)...Cl(2)	0.709(16)	2.397(17)	3.0789(11)	161.8(17)
O(1)-H(1OB)...Cl(1)#1	0.827(16)	2.337(16)	3.1630(10)	175.6(14)
O(2)-H(2OA)...Cl(1)#2	0.754(17)	2.405(17)	3.1361(10)	163.8(16)
O(2)-H(2OB)...Cl(2)	0.809(16)	2.217(16)	3.0251(10)	177.3(15)
O(3)-H(3OA)...Cl(1)	0.850(17)	2.286(17)	3.1319(11)	173.1(16)
O(3)-H(3OB)...Cl(1)#2	0.791(16)	2.401(16)	3.1622(10)	161.9(15)

Symmetry transformations used to generate equivalent atoms:

#1 x-1/2,-y+1/2,-z+1 #2 x+1/2,-y+1/2,-z+1

Appendix 3: Reaction conditions for polymerization of ethylene and propylene

Below is the correspondence between Dr. White from Exova in regard to the reaction condition for polymerization of ethylene and propylene carried out by **1**.

Background Information

Gossage and co-workers have demonstrated the potential of a new air stable nickel catalyst by polymerizing styrene and methyl methacrylate.[64] They would like to extent their work to include two gaseous monomers – ethylene and propylene.

Safety concerns and Work Plan

1. *Polymerization* - Polymer yields appear low and polymerization rates lower than for typical free radical or Zeigler Natta type processes. Polymerization times of 2-3 days are expected. Since we cannot run the reaction overnight due to safety concerns we propose to stop the flow of gas at the end of the day and then continue the polymerization the following morning for up to a maximum of 3 days polymerization (total reaction time about 20 hours). Does this sound OK? Any comments!

2. *MAO to catalyst ratio* - About 1.2 equivalent of MAO (methylaluminoxane) per nickel cluster was found to be optimal for good yields (see table below). We will polymerize at a MAO to catalyst ratio of 1.2-1.3 to 1(see table below).

3. *Reaction temperature* – because we are anticipating relatively low rate of polymerization we will perform the polymerization at 45ºC.

Starting Recipe

Reagent	**Amount**	**Millimoles**
Isopar H	400 mL	not
Nickel catalyst, crushed crystalline form	250 mg	0.308
MAO	0.6 mL	Molar ration cat:Mao1:3
Monomer feed flow	500 mL/min	not
Reaction time	6 hours	Not
Anticipated volume of gas consumed assuming above feed	180 L	Not
Mass (based on ideal gas equation)	205 g	About 7300 for ethylene

Materials

Isopar H will be used as received (no further drying) CAS # 64742-48-9, b_p range 179-187ºC, density 0.759

MAO Sigma-Aldrich a 10% (w/w) solution in toluene – Aldrich, page 1800, CAS # [120144-90-3], $[Al(CH_3)O-]_n$ MW 58.02, density of MAO dispersion 0.875 g/cm^3.

Nickel catalyst (MW, number of nickel atoms per molecule) equivalent MW 812.9 g/mol, 3 Ni per cluster.

Monomer will be introduced into the reactor as a gas which will dissolve in the Isopar H and then polymerize with the aid of the Ni catalyst.

Nitrogen gas will be used as a purge gas during drying of the reactor vessel prior to polymerization

Ryerson - General Synthesis Procedure

Step 1 – Conditioning of the Reactor Vessel

1. Wipe vessel walls using kimwipes soaked with Isopar H or toluene to remove particulate and other foreign debris;
2. Seal reactor and begin purging vessel with nitrogen gas;
3. Dry reactor by heating walls of the vessel at 120-130ºC for at least 4 hours while passing ultra dry nitrogen through the reactor;
4. Stop heating and continue purging reactor with N_2 gas overnight;

Status 1. _____

2._____

3._____

4._____

Step 2 – Weighing and drying of Isopar H

5. Dry glassware and other required transfer equipment such as dispensing syringes, needles and fittings at 150ºC for at least 16 hours;

6. Remove a flat bottom round flask (RBF) and rubber septum from oven set at 150ºC. Seal RBF with septum and purge head space with nitrogen gas until flask is at room temperature. Weigh target mass of Isopar H directly into RBF over a stream of nitrogen gas as quickly as possible to minimize exposure of solvent/glassware to the atmosphere.

7. Inject 0.2 mL MAO into RBF containing Isopar H. To accomplish this task remove syringe from oven and insert syringe needle into PTFE tubing. Fill syringe with nitrogen gas and then push down on the plunger to release the gas. Repeat this operation at least four more times to ensure that the air inside the syringe has been displaced with nitrogen gas. Inject syringe into bottle containing MAO activator. Withdraw 0.2 mL MAO solution and inject immediately into RBF. *Note some white precipitate will form over surfaces exposed to atmospheric moisture.*

Weight of Isopar H _____ Volume of MAO

_____

Step 3 – Weighing and addition of Nickel Catalyst into RBF

8. Grind the as received Ni catalyst using motor/pestle (this step is optional). If the catalyst has been crushed then weigh catalyst directly into pre-weighed vial, purge head

space with nitrogen gas and weigh vial again. Continue adding catalyst to the vial until target weight has been reached. *Note transfer vials should be heated at 150ºC for at least 2 hours prior to beginning this step*.

9. Transfer catalyst in powered state to RBF. Determine the weigh of catalyst transferred to the RBF by difference.

10. Stir catalyst/Isopar H dispersion overnight. The mechanical action from the stirring bean is expected to slowly break down the remaining larger crystal.

Weight of Vial _____ Weight of Ni catalyst _____

Step 4 – Addition of MAO to RBF and Transfer to Reactor Vessel

11. Inject target volume (about 0.6 mL MAO) into RBF containing Isopar H. Remove syringe from oven and insert syringe needle into PTFE tubing. Fill syringe with nitrogen gas and then push down on the plunger to release the gas. Repeat this operation at least six more times to ensure that the air inside the syringe barrel has been displaced with nitrogen gas. Inject syringe into bottle containing MAO activator. Withdraw 0.6 mL MAO solution and inject immediately into RBF. *Note some white precipitate will form over surfaces where MAO has been exposed to atmospheric moisture.*

12. Mix contents for 30-60 minutes.

13. Transfer by cannula catalyst/MAO dispersion into vessel through entry port;

14. Bring reactor to temperature (45ºC) and set stir speed to 420 rpm;

15. Open cylinder regulator valve and set the flow rate using mass flow detector (500 mL/min). Monitor the reactor and alter ethylene flow accordingly;

16. Run reaction for 5-7 hours monitoring temperature and pressure;

17. Sample vessel contents for evidence of polymerization.

Please add comments or preferably call me at (905)-822-4111 ext 752. We are hoping to start drying the vessel on Wednesday and begin polymerizing on Thursday.

Appendix 4: Data of conversion of each polymerization trial for kinetic studies

Run 1: 0.2109 g of 1; R.T.; 10% (v/v) in a total of 20mL solution				
Hours	Flask before (g)	Aliquot (mL)	Flask after (g)	**Conversion (%)**
144	19.582	0.32	19.590	**5.518763797**
168	20.020	0.20	20.025	**5.430463576**
192	20.611	0.20	20.620	**9.675496689**

Run 2: 0.2107 g of 1; R.T.; 50% (v/v) in a total of 20mL solution				
Hours	Flask before (g)	Aliquot (mL)	Flask after (g)	**Conversion (%)**
144	19.029	0.27	19.041	**9.811135639**
168	20.748	0.18	20.759	**13.3081923**
192	20.27	0.18	20.280	**11.98798136**

Run #3: Polymerization abort

Run 4: 0.2095 g of 1; R.T.; 50% (v/v) in a total of 20mL solution				
Hours	Flask before (g)	Aliquot (mL)	Flask after (g)	**Conversion (%)**
264 hours	19.661	0.15	19.671	**1.28E+01**
312 hours	19.666	0.18	19.679	**1.40E+01**
336 hours	30.321	0.14	30.333	**1.68E+01**
360 hours	22.084	0.23	22.107	**1.97E+01**

Run 5: 0.2108 g of 1; R.T.; 50% (v/v) in a total of 100mL solution				
Hours	Flask before (g)	Aliquot (mL)	Flask after (g)	**Conversion (%)**
24	19.665	0.18	19.671	**7.36E+00**
72	21.712	0.19	21.721	**1.04E+01**
96	18.649	0.185	18.659	**1.19E+01**
120	24.819	0.3	24.831	**8.78E+00**

Run 6: 0.2103 g of 1; R.T.; 10% (v/v) in a total of 100mL solution				
Hours	Flask before (g)	Aliquot (mL)	Flask after (g)	**Conversion (%)**
24	18.653	0.38	18.656	1.74E+00
72	19.939	0.22	19.944	5.00E+00
96	23.519	0.2	23.524	5.49E+00
120	19.936	0.19	19.941	5.76E+00

Run 7: 0.2095 g of 1; R.T.; 50% (v/v) in a total of 100mL solution				
Hours	Flask before (g)	Aliquot (mL)	Flask after (g)	**Conversion (%)**
24	23.519	0.23	23.529	**9.60E+00**
72	24.808	0.18	24.814	**7.34E+00**
96	19.283	0.2	19.288	**5.50E+00**
120	21.712	0.29	21.729	**1.29E+01**

Run 8: 0.2095 g of 1; 70˚C; 50% (v/v) in a total of 100mL solution				
Hours	Flask before (g)	Aliquot (mL)	Flask after (g)	**Conversion (%)**
24	20.608	0.14	20.612	**6.31E+00**
72	23.518	0.17	23.522	**5.04E+00**
96	21.719	0.32	21.729	**6.88E+00**
120	20.754	0.20	20.782	**3.07E+01**

Run #9,10: Blank

Run 11: 1.0505 g of 1; 70˚C; 50% (v/v) in a total of 100mL solution				
Hours	Flask before (g)	Aliquot (mL)	Flask after (g)	**Conversion (%)**
3.33	18.649	0.16	18.655	**8.28E+00**
4.33	19.938	0.16	19.943	**6.90E-01**
24	20.023	0.35	20.061	**2.40E+01**
48	21.721	0.31	21.796	**5.34E+01**

Run 12: 1.0523 g of 1; 70˚C; 50% (v/v) in a total of 100mL solution				
Hours	Flask before (g)	Aliquot (mL)	Flask after (g)	**Conversion (%)**
1.5	20.0258	0.375	20.0381	**5.53E+00**
3	18.6569	0.36	18.6715	**7.26E+00**
4	21.7237	0.43	21.7445	**9.00E+00**
5	18.5801	0.285	18.5941	**9.13E+00**
6	24.8159	0.28	24.8313	**1.04E+01**
22.75	18.58	0.26	18.6131	**2.66E+01**
25	19.6694	0.25	19.7033	**2.83E+01**
27	21.7238	0.21	21.7505	**2.64E+01**
44.25	20.0265	0.25	20.0697	**3.65E+01**
48.25	21.7147	0.215	21.7546	**3.92E+01**
73	20.7532	0.22	20.802	**4.71E+01**
97	20.6116	0.4	20.6989	**4.62E+01**

Run 13: 0.2100 g of 1; 70°C; 50% (v/v) in a total of 100mL solution				
Hours	Flask before (g)	Aliquot (mL)	Flask after (g)	**Conversion (%)**
1.5	20.7538	0.52	20.7604	**9.31E-01**
3	20.6118	0.425	20.6196	**2.18E+00**
4	19.6717	0.4	19.679	**2.14E+00**
5	19.4838	0.5	19.4956	**3.31E+00**
6	20.2744	0.29	20.2835	**4.99E+00**
22.75	20.7538	0.24	20.772	**1.46E+01**
25	18.655	0.25	18.6745	**1.51E+01**
27	20.6118	0.24	20.6306	**1.51E+01**
44.25	19.0334	0.26	19.0591	**1.95E+01**
48.25	19.2863	0.2	19.3088	**2.24E+01**
73	19.4835	0.19	19.5073	**2.51E+01**
97	18.5811	0.5	18.6652	**3.42E+01**

Run 14: 1.0573 g of 1; 70°C; 50% (v/v) in a total of 100mL solution				
Hours	Flask before (g)	Aliquot (mL)	Flask after (g)	**Conversion (%)**
1.5	23.748	0.3	23.761	**7.91E+00**
3	20.02	0.24	20.032	**9.40E+00**
6	24.8161	0.19	24.8288	**1.32E+01**
19	20.0122	0.23	20.037	**2.24E+01**
22.5	19.9422	0.24	19.9679	**2.22E+01**
24	19.585	0.23	19.613	**2.54E+01**
27	19.672	0.25	19.699	**2.23E+01**
30	20.6107	0.23	20.6376	**2.42E+01**
43	20.7535	0.26	20.7908	**3.01E+01**
76	19.9422	0.2	19.9824	**4.28E+01**

Run 15: 1.0549 g of 1; 70°C; 50% (v/v) in a total of 100mL solution				
Hours	Flask before (g)	Aliquot (mL)	Flask after (g)	**Conversion (%)**
1.5	18.574	0.175	18.582	**8.45E+00**
3	19.935	0.23	19.946	**8.92E+00**
6	19.4836	0.24	19.5005	**1.40E+01**
19	19.2859	0.19	19.308	**2.43E+01**
22.5	21.7145	0.3	21.749	**2.40E+01**
24	20.274	0.228	20.3016	**2.53E+01**
27	21.7239	0.31	21.7667	**2.90E+01**
30	19.2858	0.28	19.3245	**2.90E+01**
43	20.2738	0.28	20.3151	**3.10E+01**
76	23.5247	0.29	23.5748	**3.65E+01**

Run 16: 1.0519 g of 1;R.T.; 50% (v/v) in a total of 100mL solution				
Hours	Flask before (g)	Aliquot (mL)	Flask after (g)	**Conversion (%)**
1.5	19.033	0.18	19.0375	**3.75E+00**
3	21.7146	0.49	21.7242	**2.52E+00**
6	23.5248	0.2	23.5286	**2.37E+00**
19	20.611	0.4	20.6206	**3.49E+00**
22.5	23.5251	0.4	23.535	**3.65E+00**
24	20.7531	0.33	20.7613	**3.65E+00**
27	18.58	0.32	18.5868	**2.84E+00**
30	20.0112	0.34	20.0192	**3.34E+00**
43	24.8151	0.28	24.8215	**3.18E+00**

Run 17: 1.0529 g of 1; 70°C; 50% (v/v) in a total of 100mL solution				
Hours	Flask before (g)	Aliquot (mL)	Flask after (g)	**Conversion (%)**
1.5	19.713	0.175	19.7163	**2.35E+00**
3	20.2741	0.36	20.279	**1.16E+00**
6	21.725	0.26	21.7287	**1.29E+00**
19	23.7561	0.28	23.7625	**3.24E+00**
22.5	20.0261	0.29	20.0327	**3.21E+00**
24	24.8154	0.33	24.8225	**2.92E+00**
27	19.484	0.43	19.4925	**2.52E+00**
30	19.7128	0.25	19.7182	**2.91E+00**
43	20.026	0.34	20.0331	**2.75E+00**

Run 18: 1.0516 g of 1; 70°C; 50% (v/v) in a total of 100mL solution				
Hours	Flask before (g)	Aliquot (mL)	Flask after (g)	**Conversion (%)**
3	21.714	0.35	21.722	**3.26E+00**
6	19.5923	0.22	19.6036	**9.70E+00**
9	20.2744	0.24	20.2884	**1.13E+01**
12	21.7238	0.23	21.7399	**1.39E+01**
24	20.6104	0.25	20.6375	**2.25E+01**
27	19.285	0.27	19.3164	**2.42E+01**
30	23.5245	0.28	23.5582	**2.50E+01**
33	21.7142	0.26	21.7462	**2.56E+01**
36	19.942	0.22	19.9685	**2.49E+01**
48	19.67	0.22	19.7031	**3.15E+01**
60	19.2851	0.26	19.3304	**3.67E+01**
78	23.5243	0.28	23.5899	**4.99E+01**

Run 19: 1.0516 g of 1; 70°C; 50% (v/v) in a total of 100mL solution				
Hours	Flask before (g)	Aliquot (mL)	Flask after (g)	**Conversion (%)**
3	23.7563	0.53	23.7745	**5.70E+00**
6	23.5252	0.25	23.5367	**8.23E+00**
9	19.9425	0.34	19.9612	**1.02E+01**
12	19.67	0.3	19.6892	**1.21E+01**
24	24.8153	0.29	24.8423	**1.84E+01**
27	19.7127	0.35	19.7484	**2.03E+01**
30	20.7533	0.29	20.7821	**1.96E+01**
33	19.5921	0.28	19.6228	**2.18E+01**
36	20.6111	0.38	20.6541	**2.25E+01**
48	18.5792	0.25	18.6135	**2.76E+01**
60	20.7529	0.27	20.7945	**3.11E+01**
78	20.0262	0.33	20.0954	**4.28E+01**

Run 20: 1.0520 g of 1; R.T.; 50% (v/v) in a total of 100mL solution				
Hours	Flask before (g)	Aliquot (mL)	Flask after (g)	**Conversion (%)**
6	19.0336	0.82	19.049	**2.27E+00**
12	20.026	0.47	20.0359	**2.75E+00**
24	19.4833	0.59	19.4993	**4.06E+00**
30	23.7563	0.29	23.7642	**4.06E+00**
36	20.2736	0.38	20.2847	**4.47E+00**
48	20.0118	0.34	20.0221	**4.69E+00**
60	21.7233	0.38	21.7364	**5.57E+00**
102	19.4833	0.38	19.5003	**7.74E+00**

Run 21: 1.0523 g of 1; R.T.; 50% (v/v) in a total of 100mL solution				
Hours	Flask before (g)	Aliquot (mL)	Flask after (g)	**Conversion (%)**
6	20.7535	0.46	20.7689	**5.30E+00**
12	20.0118	0.34	20.0282	**9.08E+00**
24	18.5796	0.31	18.6054	**1.70E+01**
30	19.0335	0.28	19.0542	**1.49E+01**
36	23.753	0.23	23.765	**9.89E+00**
48	20.0118	0.2	20.0221	**9.71E+00**
60	19.0333	0.24	19.0738	**3.61E+01**

PS#22: 1.0536 g of 1; blank at 90°C ; 50% (v/v) styrene in a total of 100mL solution					
First, the 7 samples were taken before putting into the oil bath					
	Flask before	Flask after	Weight	mL of aliquot	Weight of cat/mL
bottom	24.8163	24.8255	0.0092	1.08	0.0085
middle	20.0129	20.0268	0.0139	1.61	0.0086
middle	19.6710	19.6854	0.0144	1.71	0.0084
bottom	19.4838	19.4980	0.0142	1.60	0.0089
bottom	20.0267	20.0411	0.0144	1.63	0.0088
middle	23.7568	23.7685	0.0117	1.40	0.0084
middle	19.9428	19.9539	0.0111	1.38	0.0080
				Average	0.0085
	19.2861	19.2995	0.0134	1.70	0.0079
	23.5257	23.5383	0.0126	1.50	0.0084
	18.5802	18.5928	0.0126	1.30	0.0097
	21.7244	21.7367	0.0123	1.50	0.0082
				Average Wt cat/mL	0.0085
				Std. Dev	0.1024

Run #23: Aborted reaction. Wrong amount of monomer was added.

PS#24: 1.0543 g of 1; blank at 90°C ; 50% (v/v) styrene in a total of 100 mL solution						
1.0543g cat in total 100 mL solution						
Run	Time	Flask before	Flask after	Weight	Aliquot (mL)	Weight of cat/mL
1	0	19.4840	19.4991	0.0151	1.70	0.0089
2	0	19.7134	19.7286	0.0152	1.79	0.0085
3	30	20.0126	20.0257	0.0131	1.50	0.0087
4	30	20.7534	20.7657	0.0123	1.50	0.0082
5	60	20.6116	20.6258	0.0142	1.70	0.0084
6	60	20.0265	20.0415	0.0150	1.80	0.0083
7	90	19.6708	19.6831	0.0123	1.50	0.0082
8	90	19.0338	19.0473	0.0135	1.60	0.0084
9	120	19.2858	19.2972	0.0114	1.30	0.0088
10	120	19.9422	19.9539	0.0117	1.33	0.0088
11	150	19.5920	19.6047	0.0127	1.50	0.0085
12	150	21.7146	21.7268	0.0122	1.40	0.0087
13	180	24.8150	24.8293	0.0143	1.50	0.0095
14	180	23.7562	23.7672	0.0110	1.30	0.0085
15	240	20.2748	20.2872	0.0124	1.40	0.0089
16	240	20.0127	20.0247	0.0120	1.40	0.0086
17	300	19.6713	19.6856	0.0143	1.70	0.0084
18	300	20.0270	20.0395	0.0125	1.40	0.0089
					Average Wt cat/mL	0.0085
					standard dev	0.0003

Run 25: 1.0522 g of 1; 90°C.; 50% (v/v) in a total of 100mL solution				
Hours	Flask before (g)	Aliquot (mL)	Flask after (g)	**Conversion (%)**
0	19.5931	2.2	19.6387	**2.70E+00**
0.25	19.9423	2.1	20.0096	**5.08E+00**
0.5	20.6122	1.7	20.6753	**6.05E+00**
0.75	23.7567	1.7	23.8168	**5.57E+00**
1	19.714	1.49	19.7797	**7.25E+00**
1.25	20.0125	1.2	20.0638	**6.87E+00**
1.5	23.5256	1.1	23.5793	**7.98E+00**
1.75	20.2741	1.4	20.35	**8.93E+00**
2	20.754	1.3	20.824	**8.72E+00**
2.25	19.0341	1.35	19.1131	**9.47E+00**
2.5	19.6713	1.2	19.7426	**9.49E+00**
2.75	18.5799	1.28	18.6555	**9.29E+00**
3	19.485	1.25	19.5634	**9.81E+00**
3.25	21.7156	1.3	21.8121	**1.17E+01**
3.5	20.0272	1.5	20.1399	**1.17E+01**

Run 26: 1.0551 g of 1; 90°C.; 50% (v/v) in a total of 100mL solution				
Hours	Flask before (g)	Aliquot (mL)	Flask after (g)	**Conversion (%)**
0	20.7538	2.2	20.7828	**1.03E+00**
0.25	19.0337	2.6	19.0978	**3.49E+00**
0.5	19.6708	1.95	19.7293	**4.52E+00**
0.75	23.757	2.2	23.8339	**5.45E+00**
1	19.9424	2.1	20.0288	**6.56E+00**
1.25	19.7133	2.5	19.848	**8.91E+00**
1.5	21.715	1.8	21.8007	**7.46E+00**
1.75	24.8161	1.6	24.9023	**8.48E+00**
2	18.5799	1.7	18.6745	**8.64E+00**
2.25	20.6119	1.3	20.6836	**8.38E+00**
2.5	20.2744	1.2	20.3479	**9.32E+00**
2.75	20.6776	2.1	20.8175	**1.01E+01**
3	19.5921	1.2	19.6814	**1.12E+01**

Run 27: 1.0564 g of 1; 90°C.; 50% (v/v) in a total of 100mL solution				
Hours	Flask before (g)	Aliquot (mL)	Flask after (g)	**Conversion (%)**
0	19.484	2.8	19.5177	**7.81E-01**
0.25	22.6172	2.6	22.664	**2.04E+00**
0.5	21.7244	2.1	21.7838	**4.13E+00**
0.75	19.2855	1.98	19.353	**5.23E+00**
1	22.443	2.1	22.527	**6.29E+00**
1.25	19.6713	1.95	19.7692	**8.14E+00**
1.5	20.2744	2.3	20.3931	**8.23E+00**
1.75	20.0269	2.1	20.1441	**8.79E+00**
2	19.9427	2.03	20.0618	**9.09E+00**
2.25	19.034	1.8	19.1547	**1.03E+01**
2.5	21.7149	1.8	21.8413	**1.07E+01**
2.75	20.0123	1.8	20.1698	**1.33E+01**
3	20.7537	2.38	20.945	**1.18E+01**

Run 28: 1.0538 g of 1; 90°C.; 25% (v/v) in a total of 100mL solution				
Hours	Flask before (g)	Aliquot (mL)	Flask after (g)	**Conversion (%)**
0	20.0133	2.1	20.0407	**1.96E+00**
0.25	20.2745	2.2	20.3067	**2.59E+00**
0.5	19.4843	2.5	19.5307	**4.14E+00**
0.75	19.2860	1.7	19.3174	**4.00E+00**
1	20.0265	1.7	20.0618	**4.83E+00**
1.5	18.5801	1.7	18.6219	**6.21E+00**
2	21.7149	1.9	21.7627	**6.30E+00**
2.5	23.7565	2.2	23.8212	**7.74E+00**
3	24.8161	2.38	24.8914	**8.34E+00**
4	21.7241	1.45	21.8013	**1.57E+01**

Run 29: 1.0527 g of 1; 90°C.; 50% (v/v) in a total of 100mL solution				
Hours	Flask before (g)	Aliquot (mL)	Flask after (g)	**Conversion (%)**
0	20.7539	2	20.7835	**1.39E+00**
0.25	20.0266	1.7	20.0712	**3.84E+00**
0.5	20.2744	1.7	20.3354	**5.82E+00**
0.75	21.7143	1.8	21.7892	**6.91E+00**
1	18.5799	1.9	18.6675	**7.70E+00**
1.25	20.0125	1.7	20.1025	**8.92E+00**
1.5	19.0338	2	19.1462	**9.39E+00**
1.75	22.4414	1.7	22.5478	**1.04E+01**
2	19.4839	1.8	19.6054	**1.11E+01**
2.25	19.9426	1.6	20.0603	**1.20E+01**
2.5	21.7238	1.9	21.871	**1.25E+01**
2.75	20.6775	1.6	20.8117	**1.33E+01**
3	23.525	1.7	23.666	**1.29E+01**
4	23.7564	1.5	23.9007	**1.49E+01**
5	22.6149	1.7	22.8241	**1.91E+01**
6	19.5921	1.55	19.7875	**1.91E+01**
8	24.8157	1.45	25.0278	**2.19E+01**
10	20.612	1.45	20.8577	**2.51E+01**
12	19.2861	1.2	19.4773	**2.31E+01**
14	19.714	0.8	19.8821	**3.03E+01**
16	20.754	1	20.9635	**2.98E+01**
18	18.5803	0.7	18.7425	**3.26E+01**
20	20.0268	0.9	20.2095	**2.81E+01**
24	20.012	0.9	20.2333	**3.39E+01**

Run 30: 1.0547 g of 1; 90°C.; 75% (v/v) in a total of 100mL solution				
Hours	Flask before (g)	Aliquot (mL)	Flask after (g)	**Conversion (%)**
0	21.7144	3.2	21.7675	**1.79E+00**
0.25	19.4842	2.3	19.5757	**6.68E+00**
0.5	19.2857	1.7	19.3784	**9.60E+00**
0.75	20.6775	1.9	20.7906	**1.05E+01**
1	19.9428	2.2	20.0953	**1.22E+01**
1.25	19.034	2.3	19.223	**1.44E+01**
1.5	18.8046	1.8	18.9661	**1.55E+01**
1.75	20.6663	2.1	20.8701	**1.65E+01**
2	22.615	1.9	22.8006	**1.62E+01**
2.25	19.5921	1.75	19.7921	**1.88E+01**
2.5	22.6079	1.5	22.7864	**1.92E+01**
2.75	23.8344	1.5	24.0415	**2.21E+01**
3	21.7238	1.5	21.9304	**2.16E+01**
3.5	23.7563	1.25	23.9644	**2.59E+01**
4	23.5249	1.3	23.712	**2.19E+01**
4.5	22.4417	1.5	22.686	**2.45E+01**

Run 31: 1.0531 g of 1; 25.5°C.; 25% (v/v) in a total of 100mL solution				
Hours	Flask before (g)	Aliquot (mL)	Flask after (g)	**Conversion (%)**
0	19.2851	2.4	19.3108	**4.68E-01**
0.25	20.0258	1.8	20.0476	**8.09E-01**
0.5	22.6074	1.6	22.6279	**9.49E-01**
0.75	20.7532	1.8	20.7746	**7.33E-01**
1	18.8033	1.7	18.8273	**1.19E+00**
1.25	22.4412	1.5	22.4629	**1.24E+00**
1.5	19.0333	1.6	19.0571	**1.31E+00**
1.75	20.0114	1.5	20.0347	**1.41E+00**
2	23.7559	1.7	23.7815	**1.30E+00**
2.25	20.6775	1.9	20.7075	**1.41E+00**
2.5	20.6107	1.5	20.6359	**1.57E+00**
2.75	23.8334	1.7	23.8623	**1.58E+00**
3	21.7235	1.5	21.7488	**1.52E+00**

PS#32: 1.0527 g of 1; blank at 25 and 50°C ; 50% (v/v) of MMA in 100 mL solution						
Run	Time	Flask before	Flask after	weight	mL of aliquot	Weight of cat/mL
1	0	18.8039	18.8148	0.0109	1.40	0.0078
2	0	19.4839	19.4941	0.0102	1.30	0.0078
3	0	20.2743	20.2856	0.0113	1.40	0.0081
4	0	19.2856	19.2988	0.0132	1.50	0.0088
5	0	21.7238	21.7346	0.0108	1.30	0.0083
6	0	20.0125	20.0258	0.0133	1.50	0.0089
7	240	19.0339	19.0483	0.0144	1.65	0.0087
8	240	22.4415	22.4552	0.0137	1.65	0.0083
9	300	22.6078	22.6188	0.0110	1.30	0.0085
10	300	20.7532	20.7683	0.0151	1.70	0.0089
11	360	23.8338	23.8443	0.0105	1.20	0.0088
12	360	20.0262	20.0370	0.0108	1.30	0.0083
					Average Wt cat/mL	0.0084
					Std. Dev	0.0004

Appendix 5: Results of fitting the first order and second order model.

Calculation for fitting the model:

Take Run 27, trials at 1st hour:

Polymer recovered from aliquot: 0.06855 g (weight of flask after-flask before)

Polymer recovered =Styrene consumed and turned into the polymer

Aliquot sampling size: 2.10mL

Total solution volume before sampling: 100-2.2-2.6-1.95-2.2=91.05 (mL)

Styrene consumed (polymer formed) into polymer in the solution up to first hour:

(0.06855/2.10)×91.05= 2.9 7 (g)

Concentration of styrene in solution at this moment:

Styrene left in the solution /total volume of solution

Styrene left in the solution=initial styrene –styrene converted into polymer-styrene loss from sampling (half of the sampling volume is styrene)

Initially, styrene added was 50mL; Styrene density: 0.905 (g/mL)

Styrene left over= (50×0.905)-2.97-(2.2+2.6+1.95+2.2)×0.5×0.905=32.32(g)

Styrene M.W: 104.15 (g/mol)

Styrene concentration at first hour: (32.32/104.15)/0.09105=3.409M

Or use weight to express the changes in regards to the styrene concentration, this became:

Styrene consumed=2.97(g)

Initial styrene weight=5×0.905=4.525 (g)

Then $\ln([M]_0/[M])=0.421$, this value is calculated for each trial in each run to fit a model of first order reaction.

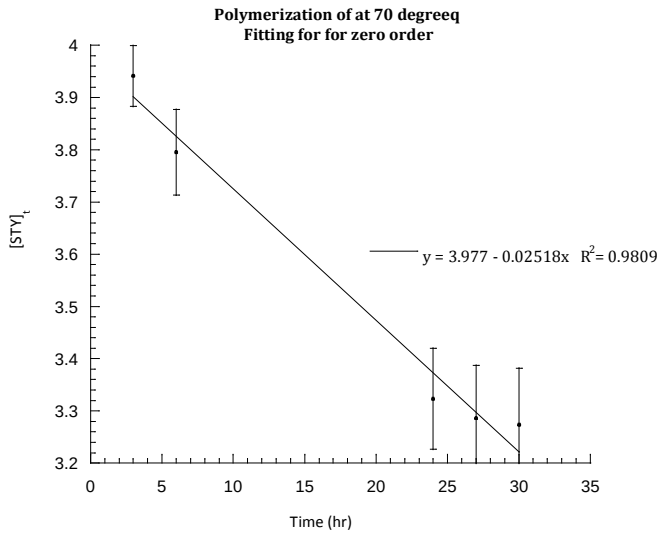

Figure 52: Polymerization of STY fitted as a zero-order reaction at 70˚C. Data are averaged numbers from 4 trials (Run 14,15,18 and 19)

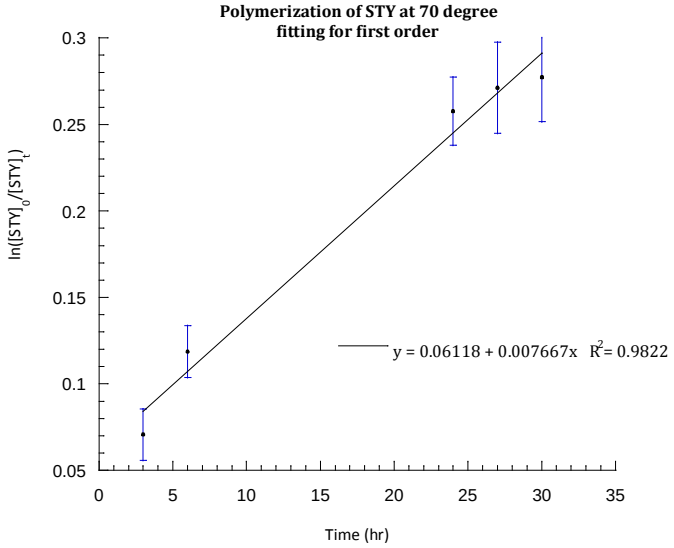

Figure 53: Polymerization of STY fitted as a first-order reaction at 70˚C. Data are averaged numbers from 4 trials (Run 14, 15,18 and 19)

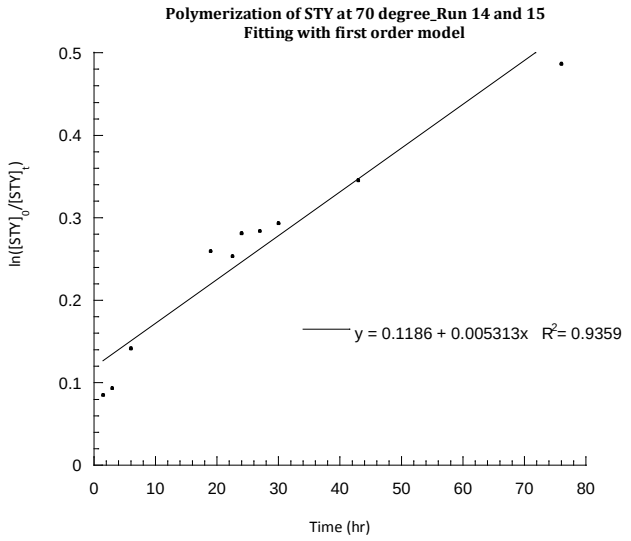

Figure 54: Polymerization of STY fitted as a first-order reaction at 70˚C. Data points are averaged values from trial of Run 18, 19.

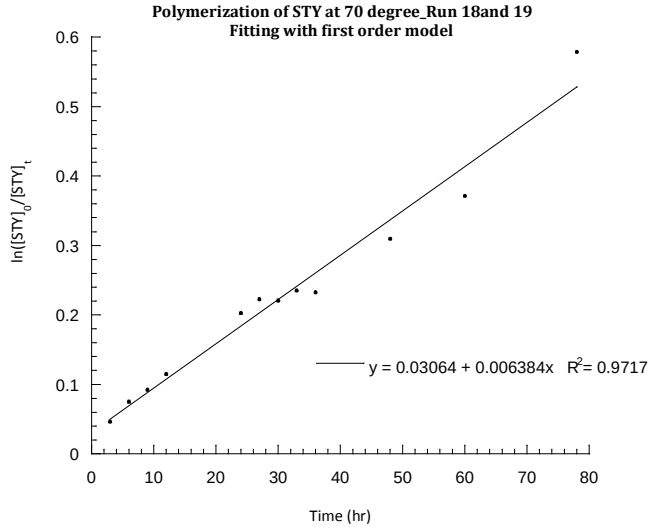

Figure 55: Polymerization of STY fitted as a first-order reaction at 70°C. Data points are averaged values from trial of Run 18, 19.

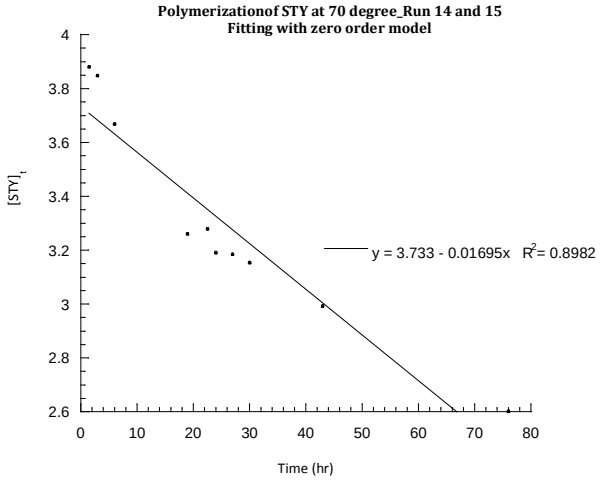

Figure 56: Polymerization of STY fitted as a zero-order reaction at 70˚C. Data are averaged values from trial of Run 14 and 15.

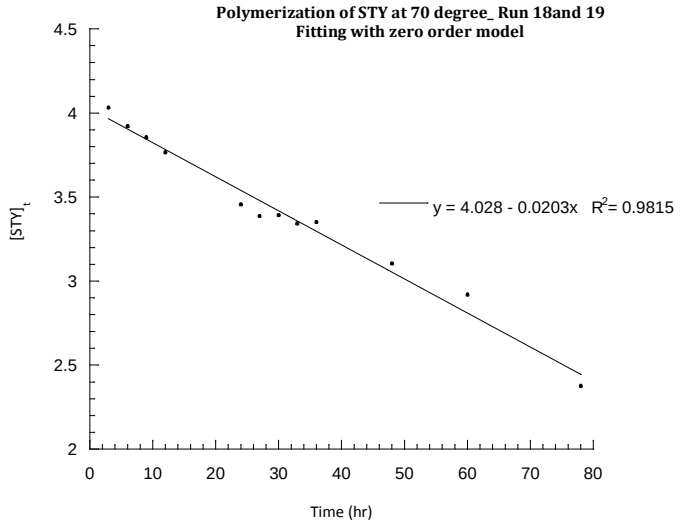

Figure 57: Polymerization of STY fitted as a zero-order reaction at 70˚C. Data are averaged values from Run 18 and 19.

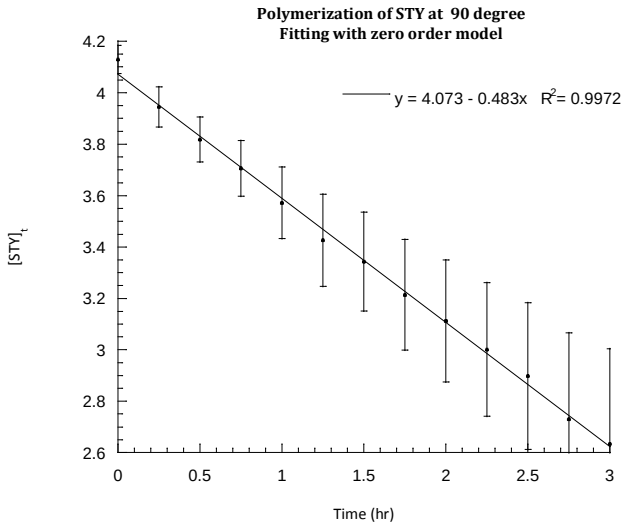

Figure 58: Polymerization of STY fitted as a zero-order reaction at 90C. Data are averaged values from trial of run 25,26,27 and 29.

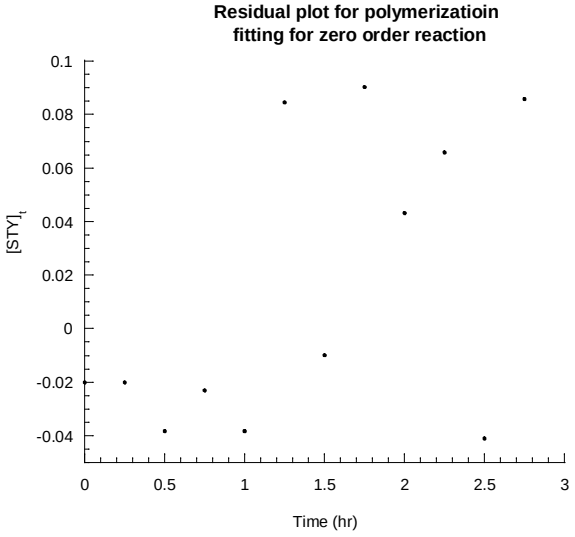

Figure 59: Residual plot for Fig. 50.

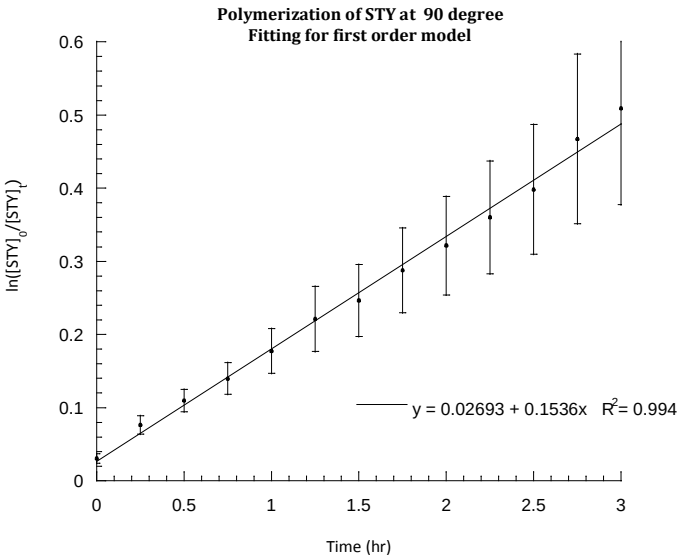

Figure 60: Polymerization of STY fitted as a first-order reaction at 90C. Data are averaged values from trial of run 25, 26, 27 and 29.

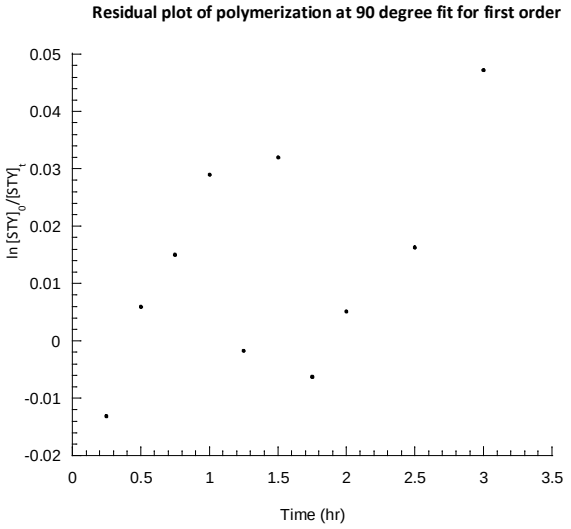

Figure 61: Residual plot for Fig. 52.

References:

1: Aggarwal, S. L.; Sweeting, O. J. *Chem. Rev.* **1957**, *57*, 665.

2: Chandrasekhar, V. *Inorganic and Organometallic Polymers*. **2005**, Springer-Verlag, Berling, Chapter 2.

3: Singh, D.; Merrill, R. P. *Macromolecules*, **1971**, *4*, 599.

4: Belov, G. P.; Lisitskaya, A. P.; Solovyeva, T. I.; Chirkov, N. M. *Eur. Polym. J.* **1970**, *6*, 29.

5: Odian, G. C. *Princlple of Polymerization.* 4th ed. **2004**, John Wiley & Sons. Inc. Chapter 8.

6 : Zambelli, A.; Natta, G.; Pasquon, I. *J. Polym. Sci. C*, **1963**, *4*, 411.

7 : Natta, G.; Zambelli, A.; Lanzi, G.; Pasquon, I.; Mognaschi, E. R.; Segre, A. L.; Centola, P. *Die Makromol. Chem.* **1965**, *81*, 161.

8: Natta, G.; Pino, P.; Mazzanti, G.; Giannixi, U. *J. Am. Chem. Soc.* **1957**, *79*, 2975.

9: Breslow, D. S.; Newburg, N. R. *J. Am. Chem. Soc.* **1957**, *79*, 5072.

10: Kaminsky, W. *J. Polym. Sci. Part A: Polym. Chem*. **2004**, *42*, 3911.

11: Kazuo, S.; Takeshi, S. *Prog. Polym. Sci.* **1997**, *22*, 1503.

12: Brintzinger, H. H.; Fischer, D.; Mulhaupt, R.; Rieger, B.; Waymouth, R. M. *Angew. Chem. Int. Ed. Eng.* **1995**, *34*, 1143.

13: Shinn, H. *Macromol. Symp*. **1995**, *97*, 27.

14: Kaminsky, W.; Funck, A.; Hahnsen, H. *Dalton Trans.* **2009**, *41*, 8803.

15: Kaminsky, W. *Catalysis Today* **1994**, *20*, 257.

16: Huang, J.; Pempel, G. L. *Prog. Polym. Sci* .**1995**, *20*, 459.

17: Edited by Baugh, L. S.; Canich, J. A. M. *Stereoselective Polymerization with Single Site Catalysts.* **2008**, Taylor & Francis Group, Boca Raton. Ch 1 and 3.

18: Kaminsky, W.; Kulper, K.; Niedoba, S. *Makromol. Chem. Macromol. Symp.* **1986**, *3*, 377.

19: Kaminsky, W.; Hopf, A.; Arndt-Rosenau, M. *Macromol. Symp.* **2003**, *201*, 301.

20: Annunziata, L.; Pragliola, S.; Pappalardo, D.; Tedesco, C.; Pellecchia, C. *Macromolecules*, **2011**, *44*, 1934.

21: Haruyuki, M.; Hiroshi, T.; Akihiko, I.; Terunori, F. *Chem. Rev.* **2011**, *111*, 2363.

22: Mulhaupt, R. *Macromol. Chem.Phys.* **2003**, *204*, 289.

23: Ittel, S. D.; Johnson, L. K.; Brookhart, M. *Chem. Rev.* **2000**, *100*, 1169.

24: Peuckert, M.; Keim, W. *Organometallics*, **1983**, *2*, 594.

25: Jacobsen, E. N.; Breinbauer, R. *Science*, **2000**, *287*, 437.

26: Gibson, V. C.; Spitzmesser, S. K. *Chem. Rev.* **2003**, *103*, 283.

27: Klabunde, U.; Ittel, S. D. *J. Mol. Catal.* **1987**, *41*, 123.

28: Johnson, L. K.; Killian, C. M.; Brookhart, M. *J. Am. Chem. Soc.* **1995**, *117*, 6414.

29: Rose, J. M.; Cherian, A. E.; Coates, G. W. *J. Am. Chem. Soc.* **2006**, *128*, 4186.

30: Camacho, D. H.; Guan, Z. *Chem. Commun.* **2010**, *46*, 7879.

31: Gates, D. P.; Svejda, S. A.; Onate, E.; Killian, C. M.; Johnson, L. K.; White, P. S.; Brookhart, M. *Macromolecules*, **2000**, *33*, 2320.

32: Deng, L.; Margl, P.; Ziegler, T. *J. Am. Chem. Soc.* **1997**, *119*, 1094.

33: Deng, L.; Woo, T. K.; Cavallo, L.; Margl, P. M.; Ziegler, T. *J. Am. Chem. Soc.* **1997**, *119*, 6177.

34: Guan, Z.; Popeney, C. S. *Top Organomet. Chem.* **2009**, *26*, 179.

35: Britovsek, G. J. P.; Gibson, V. C.; Wass, D. F. *Angew. Chem. Int. Ed.* **1999**, *38*, 428.

36: Bryliakov, K. P. *Russ. Chem. Rev.* **2007**, *76*, 253.

37: Gibson, V. C.; Solan, G. A. *Top. Organomet. Chem.* **2009**, *26*, 107.

38: Pellecchia C.; Mazzeo, M.; Pappalardo, D. *Macromol. Rapid Commun.* **1998**, *19*, 651.

39: Small, B. L.; Brookhart, M. *Macromolecules*. **1999**, *32*, 2120.

40: Michalak, A.; Ziegler, T. *J. Am. Chem. Soc.* **2001**, *123*, 12266.

41: Szabo, M. J.; Jordan, R. F.; Michalak, A.; Piers, W. E.; Weiss, T.; Yang, S. Y.; Ziegler, T. *Organometallics*, **2004**, *23*, 5565.

42: Younkin, T. R.; Connor, E. F.; Henderson, J. I.; Friedrich, S. K.; Grubbs, R. H.; Bansleben, D. A. *Science*, **2000**, *287*,460.

43: Pellecchia, C.; Zambelli, A. *Macromol. Rapid Commun.* **1996**, *17*, 333.

44: Pappalardo, D.; Mazzeo, M.; Antinucci, S.; Pellecchia C. *Macromolecules*, **2000**, *33*, 9483.

45: Cherian, A. E.; Rose, J. M.; Lobkovsky, E. B.; Coates, G. W. *J. Am. Chem. Soc.* **2005**, *127*, 13770.

46: Azoulay, J. D.; Gao, H.; Koretz, Z. A.; Kehr, G.; Erker, G.; Shimizu, F.; Galland, G. B.; Bazan, G. C. *Macromolecules*, **2012**, *45*, 4487.

47: Milano, G.; Guerra, G.; Pellecchia, C.; Cavallo, L. *Organometallics*, **2000**, *19*, 1343.

48 : Pellecchia, C.; Zambelli, A.; Oliva, L.; Pappalardo, D. *Macromolecules*, **1996**, *29*, 6990.

49 : Pellecchia, C.; Zambelli, A.; Mazzeo, M.; Pappalardo, D. *J. Mol. Catal. A: Chemical*, **1998**, *28*, 229.

50 : Ruiz-Orta, C.; Fernandez-Blazquez, J. P.; Anderson-Wile, A. M.; Coates, G. W.; Alamo, R. G. *Macromolecules*, **2011**, *44*, 3436.

51: Kim, I.; Kim, J. S.; Ha, C. S.; Park, D. W. *Macro. Res.* **2003**, *11*, 514-517.

52: Schellenberg, J. *Eur. Polym. J.* **2006**, *42*, 487.

53: Ishihara, N.; Seimiya, T.; Kuramoto, M.; Uoi, M. *Macromolecules* **1986**, *19*, 2464.

54: Edited by Schellenberg, J. *Syndiotactic polystyrene : synthesis, characterization, processing, and applications* **2010** Wiley and Sons Chapter 1

55: Longo, P.; Grassi, A.; Oliva, L.; Ammendola, P. *Makromol. Chem.***1990**, *191*, 237.

56: Beckerle, K.; Capacchione, C.; Ebeling, H.; Manivannan, R.; Mulhaupt, R.; Proto, A.; Spaniol, T. P.; Okuda, J. *J. Organo. Chem.* **2004**, *689*, 4636.

57: Po, R.; Cardi, N.; Santi, R.; Romano, A. M.; Zannoni, C.; Spera, S. *J. Poly. Sci. Part A : Poly. Chem.* **1998**, *36*, 2119.

58: Ferreira Jr. L. C.; Costa, M. A. S.; Guimaraes, P. I. C.; Santa Maria, L. C. *Polymer* **2002**, *43*, 3857.

59: Ishihara, N.; Kuramoto, M.; Uoi, M. *Macromolecules* **1988**, *21*, 3356.

60: Lena, F.; Matyjaszewski, K. *Prog. Poly. Sci.* **2010**, *35*, 959.

61: Matyjaszewski, K. *Macromolecules* **2012**, *45*, 4015.

62: Edited by Schellenberg, J. ***Syndiotactic polystyrene****: synthesis, characterization, processing and applications.* **2010**, John Wiley & Sons, Inc., electronic version. Ch 1.

63: Helldorfer, M.; Backhaus, J.; Milius, W.; Alt, H. G. *J. Mol. Catal. A; Chem.* **2003**, *193*, 59.

64: a) Resanovic, S.; Wylie, R. S.; Quail, J. W.; Foucher, D. A.; Gossage, R. A. *Inorg. Chem.* **2012**, 50, 9930; b) Sanja Resanovic Thesis

65: Miller, F. A.; Wilkins, C. H. *Anal. Chem.* **1952**, *24*, 1253.

66: Pavia, D. L.; Lampman, G. M.; Kriz, G. S.; Vyvyan, J. R. *Introduction to spectroscopy* 4th edition. **2009**, Brooks/Cole, Belmont. *pg*77

67: Handley, D.A., Hitchock, P.B., Leigh, G.J. *Inorg. Chim. Acta* , **2001**, 314, 1.

68: Fontaine, F. G. *Acta Cryst.* **2001**, *57*, m270.

69: Perrier, S., Kowollik, C. B., Quinn, J. F., Vana, P., Davis, T. P. *Macromolecules* **2002**, *35*, 8300.

70: Haken, J. K., Werner, R. L. *Br. Polym. J.* **1971**, 263.

71: Arehart, S. V.; Matyjaszewski, K. *Macromolecules*, **1999**, *32*, 2221.

72: Koinuma, H.; Tanabe, T.; Hirai, H. *Macromolecules*, **1981**, *14*, 883.

73 : Dancalf, D. J.; Wade, H. J.; Waterson, C.; Derrick, P. J.; Haddleton, D. M.; McCamley, A. *Macromolecules* **1996**, *29*, 6399.

74: Davies, S.C., Hughes, D.L., Leigh, G.F., Sanders, J. R., Souza, J. S. **1997**, *J. Chem. Sco., Dalton Trans.,1*. **1997,** 1981.